

**Functional Characterisation of Two Channels Proteins
Involved in Leguminous Symbiosis**

Dissertation
der Fakultät für Biologie
der Ludwig-Maximilians-Universität München

vorgelegt von

Charpentier Myriam

München
im September 2008

Dekan: Prof. Dr. Jürgen Soll

Gutachter: Prof. Dr. Martin Parniske

Gutachter: Prof. Dr. Heinrich Jung

Datum der Disputation: 18.12.2008

To my father

(1949-1999)

Table of contents

List of abbreviations	7
List of Units	9
Abstract	10
Zusammenfassung	11
1. Introduction	12
1.1 Endosymbiotic plant-microbe interactions	12
1.2 Root-nodule-symbiosis early ion fluxes	17
1.3 Dissection of the calcium-spiking pathway	22
1.4 <i>Castor</i> and <i>pollux</i> mutant and aim of the study	23
2. Results	28
2.1 CASTOR and POLLUX identification	28
2.2 Sequence analyses	31
2.3 Nuclear localization of CASTOR and POLLUX	35
2.4 Homodimerization of CASTOR and POLLUX	40
2.5 Expression of POLLUX and DMI1 under the control of P35S restore the nodulation phenotype of <i>castor-12</i> mutant	43
2.6 Functional characterization	47
2.6.1 Yeast complementation assays	47
2.6.1.1 <i>cch1Δmid1Δ</i> and <i>trk1Δ</i> yeast mutants complementation assays	47
2.6.1.2 MAB2d yeast mutant complementation assays	48
2.6.2 Electrophysiological analysis	50
2.6.2.1 CASTOR is a cation channel	50
2.6.2.2 Magnesium mediates voltage-dependent blockage of CASTOR	54
2.6.2.3 CASTOR sensitivity to putative binding ligands	55
2.7 CASTOR interacting component	57
2.7.1 Yeast-two-hybrid assay with common symbiotic components	58
2.7.2 Screening of a <i>L. japonicus</i> roots cDNA libraries using yeast-two-hybrid system	59
2.7.2.1 Root nodule phenotype of transformed <i>L. japonicus</i> roots expressing RNAiLjSNF7 construct	61
2.7.2.2 Sub-cellular localization of LjSNF7	62

3. Discussion	64
3.1 Nuclear localization of CASTOR and POLLUX	64
3.2 CASTOR and POLLUX are non-selective cation channels	65
3.3 Channel gating	67
3.4 Hypothetical role of LjSNF7 in the root nodule symbiosis	68
3.5 CASTOR and POLLUX are required for calcium spiking	70
4. Material and methods	73
4.1 Material	73
4.1.1 Plants and chemicals	73
4.1.2 Enzymes and kits	73
4.1.3 Strains, oligonucleotides, vectors and clones	73
4.1.4 Antibodies	74
4.2 Methods	76
4.2.1 Bioinformatics	76
4.2.2 Genetics methods	76
4.2.3 Molecular biological methods	77
4.2.3.1 General molecular biological methods	77
4.2.3.2 TILLING	77
4.2.3.3 Cloning strategies	78
4.2.3.4 RNA isolation	78
4.2.3.5 Reverse transcription (RT)-PCR, Rapid Amplification of cDNA ends (RACE)-PCR and quantitative Reverse Transcription (qRT)-PCR	78
4.2.3.6 Site directed mutagenesis	79
4.2.3.7 Yeast transformation methods	79
4.2.4 Biochemical methods	79
4.2.4.1 General biochemical methods	79
4.2.4.2 Protein extraction from <i>L. japonicus</i> root	79
4.2.4.3 Protein extraction from <i>N. benthamiana</i> leaves	80
4.2.4.4 Protein extraction from <i>S. cerevisiae</i>	80
4.2.4.5 <i>In vitro</i> expression and purification	80
4.2.5 Electrophysiological methods	81
4.2.6 Plant transformation methods	82

4.2.6.1 <i>A. tumefaciens</i> -mediated transient transformation	82
4.2.6.2 <i>A. rhizogenes</i> -mediated transient transformation	82
4.2.7 Cell biological methods	83
4.2.7.1 <i>L. japonicus</i> cell culture protoplast transfection	83
4.2.8 Histochemical methods	84
4.2.8.1 Immunogold electron microscopy	85
4.2.8.2 GUS assay	85
4.2.8.3 Mycorrhiza staining	85
4.2.9 Fungal and bacterial inoculation methods	85
4.2.9.1 Inoculation with <i>G. intraradices</i>	85
4.2.9.2 Inoculation with <i>M. loti</i>	85
5. References	86
6. Acknowledgement	102
7. Appendix	103
7.1 List of publication	103
7.1.1 Papers	103
7.1.2 Posters and conferences	103
7.1.3 Talks	104
7.2 List of figures	105
7.3 List of tables	106
7.4 Erklärung	107
7.5 Curriculum vitae	108

List of abbreviations

a.a.	Amino acid
AFLP	Amplified fragment length polymorphism
AM	Arbuscular mycorrhiza
AS	Alternative spliced
BAC	Bacterial artificial chromosomes
BiFC	Bimolecular fluorescence complementation
bp	Base pair
Ca ²⁺	Calcium
CaCl ₂	Calcium chloride
cADP-rib	1-(5-phospho-b-D-ribosyl) adenosine 5-phosphate cyclic anhydride
CAPS	Cleaved amplified polymorphic sequence
CDD	Conserved domain database
cDNA	Complementary deoxyribonucleic acid
CODDLE	Codons Optimized to Discovered Deleterious Lesions
DNA	Deoxyribonucleic acid
DGPP	Diacylglycerol pyrophosphate
DMI	Does not make infection
DsRed	<i>Discosoma sp.</i> red fluorescent protein
DTT	Dithiothreitol
DUF	Domain of unknown function
EDTA	Ethylenediaminetetraacetic acid
EMS	Ethyl methane-sulfonate
ENOD	Early nodulation
ER	Endoplasmic reticulum
Erev	Reverse potential
ESCRT	Endosomal sorting complex required for transport
EST	Expressed sequence tags
F	Faraday constant; $N_{qe} = 9.6485 \times 10^4 \text{ C mol}^{-1}$
FNR	Ferredoxin NADP(H) oxidoreductase
GFP	Green fluorescent protein
GUS	β -glucuronidase
HRP	Horseradich peroxidase
INM	Inner nuclear membrane
InsP ₃	Inositol triphosphate
IPD	Interacting protein of DMI3
IT	Infection thread
ITD	Infection thread deficient
K ⁺	Potassium
kb	Kilobase
KCl	Potassium chloride
Li ⁺	Lithium
MtPT4	<i>Medicago truncatula</i> phosphate transporter
MEGA-9	N-Nonanoyl-N-methylglucamine
Na ⁺	Sodium
NaCl	Sodium chloride

NAADP	Nicotinic acid adenine dinucleotide phosphate
NAD ⁺	Nicotinamide adenine dinucleotide
NADP ⁺	Nicotinamide adenine dinucleotide phosphate
NAD(P)bd	Nicotinamide adenine dinucleotide phosphate binding domain
NCBI	National Centre for Biotechnology Information
NE	Nuclear envelope
NFR	Nod factor receptor
NLS	Nuclear localization signal
nt	nucleotide
NUP	Nucleoporin
ONM	Outer nuclear membrane
PA	Phosphatidic acid
PCR	Polymerase chain reaction
PLD	Phospholipase D
PHYLIP	Phylogeny inference package
PPA	Pre-penetration apparatus
PI-PLC	Phosphoinositide-dependent phospholipase C
PIP ₂	Phosphatidylinositol 4,5-bisphosphate
PIT	Pre-infection thread
PTC	Premature termination codon
QAs	Quaternary ammonium ions
qRT	Quantitative Reverse Transcription
R	Molar gas constant; 1.987 cal mol ⁻¹ K ⁻¹
RACE	Rapid Amplification of cDNA ends
RFP	Red fluorescent protein
RNAi	Ribonucleic acid interference
RNS	Root nodule symbiosis
SINA	Seven in absentia
SD	Yeast synthetic defined medium
SDS	Sodium dodecyl sulfate
SNF7p	sucrose non-fermenting protein 7
SSR	Simple sequence repeat
SYMRK	Symbiosis receptor-like kinase
T	Thermodynamic temperature
TAC	Transformable bacterial artificial chromosomes
TBA	Tetrabutylammonium
TILLING	Targeted induced local lesions in genomes
Tm	Annealing temperature
TP	Transit peptide
v/v	By volume
YFP	Yellow fluorescent protein

List of Units

A	Ampere
C	Celsius
Da	Dalton
g	Times gravity
L	Liter
m	Meter
M	mol/L
OD _x	Optical density of an element for a given wavelength x
pH	“Power of hydrogen” or measure of the activity of dissolved hydrogen ions
rpm	Centrifuge rotor speed
s	second
S	Siemens
V	Volt

Abstract

Legume-rhizobial symbiosis results in the formation of a new organ, the nitrogen-fixing root nodule. A chemical communication between both partners accompanies the invasion of plant host cells by bacteria and the development of the root nodule. In response to plant-released flavonoids, rhizobia produce lipo-chito-oligosaccharide signalling molecules, so called Nod factors. Early signal transduction in legumes such as *Lotus japonicus* and *Medicago truncatula*, is associated with a succession of tightly orchestrated ion fluxes across different membrane systems of the host cell. The Nod factor perception at the plasma membrane triggers Ca^{2+} oscillations that are associated with the nucleus. *CASTOR* and *POLLUX* are required for Ca^{2+} spiking. Homology modeling suggested *CASTOR* and *POLLUX* might be ion channels. However, experimental confirmation was lacking. Therefore we performed biochemical and electrophysiological analysis to define their role. Here we show that *CASTOR* and *POLLUX* form two independent homocomplexes in the nuclear rim *in planta*. We reconstituted *CASTOR* in planar lipid bilayers and electrophysiological measurements revealed that *CASTOR* is a cation channel preferentially permeable to potassium. The permeability of the sequence-related *POLLUX* for cation could be as well demonstrated through expression of *POLLUX* in different yeast mutants. Furthermore, we demonstrate that a voltage-dependent magnesium blocking mechanism contributes to reduce the conductance of *CASTOR* at negative membrane potential. By screening a *L. japonicus* roots cDNA library using yeast-two-hybrid system, a SNF7 protein interacting with *CASTOR* was found which acts as positive regulator in the nodulation pathway. Collectively the data demonstrate that both *CASTOR* and *POLLUX* are nuclear localized cation channels. Therefore, we propose that *CASTOR* and *POLLUX* may act as counter ion channels to facilitate a rapid efflux of charge associated with the calcium efflux. Alternatively and not mutually exclusive, they may catalyze a nuclear membrane depolarization leading to the activation of calcium channels responsible for calcium spiking.

Zusammenfassung

Leguminosen können mit Bakterien, den so genannten Rhizobien, eine Symbiose eingehen, wobei in neu gebildeten Pflanzenorganen, den Wurzelknöllchen, molekularer Stickstoff aus der Luft fixiert wird. Das Eindringen der Bakterien in die Pflanzenzellen und die darauf folgende Entstehung der Wurzelknöllchen sind Folge eines molekularen Signalaustauschs zwischen beiden Partnern. Als Reaktion auf Flavonoide, die von der Pflanze ausgeschüttet werden, produzieren Rhizobien Lipochitooligosaccharide, die so genannten Nod-Faktoren. Perzeption dieser bakteriellen Signalmoleküle in Leguminosen wie *Lotus japonicus* und *Medicago truncatula* induziert nukleäre Kalzium-Oszillationen, die die Funktion von zwei Proteinen, CASTOR und POLLUX, erfordern. Strukturvorhersagen, die auf Sequenzvergleichen mit bereits bekannten Proteinen basieren, legen die Vermutung nahe, dass es sich bei CASTOR und POLLUX um Ionenkanäle handelt. Ein experimenteller Nachweis fehlte jedoch. Daher wurden in dieser Arbeit CASTOR und POLLUX mit biochemischen und elektrophysiologischen Methoden analysiert, um ihre genaue Funktion zu identifizieren. Es konnte gezeigt werden, dass CASTOR und POLLUX *in planta* zwei voneinander unabhängige Homokomplexe in der Kernmembran bilden. Wir rekonstituierten CASTOR in planaren Lipiddoppelschichten für elektrophysiologische Messungen, die ergaben, dass CASTOR ein kationenpermeabler Ionenkanal mit einer schwachen Präferenz für Kalium ist. Die Permeabilität für Kalium von POLLUX, dessen Sequenz mit der von CASTOR verwandt ist, wurde durch die Expression von *POLLUX* in einer Hefe-Mutante mit defektem Kaliumtransport bestätigt. Anhand einer ‚Yeast-two-hybrid‘-Sichtung einer *L. japonicus* cDNA-Bibliothek, wurde ein SNF7 Protein identifiziert, das mit CASTOR interagiert und ein positiver Regulator der Signaltransduktionskette der Wurzelknöllchensymbiose ist. Die in dieser Arbeit gewonnenen Daten belegen, dass CASTOR und POLLUX Kationenkanäle in der Kernmembran sind, die den schnellen Efflux von Kalzium durch einen gegensätzlichen Ladungsausgleich ermöglichen. Eine alternative oder zusätzliche Funktion der beiden Proteine könnte die Depolarisierung der Kernmembran darstellen, die für die Aktivierung der Kalziumkanäle und somit für die Kalzium-Oszillationen verantwortlich ist.

1. Introduction

1.1 Endosymbiotic plant-microbe interactions

In the mid-nineteenth century, de Bary defined the term “symbiosis” (from the Greek: *sym* = together, *bio* = life) as a close physical association between two organisms of different species. This definition which could be applied to a wide range of biological interaction, was then narrowed by Pierre-Joseph van Benedén who restricted as symbiotic, a mutually beneficial relationships between two organisms (Wilkinson, 2001). Most land plants rely on symbiosis with soil microorganisms such as fungi and bacteria to provide them with inorganic compounds and trace elements. Among microorganisms, some symbionts accommodate within the host plants cells to form an endosymbiosis (*endo* = inner).

The arbuscular mycorrhiza (AM), endomycorrhiza formed by fungi of the phylum *Glomeromycota* and the majority of land plants, is one of the most significant plant-fungal endosymbiosis (Schüssler, 2001; Trappe, 1987). In this mutually beneficial association, AM fungi provide the plants with phosphate and other mineral nutrients and in return obtain carbohydrates from their hosts (Hodge et al., 2001). The fossil record for existence of AM, 450 million years ago, demonstrates that the AM is as old as the earliest land plants (Remy et al., 1994). In comparison, root nodule symbiosis (RNS), endosymbiosis between soil nitrogen-fixing bacteria and plants belonging to a clade within the Eurosoid, including the Fabales, Fagales, Cucurbitales and Rosales, is more recent; the oldest fossil nodule-like structures are dated at 65 million years (Herendeen et al., 1999; Soltis et al., 2000). RNS occurs with two different types of soil bacteria: Gram-positive bacteria of the genus *Frankia* and members of Gram-negative bacteria, termed rhizobia. Plants of the Fabales, Cucurbitales and Rosales nodulate with gram-positive actinobacteria *Frankia* (Swensen and Benson, 2008). In contrast, with the exception of the genus *Paranosporia* in the *elm* family, the rhizobia, including the *Rhizobium*, *Bradyrhizobium*, *Azorhizobium*, *Mesorhizobium* and *Sinorhizobium*, associate with plants of exclusively one order, the Fabales (Doyle, 1998; Marvel et al., 1987).

The phenotypic analysis of legume mutants impaired in both RNS and AM revealed a genetic link between both symbioses (Catoira et al., 2000; Kistner et al., 2005). From the existence of this common genetic program the hypothesis arises that pre-existing AM genetic program has been recruited to serve the bacterial endosymbiosis development (Albrecht et al., 1999; LaRue and Weeden, 1994). For both AM and rhizobia RNS, the success of the relationship between the symbionts and the plants depend on four major steps: recognition, penetration, proliferation and nutrient transfer. During these steps, structural and physiological similarity can be observed between the two endosymbioses.

In the case of the interaction between the AM fungi and the plant host, the signalling events responsible for mutual recognition are not fully understood. Spores of AM fungi can germinate spontaneously without plant-derived signals (Juge et al., 2002). Nevertheless, depending on the fungi/host interaction, flavonoids-containing roots exudates can enhance or decrease the spore germination, indicating that those plant-phenolics are perceived by the fungi (Nair et al., 1991; Vierheilig et al., 1998). The spore germination can also be enhanced by the host plant-derived strigolactone. The strigolactone, newly identified as endogenous plant hormones (Umehara et al., 2008), has been shown to induce hyphal branching and metabolic activity of the fungi (Akiyama et al., 2005; Besserer et al., 2006; Buee et al., 2000). In addition to the growth and metabolic changes, the fungi respond to the plant by releasing signalling molecules which are key messengers to alert the plant of the symbiont presence and trigger the plant symbiosis program. The first evidence for fungal signalling molecules, so-called “Myc factors”, was gained from experiments using a *Medicago truncatula* *EARLY NODULATION11* promoter (P_{ENOD11}): β -glucuronidase (GUS) fusion, which is induced in response to both AM fungi and rhizobia (Journet et al., 2001). The *ENOD11* gene encodes a repetitive Pro-rich protein, believed to be a functional component of the plant extracellular matrix and induced upon AM and RNS (Journet et al., 2001). The AM branching hyphae, localized in the vicinity of the host root but physically separated by a permeable cellophane membrane, induced GUS expression in epidermal and cortical roots cells (Kosuta et al., 2003). This experiment indicates that the host roots perceive the diffusible “Myc factor(s)”. Multiple experiments confirmed the presence of diffusible fungal factor(s) (Navazio et al., 2007; Olah et al., 2005; Weidmann et al., 2004). In

soybean cell culture stably expressing the bioluminescent calcium indicator aequorin, diffusible fungal factor(s) of small molecular mass (< 3KDa) are able to elicit AM specific transient elevations of cytosolic free calcium (Navazio et al., 2007).

Upon contact with the fungi, the expression pattern of the $P_{ENOD11}:ENOD11$ changes and is restricted to the epidermal cells directly associated with visible appressoria, flattened hyphal tips adhering to the host epidermal cells (Chabaud et al., 2002). Studies using $P_{ENOD11}:GFP-HDEL$ fusion in transgenic *Medicago truncatula* roots confirmed that the induction of *ENOD11* expression occurs in the epidermal cell after the fungal appressorium differentiation (Genre et al., 2005). In this study, *ENOD11* induction is also synchronized with an AM specific plant cellular reorganisation occurring before the fungus penetrates into the first cell at the epidermis or exodermis (Genre and Bonfante, 2007; Genre et al., 2005). Indeed, from the site of the infection, a pre-penetration apparatus (PPA) is formed. The PPA is a trans-cellular column of cytoplasm, rich in cytoskeletal elements and endoplasmic reticulum which define the future path for the hyphal penetration (Genre et al., 2005). The assembly of the PPA is coupled with an initial repositioning of the nucleus at the site of fungal adhesion and subsequent transcellular migration (Genre et al., 2008; Genre et al., 2005). Using vital lipophilic fluorescent dye, a putative membrane structure that colocalizes with the cytoplasmic column and associated PPA is labelled. This suggests that the PPA could be a player in the synthesis of the membrane that surrounds and isolates the infection hypha from the cell cytoplasm (Genre et al., 2005). Once the PPA and the perifungal membrane have traversed the cell lumen, the fungal hypha penetration starts.

The fungus progresses through exodermal and outer cortical cells in a PPA dependent manner and reaches the apoplast between inner cortical cells where it proliferates (Genre et al., 2008; Parniske, 2004). This intercellular hyphal progression is accompanied by cytoplasmic reorganisation, nuclear enlargement and repositioning opposite to the site of fungal contact of the inner cortical cells (Genre et al., 2008). Then, without apparent appressorium formation, the fungus invades the inner cortical cells where it differentiates an ephemeral tree-like structure, the so-called arbuscule, which will reach full development within several days, and then senesce (Alexander et al., 1988; Javot et al., 2007). The arbuscule is enveloped in a membrane known as periarbuscular membrane, derived from the host plasma membrane. The resulting surface between the

periarbuscular membrane and the arbuscule membrane constitutes a symbiotic interface for nutrient exchange between the two symbionts (Gianinazzi-Pearson, 1996).

The arbuscular mycorrhizal fungi obtain carbohydrates from the host and in exchange improve the plant acquisition in mineral nutrients, specially phosphate but also nitrogen (Govindarajulu et al., 2005; Pearson and Jakobsen, 1993; Smith et al., 2003). Today, few periarbuscular membrane transporters have been identified. The up-regulation of plant proton ATPases during AM interaction as well as their specific expression in arbuscule containing cells, suggest their involvement in the AM mechanism (Gianinazzi-Pearson et al., 2000; Murphy et al., 1997). Furthermore, expression profiling studies have revealed upon AM inoculation specific up-regulation of plant high-affinity nitrate transporter as well as plant hexose transporter functionally characterized as glucose and fructose transporter in yeast (Harrison, 1996; Hohnjec et al., 2005). So far, the most characterized transporter involved in the AM nutrient exchange is the *Medicago truncatula* phosphate transporter, MtPT4 (Harrison et al., 2002). Also mycorrhiza-induced, MtPT4 localize to the periarbuscular membrane where it contributes to the plant phosphate uptake (Harrison et al., 2002; Javot et al., 2007). Without MtPT4, the arbuscules die prematurely (Javot et al., 2007). Recently the arbuscular mycorrhizal molecule involved in the induction of MtPT4 tomato and potato orthologous has been identified (Drissner et al., 2007). By chromatography and mass spectrometric analyses, the active component was characterized as a lyso-phosphatidylcholine (Drissner et al., 2007). Today, the receptor to lyso-phosphatidylcholine is unknown.

Similarly to AM symbiosis, a molecular dialogue is established between the plant host and rhizobia in order to establish the RNS. While in the AM formation there is little host specificity, the rhizobia-legume interaction is typically specific. The host specificity is controlled at several levels of the molecular dialogue. At the first step of the recognition, the bacteria perceive flavonoid, chemo-attractant, secreted by the host. The flavonoids induce the production of a bacterial-nodulation factor, lipo-chitin-oligosacharides, so-called Nod-factor. The nature of the flavonoids play a role in the specific activation of the transcriptional regulator NodD which induces the expression of the *nod* genes involved in the production of the Nod factor (Cardenas et al., 1995; Fisher and Long, 1992; Long, 1996). The Nod factor is the major player of the host specificity

and consists of a β -1,4-linked N-acyl-D-glucosamine backbone of three to five units, N-acetylated at the nonreducing-terminal residue by a fatty acid and containing a variety of additional decorations at the end reducing or non-reducing terminal residue, or both (Lerouge et al., 1990; Spaink et al., 1991). The length of the glucosamine backbone, the modification of the terminal sugar residue or the nature of the acyl chain can all define the biological activity and host specificity of the Nod factor (Carlson et al., 1995).

The recognition by the host plant of the Nod-factor-secreting rhizobia elicits the growth of the root hair cell which leads to deformation and “Shepherd’s crook”-like curling of the root hair tip within hours (Heidstra et al., 1994; Yao and Vincent, 1969). The application of the Nod-factor alone is sufficient to induce the transient actin fragmentation which precedes the root hair tip deformation and curling (Cardenas et al., 1998), as well as the activation of early nodulation genes expression like *ENOD11* and cortical cells division (Catoira et al., 2001; Esseling et al., 2003; Truchet et al., 1991). Entrapped in the curl, rhizobia enter the root hair *via* degradation of the cell wall, invagination of the plasma membrane and deposition of new plant and bacterial materials forming a new tubular structure, the infection thread (IT) (Ridge and Rolfe, 1985; Turgeon and Bauer, 1985). The IT grows centripetally towards the cortex with rhizobia continuously dividing (Napoli and Hubbell, 1975; Ridge and Rolfe, 1985). Similarly to AM penetration, a reorganisation of the cytoskeleton precedes the infection thread progression. Cytoplasmic bridge from one side of the cell to the other, the so-called pre-infection thread (PIT), is formed which guides the infection thread passage (Timmers et al., 1999; van Brussel et al., 1992). Likewise to the AM pre-penetration apparatus, the PIT is closely connected to the nucleus (Timmers et al., 1999). Concomitant with the epidermal infection thread progression, the cortical cells below the site of infection divide to form the nodule primordium (Yang et al., 1994). The nature of the cortical cells which differentiate into meristematic cells is determined by the plant and will specify the type of nodule; indeterminate or determinate (Hirsch, 1992). When the infection thread reaches the primordium, the rhizobia are released. They enter the cytoplasm *via* invagination of the host-cell membrane. Similarly to the arbuscule, the bacterial surface is not in direct contact with the cytoplasm but remains surrounded by a plant-derived membrane, the peribacteroid membrane, and together form a so-called symbiosome (Oke and Long, 1999). In this microaerobic environment, the bacteria differentiate into bacteroids in

which nitrogen reduction into ammonia occurs (Oke and Long, 1999). On the peribacteroid membrane that is highly permeable to NH_4^+ , ammonium transporter has been characterized (Kaiser et al., 1998; Niemietz and Tyerman, 2000).

Among legumes, two types of root nodules are found; determinate and indeterminate nodules (Hirsch, 1992). On pea and alfalfa roots for example, indeterminate nodules are formed. The cell division that initiates this type of nodule takes place in the inner cortex and leads to the formation of a nodule with a persistent apical meristem (Robertson et al., 1985). The constant addition of new cells leads to the formation of an egg-shape nodule. In comparison, in lotus and soybean roots, determinate nodules are developed from outer cortical cells. The meristematic activity stop in an early stage and the subsequent nodule growth depends on cell expansion leading to a mature spherical nodule (Stougaard, 2000). In most species, nodules are visible within 7 days after inoculation (Albrecht et al., 1999).

1.2 Root-nodule-symbiosis early ion fluxes

Using a combination of electrophysiology and fluorescence microscopy with ion sensitive dyes, specific ion fluxes preceding root hair deformation have been measured in response to Nod factor (Felle et al., 1998; Shaw and Long, 2003).

Within one minute after addition of at least 10 nM Nod factor, a rapid calcium influx into the cytoplasm of the root hair tip of alfalfa is recorded (Ehrhardt et al., 1996; Felle et al., 1998). The calcium influx can raise the intracellular calcium concentration to 1500 nM at the root hair tip (Cardenas et al., 1999). In *Medicago truncatula* the calcium influx is biphasic, with a first increase in calcium followed by an elevated level of calcium lasting for several minutes (Shaw and Long, 2003). The calcium influx induces secondary responses including membrane depolarization of 10-15 mV and transient intracellular alkalization of 0,3 pH units (Ehrhardt et al., 1992; Felle et al., 1995; Felle et al., 1996; Felle et al., 1998; Kurdjian, 1995). By using stationary ion-selective extracellular electrodes, a chloride efflux triggered by the calcium influx is proved to be responsible for the membrane depolarization (Felle et al., 1998). The charge balance which eventually stops the depolarization and initiates the repolarization is provided by

potassium efflux (Felle et al., 1998). During Nod-factor-induced membrane depolarization, addition of H⁺-ATPase inhibitor abolishes the membrane repolarization suggesting that a proton efflux is responsible for the membrane potential recovery (Felle et al., 1998). Concomitant to the membrane depolarization, the calcium influx triggers a transient alkalinization of the root hair surface. Upon H⁺-ATPase inhibitor treatment, the alkalinization becomes persistent suggesting that it could be due to a transient Nod factor-induced inhibition of a H⁺-ATPase (Felle et al., 1998). So far, no causal link has been proved between the membrane depolarization and the transient alkalinization.

Subsequently, with a delay of 10-20 min, transient oscillations of the calcium concentration rising from 50 to 600 nM, so-called calcium spiking, are observed around the nucleus (Ehrhardt et al., 1996; Shaw and Long, 2003). Due to the nucleoplasmic and perinuclear localization of the Ca²⁺ spiking, cisterns of the endoplasmic reticulum (ER) and the nuclear envelope are likely to be the corresponding Ca²⁺ stores (Oldroyd and Downie, 2006). The calcium oscillations, which can last 1 to 3 hours, are regular with a mean period of 60 seconds for a single spike and can be induced with a Nod factor concentration as low as 1 pM (Ehrhardt et al., 1996; Shaw and Long, 2003). The spike is imposed on a baseline with a raising phase of each peak typically faster than the falling phase (Ehrhardt et al., 1996).

So far, the calcium influx and the calcium spiking have been reported from six and five different legumes, respectively (Cardenas et al., 1998; de Ruijter et al., 1998; Harris et al., 2003; Miwa et al., 2006; Shaw and Long, 2003; Wais et al., 2000; Walker et al., 2000). In addition to those reports, Nod factor fails to induce calcium spiking and calcium influx in root hair cells of non-leguminous plants (Ehrhardt et al., 1996). All together these results suggest that the calcium fluxes are specific and common features of Legume-rhizobia interactions.

The calcium spiking and the calcium influx responses are spatially distinct and appear to be causally unlinked (Shaw and Long, 2003). Various non-nodulating mutants impaired for the calcium spiking still show calcium influx (Miwa et al., 2006; Shaw and Long, 2003). In wild-type legumes, Nod-factor-like molecules, N-acetylglucosamine tetramers or partially decorated Nod factors can trigger calcium spiking but fail to induce calcium influx (Ardourel et al., 1994; Shaw and Long, 2003; Walker et al., 2000). In calcium-spiking-deficient mutants, these molecules cannot cause the calcium spiking

which suggests that both stringent and non-stringent perceptions of Nod factor involve the same Nod factor pathway (Oldroyd et al., 2001). Furthermore, the minimal concentration of Nod factor required to induce the calcium spiking is three orders of magnitude lower than the concentration needed to trigger the calcium influx (Shaw and Long, 2003). Collectively, these results suggest that there is a lower stringency of Nod factor perception required for induction of calcium spiking, whereas a relatively high concentration and specific Nod factor structures are required to induce distinctly the calcium influx.

Forward genetics approaches, using ethyl methane-sulfonate (EMS) or T-DNA insertion as mutagen tools, yielded at least seven distinct mutants impaired in the symbiotic process upstream of the calcium spiking (Miwa et al., 2006; Perry et al., 2003; Schauser et al., 1998). Among those loci, only two, *NFR1* and *NFR5*, are RNS specific, whereas the five other loci are commonly involved in AM and RNS symbioses, and so-called common *SYM* genes (Kistner and Parniske, 2002). *NFR1* and *NFR5* are required for the calcium influx, membrane depolarisation and transient alkalinisation, as well as noduline genes expression (Madsen et al., 2003; Miwa et al., 2006; Radutoiu et al., 2003). The *nfr1* and *nfr5* mutants show no root hair deformation upon *Mesorhizobium loti* inoculation (Radutoiu et al., 2003). The corresponding LysM receptor-like kinases, NFR1 and NFR5, have been shown to determine the Nod factor specificity of legume/rhizobial symbiosis. The transfer of *L. japonicus* *NFR1* and *NFR5* to *M. truncatula* enables indeed nodulation of the transformants by the *L. japonicus* symbiont *M. loti* (Radutoiu et al., 2007). The LysM-containing extracellular domains have also been proved to be directly involved in the Nod factor perception (Radutoiu et al., 2007). Although a direct Nod factor binding has not been demonstrated yet, the results suggest that NFR1 and NFR5 form the Nod factor receptor complex required for the first recognition step (Radutoiu et al., 2003; Radutoiu et al., 2007).

In all five other common symbiosis mutants impaired in the calcium spiking, so-called *symrk*, *nup85*, *nup133*, *castor* and *pollux* (Table 1), the root hair deformation phenotype is accentuated in comparison to the wild type upon incubation with rhizobia or Nod factor (Bonfante et al., 2000; Kanamori et al., 2006; Miwa et al., 2006; Stracke et al.,

2002). However, no curling of the root hair tips is observed. This phenotypic characterization suggests that the Nod factor signalling pathway is blocked downstream of Nod factor perception and that the calcium spiking would be required for root hair curling followed by bacterial entrapment. In these mutants, upon treatment with a high Nod factor concentration, calcium influx is induced (Miwa et al., 2006). Considering the amount of Nod factor required to elicit calcium influx, it is proposed that in physiological condition calcium influx is induced when the bacteria are entrapped prior to the infection thread formation (Miwa et al., 2006). This calcium influx would be necessary to the bacterial entry process through infection thread formation. Support for this model comes from the analysis of infection thread initiation in vetch by nodulation mutants of *Rhizobium leguminosarum* (Walker and Downie, 2000). The expression of the *R. leguminosarum nodO* gene in *Rhizobium* mutant can compensate the loss of the appropriate Nod factor production and induce infection thread formation (Walker and Downie, 2000). The *nodO* gene of *R. leguminosarum* encode for a secreted protein that can form cation-selective channels in lipid bilayers (Sutton et al., 1994). It has been proposed that NodO may stimulate ion flux such as calcium influx across the host plasma membrane which will be sufficient to induce infection thread formation (Walker and Downie, 2000). However, the infection threads formed have an irregular shape and are arrested prematurely (Walker and Downie, 2000). This observation suggests that a structurally specific Nod factor is necessary to pass a third “checkpoint” that controls the infection thread progression.

In this model, at least three receptor complexes, named perception, entry and progression receptor complexes, are required for the rhizobia to enter and progress into the host cells. If the putative NFR1/NFR5 receptor-like kinases complex is likely to monitor the first recognition step, other receptors and/or a different combination of receptors may be involved at the subsequent steps. *SYMRK* is encoded for an active receptor-like kinase involved downstream of NFR1 and NFR5; after treatment with purified Nod factor, double mutants *SYMRK/NRF1* or *SYMRK/NFR5* respond similarly to *NRF1* or *NFR5* mutants, respectively (Radutoiu et al., 2003; Stracke et al., 2002; Yoshida and Parniske, 2005). The phenotypic results suggest that *SYMRK* is involved in a signalling pathway leading to calcium spiking and curling. However, an additional role of *SYMRK* in the bacterial entry process cannot be excluded. Finally, several *L. japonicus*

mutants have been described as defective for infection thread growth, including *alb1*, *sym7*, *sym8*, *sym10*, *sym80*, *crinkle*, *itd1*, *itd3* and *itd4* (Lombardo et al., 2006; Schauser et al., 1998; Tansengco et al., 2003; Yano et al., 2006). For some of those mutants, the bacteria stay entrapped in the infection pocket, while in other mutants abnormal infection threads are formed. The identification of these different genes will give new insight into the mechanism of the entry and of the infection thread growth “checkpoints”.

Table 1.

Common <i>L. japonicus</i> SYM genes required for AM and RNS.				
<i>L. japonicus</i> genes	Characteristics	Orthologous		Reference(s)
		<i>M. truncatula</i>	<i>P. sativum</i>	
<i>SYMRK</i> (<i>SYM2</i>) ^a	Hac ⁻ , no Ca ²⁺ spiking	<i>DMI2</i>	<i>PsSYM19</i>	(Endre et al., 2002; Stracke et al., 2002)
<i>POLLUX</i> (<i>SYM23</i> and <i>SYM86</i>) ^a	Hac ⁻ , no Ca ²⁺ spiking	<i>DMI1</i> *	<i>PsSYM8</i> *	(Kistner et al., 2005)
<i>CASTOR</i> (<i>SYM4</i> and <i>SYM71</i>) ^a	Hac ⁻ , no Ca ²⁺ spiking			(Bonfante et al., 2000; Ovtsyna et al., 2005; Zhu et al., 2006)
<i>NUP85</i> (<i>SYM24</i> , <i>SYM73</i> and <i>SYM85</i>) ^a	Hac ⁻ , no Ca ²⁺ spiking	-	-	(Saito et al., 2007)
<i>NUP133</i> (<i>SYM3</i> and <i>SYM45</i>) ^a	Hac ⁻ , no Ca ²⁺ spiking	-	-	(Kanamori et al., 2006)
<i>CCaMK</i> (<i>SYM15</i> and <i>SYM72</i>) ^a	Hac ⁻ , Ca ²⁺ spiking	<i>DMI3</i> *	<i>PsSYM9</i> */ <i>PsSYM30</i> *	(Levy et al., 2004; Mitra et al., 2004; Ovtsyna et al., 2005; Tirichine et al., 2006)
<i>CYCLOPS</i> (<i>SYM82</i> , <i>SYM6</i> and <i>SYM30</i>) ^a	Iti ⁻ , Ca ²⁺ spiking	<i>IPD3</i> *	<i>PsSYM36</i> *	(Messinese et al., 2007; Tsyganov et al., 2002; Yano et al., 2006)

* putative orthologous of *L. japonicus* gene; ^a previous nomination used in the studies referenced; Hac⁻, no root hair curling ; Iti⁻, blockage at the stage of infection thread initiation.

1.3 Dissection of the calcium-spiking pathway

Both the rhizobial bacteria and the mycorrhizal fungi trigger nuclear-localized calcium spiking *via* the common symbiotic signalling pathway, which includes at least seven proteins (Table 1). Although components of the same signalling pathway are involved, the fungal and bacterial calcium signatures generated are very different in terms of frequency and amplitude (Kosuta et al., 2008). The AM-induced calcium spiking has an irregular spiking frequency which produces a 74-113 nM calcium change which is only 17 % of Nod factor-induced calcium change (Kosuta et al., 2008). Furthermore, in contrast to the Nod-factor induced calcium spiking which is repetitive and periodic, the AM-induced calcium spikes differ with each repetition (Kosuta et al., 2008). How those two different calcium signatures are generated and decoded by a signalling pathway involving identical components is still unclear. Among the common symbiotic proteins acting downstream of the calcium spikes, a calcium/calmodulin-dependent protein kinase, CCaMK, has been identified and constitutes an obvious candidate involved in decoding the calcium signatures (Gleason et al., 2006; Godfroy et al., 2006; Levy et al., 2004; Mitra et al., 2004; Tirichine et al., 2006).

Today, no calcium channels responsible for the generation of nuclear localized-calcium spiking have been identified in plants. In animal cells, Ca^{2+} -permeable channels such as ryanodine receptors and inositol triphosphate receptors (InsP₃-R) localized in the nuclear envelope or ER are involved in the generation of Ca^{2+} oscillation around the nucleus (Furuichi et al., 1989; Takeshima et al., 1989). These channels can be activated by secondary messengers such as nicotinic acid adenine dinucleotide phosphate (NAADP), 1-(5-phospho-b-D-ribose) adenosine 5-phosphate cyclic anhydride (cADP-Rib), inositol-1,4,5-triphosphate (InsP₃) and Ca^{2+} (Gerasimenko and Gerasimenko, 2004). InsP₃ is generated from degradation of phosphatidylinositol 4,5-bisphosphate (PIP₂) by a phosphoinositide-dependent phospholipase C (PI-PLC). The mammalian PI-PLC is primarily activated *via* heterotrimeric G-proteins (Fukami, 2002; Ross and Higashijima, 1994). Mastoparan, an agonist of heterotrimeric G-proteins in animal cells, activates PI-PLC and induces Ca^{2+} fluxes (Ross and Higashijima, 1994). Although the precise mode of action of mastoparan in plant cells is unclear (Miles et al., 2004; Pingret et al., 1998), it triggers Ca^{2+} spiking (Pingret et al., 1998; Sun et al., 2007), as well as nodulation gene

expression in *Medicago truncatula* (Pingret et al., 1998; Sun et al., 2007). In vetch roots, a synthetic analogue to mastoparan, mastoparan-7, elicits root hair deformation and activates both PI-PLC and phospholipase D (PLD), which results in an accumulation of phosphatidic acid (PA) and diacylglycerol pyrophosphate (DGPP), similarly to Nod factor treatment (den Hartog et al., 2001). Furthermore, the application of PI-PLC and PLD antagonists inhibits Nod factor-induced root hair deformation, PA accumulation and expression of nodulation genes (Charron et al., 2004; den Hartog et al., 2001; den Hartog et al., 2003; Pingret et al., 1998). The PI-PLC antagonist, U-73122, also inhibits Nod factor-elicited calcium spiking (Charron et al., 2004; Engstrom et al., 2002). All together, these results suggest that similar signalling transduction pathways lead to Ca^{2+} oscillations in plants and animals.

However, ryanodine receptors or InsP_3 -R have not been identified in the completely sequenced *Oryza sativa* and *Arabidopsis thaliana* genomes, suggesting alternative, yet unidentified channels are involved (Nagata et al., 2004). Despite the absence of clear homologs in plants, both NAADP and cADP-rib elicit Ca^{2+} release from plant ER-derived vesicles (Navazio et al., 2000; Navazio et al., 2001). Furthermore, an inhibitor of InsP_3 -activated channels, 2-aminoethoxydiphenylborate, blocks the Nod factor induced Ca^{2+} spiking (Engstrom et al., 2002). Collectively, these results suggest the presence of yet-to-be identified plant Ca^{2+} channels activated similarly to the Ca^{2+} channels responsible for Ca^{2+} oscillations in animal cells.

1.4 *Castor* and *pollux* mutants and aim of the study

The absence of Ca^{2+} spiking, root hair curling, infection thread and cortical cell division in *castor* and *pollux* mutants, suggests that *CASTOR* and *POLLUX* act early in a signal transduction chain leading to the activation of calcium-spiking and bacterial entrapment in curled root hair. It is therefore postulated that *CASTOR* and *POLLUX* are necessary to allow the passage of the bacteria through the epidermis layer (Bonfante et al., 2000; Kistner et al., 2005; Miwa et al., 2006; Schauser et al., 1998).

Similarly, fungal infection attempts on *castor* and *pollux* mutants generally abort within the epidermis (Bonfante et al., 2000; Kistner et al., 2005). The AM fungi develops

appressoria from which hyphae grows between two epidermal cells, before the progression aborts in the extracellular space. There, hyphae often show balloon-like swellings or other deformation (Bonfante et al., 2000; Kistner et al., 2005). Interestingly, two alleles of *castor*, *castor-1* and *castor-2*, present different AM phenotypic strength (Novero et al., 2002). In roots of *castor-2* mutant, fungal penetration beyond the epidermis after appressoria formation is never observed. In comparison, in roots of *castor-1*, fungal hyphae are mainly blocked at the intercellular-space of the cortex before arbuscule formation. In rare cases, arbuscules are formed. These observations suggest that *castor* could be required for infection of both epidermal and cortical cells by AM fungi (Bonfante et al., 2000; Novero et al., 2002).

The *CASTOR* and *POLLUX* genes were isolated through positional cloning and by their mutual homology. Using the collection of microsatellite (SSR) markers available for *L. japonicus* (Hayashi et al., 2001), the *CASTOR* and *POLLUX* genes were positioned close to the bottom ends of chromosome 1 and chromosome 6, respectively. Five *castor* alleles were independently mapped to the south end of chromosome 1, close to SSR marker TM0105 (Nakamura et al., 2002). Starting with this marker, a BAC/TAC (Kawasaki and Murakami, 2000; Nakamura et al., 2002) contig was constructed which extended into the telomeric region (Figure 2). Genetic mapping was affected by a 145 kb long inversion between the parental lines B-129 and MG-20 (Kawaguchi et al., 2001) with no recombination events observed upon inspection of 1,833 individuals of five different F2 populations, delimiting the *CASTOR* locus to a region of about 240 kb. PCR-marker TB2R could not be amplified from individuals homozygous for the G00472 or G00716 alleles. PCR and southern blot analysis indicated that both alleles have large deletions of more than 20 kb encompassing the *CASTOR* gene, and subsequent sequence analysis revealed that marker TB2R is located in a *CASTOR* intron.

The *POLLUX* gene was found to co-segregate with SSR marker TM0885. A TAC clone carrying SSR TM0885 was completely sequenced, and a candidate gene with high homology to *CASTOR* was identified (Figure 1).

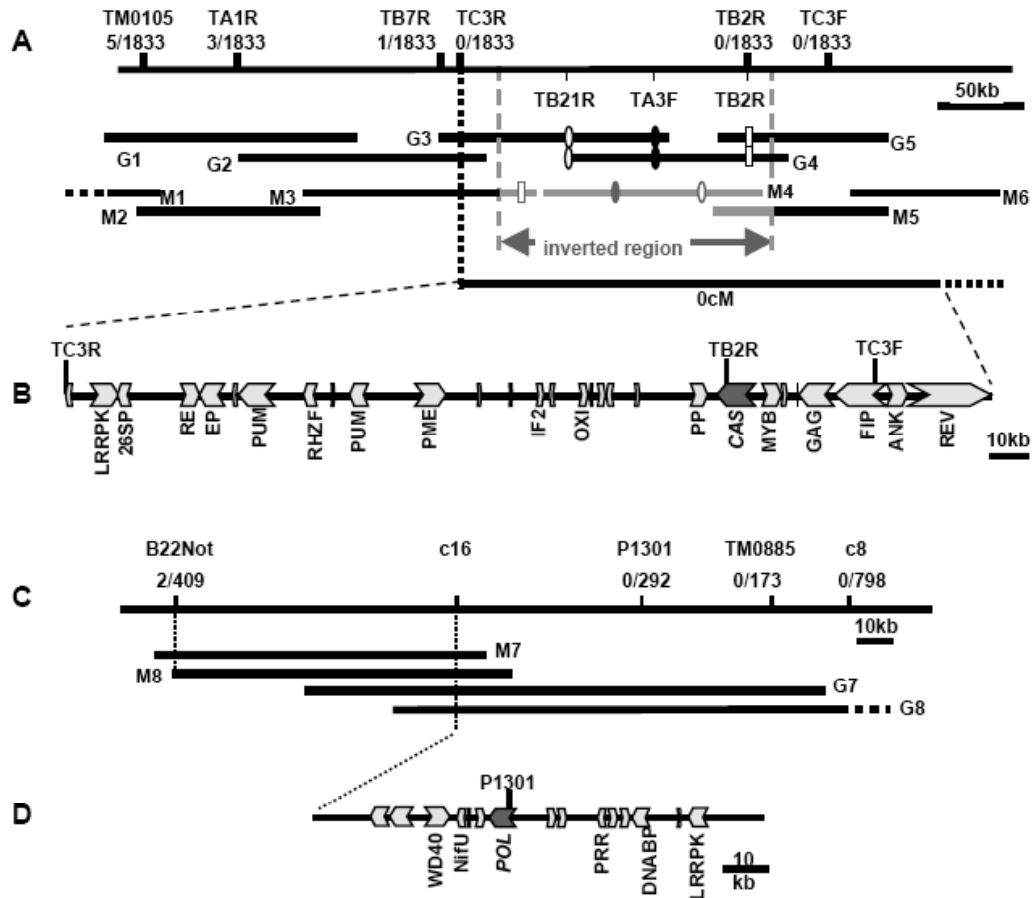


Figure 1. Positional cloning of *CASTOR* and *POLLUX* genes (Imaizumi-Anraku et al., 2005).

(A) Genetic and physical map around the *CASTOR* locus. Positions of flanking markers are indicated together with the number of recombinant plants/total number of mapping individuals. Designations of large insert clones originating from parental ecotype B-129 are; G1, BAC156-1E; G2, BAC124-7B; G3, BAC324-1D; G4, BAC104-3F; G5, BAC33-3E; and from parental ecotype MG-20: M1, LjT17M09; M2, LjT62O06; M3, LjT02K14; M4, LjT45I15; M5, LjT20F11 and M6, LjT46G19. An inverted region of 145kb between the genomes of B-129 and MG-20 was detected, which is probably responsible for the observed suppression of recombination around the *CASTOR* locus (0 cM). BAC end markers within the inverted region are: open oval, TB21R; closed oval, TA3F; open rectangle, TB2R. The TB7R marker located in the north side delimits *CASTOR* to ~240kb. (B) Candidate genes predicted within the target region. LRRPK, leucine-rich repeat receptor kinase; 26SP, 26S proteasome regulatory subunit 7; RE, retro-element; EP, Avr9/Cf-9 elicited protein; PUM, pumilio-family RNA-binding protein; RHZF, Ring H2 zinc finger protein; PME, pectin methyl esterase; IF2, initiation factor 2 subunit; OXI, oxido-reductase; PP, polyprotein; MYB, myb family protein; GAG, gag-pol polyprotein; FIP; VirF-interacting protein FIP1; ANK, ankyrin-like protein; REV; reverse transcriptase; unlabelled, hypothetical protein. (C) Genetic and physical map of the *POLLUX* locus. Positions of the flanking markers and the number of recombinant plants in the mapping populations are indicated. Abbreviations G6, G7, M7, M8 and M9 refer to large insert clones BAC131-3b, BAC45-6C, LjT39N07, LjB22b22 and LjT45B09, respectively. (D) Genes predicted on the cosegregating TAC clone LjT45B09; WD40, WD40 repeat protein; NifU, putatively involved in Fe-S cluster synthesis; PPR, pentatricopeptide repeat protein; DNABP, DNA binding protein; LRRPK, leucine-rich repeat receptor kinase; unlabelled, hypothetical protein.

In the present study, we aim to characterize CASTOR and POLLUX at molecular levels to unravel their role in the early common symbiosis-signalling pathway.

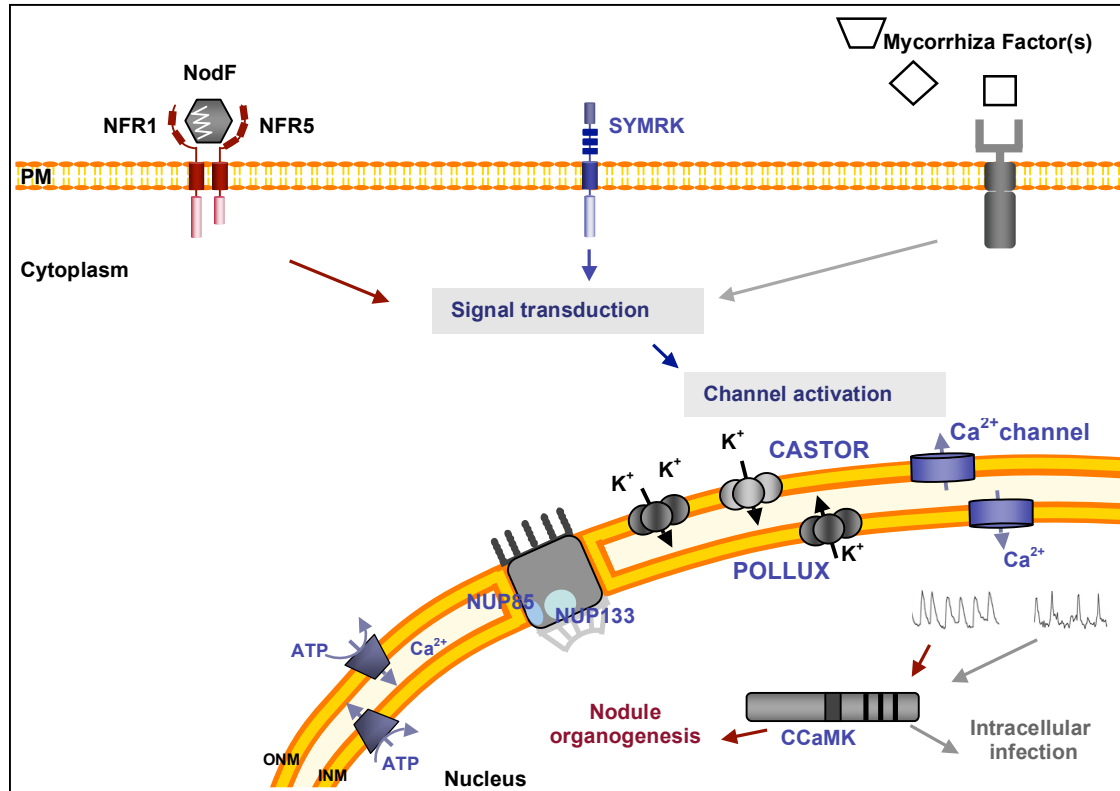


Figure 2. A model for the early symbiosis signalling pathway in the epidermis.

The receptor-like kinases, NFR1 and NFR5, are required for the Nod factor perception, which leads to the generation of the Nod factor-induced calcium spiking *via* at least five common symbiotic components; SYMRK, CASTOR, POLLUX, NUP85 and NUP133. Although no receptor has been cloned, an equivalent receptor-like kinase is presumed to exist for the recognition of mycorrhizal factor which lead to the mycorrhiza-induced calcium spiking *via* the same common symbiotic pathway (Kosuta et al., 2008). The calcium spiking is localized around the nucleus. The calcium storage compartment is believed to be the cisterns of the ER and the nuclear envelope. A yet-to-be identified calcium channel is responsible for the calcium release. The potassium influx triggers by the nuclear-localized cation channels, CASTOR and POLLUX, might compensate for the resulting charge imbalance created by the calcium released. Calcium ATPases are believed to be involved in the replenishment of the calcium storage. The CCaMK positioned downstream of the calcium spiking is believed to be involved in deciphering the calcium traces leading to either nodulation or mycorrhization programming. PM, Plasma membrane; ONM, Outer nuclear membrane; INM, Inner nuclear membrane.

We demonstrate that CASTOR and POLLUX can form two distinct homocomplexes. In electrophysiological assays or yeast complementation experiments, we show that both complexes are cation channels permeable to potassium. We further proved that CASTOR is localized in the nuclear envelope of *L. japonicus* root cells. Therefore, we propose a model in which CASTOR and POLLUX act as counter ion channels that mediate compensation of the charge imbalance associated with the calcium

efflux. Alternatively, and not mutually exclusively, they may modulate the nuclear membrane potential leading to the activation of calcium channels responsible for calcium spiking (Figure 2).

2. Results

2.1 CASTOR and POLLUX identification

Sequencing of genomic DNA in the *CASTOR* and *POLLUX* targets interval identified non-silent mutations within nine *castor* mutants and ten *pollux* mutants, respectively. Additional mutants were identified through Targeted Induced Local Lesions in Genomes (TILLING) (Perry et al., 2003). Twenty-seven and nineteen additional *castor* and *pollux* mutants, respectively, were identified through TILLING and sequencing of candidate genes (Table 2 & 3).

Full-length complementary DNAs (cDNA) sequences corresponding to the *CASTOR* and *POLLUX* genes were obtained (Imaizumi-Anraku et al., 2005). Both genes encompass 12 exons and are subject to alternative splicing, as discovered through sequence analysis of cDNA clones (Figure 3). In total, three *CASTOR* and two *POLLUX* alternative spliced (AS) variants were amplified (Figure 3).

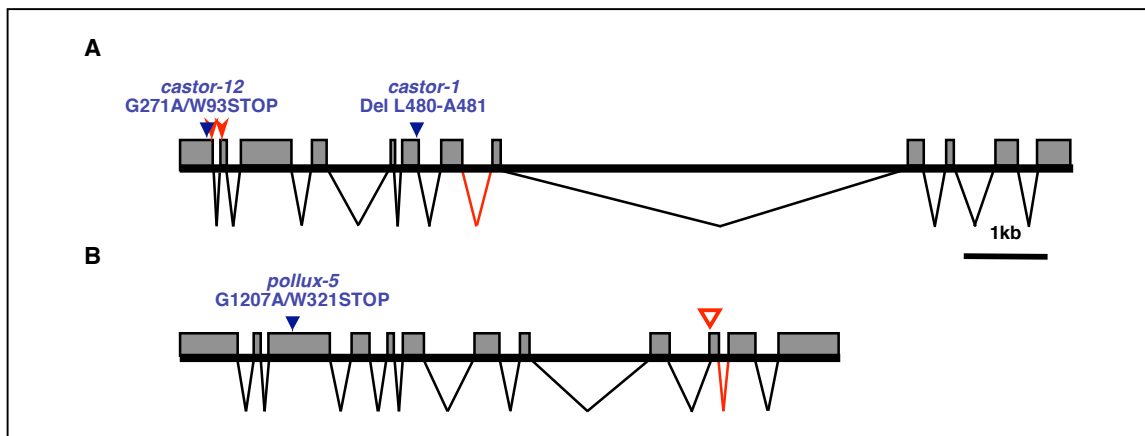


Figure 3. Alternative-spliced variants of *CASTOR* (A) and *POLLUX* (B).

Exons are indicated by upper gray boxes and introns by lower triangles. Alternative-spliced products have been found with the following change; red arrow head: alternative acceptor sites, empty red arrow head: alternative donor sites, red triangle: intron retention. Three *CASTOR* alternative-spliced variants were identified: 4-nt insertion at the 3rd end of the 1st exon, 9-nt insertion at the 5th end of the 2nd exon, retention of the 7th exon leading to a premature stop codon. Two *POLLUX* alternative-spliced variants were identified: 16-nt deletion at the beginning of the 10th exon, and retention of the first 116-nt of intron 10 leading to a premature stop codon. Blue arrow head: position of the mutation in the indicated mutant allele.

Table 2.

List of <i>castor</i> mutant alleles									
Allele	Progenitor/ mutant line	Genomic mutation ^a	Effect	Nodulation phenotype ^b	AM phenotype ^b	Detected by TILLING	Geno- type of M2 plant ^c	Refer- ences	
<i>castor-1</i>	282-227	A ₂₇₇₆ -C ₂₇₈₁ deletion	L ₄₇₉ -A ₄₈₀	-	-			This study	
<i>castor-2</i>	EMS1749	G ₁₀₅₇ to A	A ₂₆₄ to T	-	-	NODPOP	HOM	This study	
<i>castor-3</i>	EMS46	G ₁₆₅₅ to A	G ₃₈₃ to E	-	-	NODPOP	HOM	This study	
<i>castor-4</i>	25-5A	C ₇₇₆ del	Frame shift	-	n.d.			(Imaizumi- Anraku et al., 2005)	
<i>castor-5</i>	24-8B/SL1937-2	G ₃₀₅₃ to A	W ₄₈₃ to stop	-/-	n.d.,-			(Imaizumi- Anraku et al., 2005)	
<i>castor-6</i>	N5	C ₉₆₈₆ to T	P ₆₉₈ to L	-	n.d.			(Imaizumi- Anraku et al., 2005)	
<i>castor-7</i>	N10	G ₈₆₂₃ to A	V ₅₉₈ to I	-	n.d.			(Imaizumi- Anraku et al., 2005)	
<i>castor-8</i>	G00472	> 20 kb deletion	<i>CASTOR</i> deletion	-	n.d.			(Imaizumi- Anraku et al., 2005)	
<i>castor-9</i>	G00716	> 20 kb deletion	<i>CASTOR</i> deletion	-	n.d.			(Imaizumi- Anraku et al., 2005)	
<i>castor-10</i>	G00862	117 bp deletion from exon 4 to intron 4	frame shift	-	n.d.			(Imaizumi- Anraku et al., 2005)	
<i>castor-11</i>	M89-27	T ₁₀₃₇₁ del.	frame shift	-	n.d.			(Imaizumi- Anraku et al., 2005)	
<i>castor-12</i>	SL3251-2	G ₂₇₉ to A	W ₉₃ to stop	-	-	NODPOP	HOM	This study	
<i>castor-13</i>	SL0820 ^d -2,3	G ₂₆₇₂ to A	D ₄₄₄ to N	(-),(-)	(n.d.), (-)	NODPOP, NODPOP	HET, HOM	This study	
<i>castor-14</i>	SL1715-2,3,4,5,6	G ₉₈₇₁ to A	A ₇₆₀ to T	*,-*,*,-*	n.d., -, n.d., n.d., n.d.	NODPOP all in	all HOM	This study	
<i>castor-15</i>	SL1966-3	C ₁₀₁₃ to T	T ₂₄₉ to I	-	-	NODPOP	HOM	This study	
<i>castor-16</i>	SL3160-3	G ₁₆₅₅ to A	G ₃₈₃ to E	-	-	NODPOP	HOM	This study	
<i>castor-17</i>	SL6812-2	G ₃₇₃₈ to A	R ₅₉₀ to H	+/-	-	NODPOP	HOM	This study	
<i>castor-18</i>	KL549	n.d.	n.d.	-	n.d.			(Sandal et al., 2006)	
<i>castor-19</i>	G00532-21	> 20 kb deletion	<i>CASTOR</i> deletion	-	n.d.			(Sandal et al., 2006)	
<i>castor-20</i>	LKL186-4	C ₉₈₂₇ to G	S ₇₄₅ to stop	-	n.d.	NODPOP	HOM	(Sandal et al., 2006)	
<i>castor-21</i>	B32-BA ^e	G ₁₅₉₄ to A	E ₃₆₃ to K	(-)	(+)			(Murray et al., 2006)	
<i>castor-22</i>	S41-1, SL1937-2	G ₃₀₅₃ to A	W ₄₈₃ to stop	(-),-	(+),-			(Murray et al., 2006)	
<i>castor-23</i>	B5-2 ^e	G ₁₆₅₅ to A	G ₃₈₃ to E	(-)	(-)			(Murray et al., 2006)	
<i>castor-24</i>	B68-B ^e	G ₁₀₃₅₃ to A	W ₈₄₀ to stop	(-)	(-)	NODPOP	HET	(Murray et al., 2006)	
<i>castor-25</i>	S46-1 ^{e,f}	G ₁₂₅₁ to A	W ₅₂₈ to stop	(-)	(-)	NODPOP	HOM	(Murray et al., 2006)	
<i>castor-26</i>	SL6908-2	G ₁₀₈₈ to A	G ₂₇₄ to D	-	-	NODPOP	HOM	(Perry et al., ^g)	
<i>castor-27</i>	SL5136-3	G ₁₅₀₃ to A	splice site	-	-	NODPOP	HOM	(Perry et al., ^g)	
<i>castor-28</i>	282-643M1M1M3 ^g	A ₃₂₁₄ to G	D ₅₃₇ to G	n.d.	n.d.	NODPOP	HOM	(Perry et al., ^g)	
<i>castor-29</i>	SL5210-1	G ₉₁₀₅ to A	E ₆₇₂ to K	*	n.d.	NODPOP	HET	(Perry et al., ^g)	
<i>castor-30</i>	SL1415-2,3,4	G ₉₇₈₅ to A	S ₇₃₁ to N	*,*,-*	-,n.d.,n.d.	NODPOP all in	all HET	(Perry et al., ^g)	
<i>castor-31</i>	SL4162-2 ^h / SL5768-3	C ₁₇₂ to G	R ₅₈ to G	(-), +/-*	(-),n.d.			(Perry et al., ^g)	
<i>castor-32</i>	SL6453-2	T ₉₆₀ to A	V ₂₃₁ to V	-	n.d.			(Perry et al., ^g)	
<i>castor-33</i>	SL1371-2	G ₃₄₈₁ to A	intron 7	-	n.d.	NODPOP	HET	(Perry et al., ^g)	
<i>castor-34</i>	SL6077-2	G ₁₉₁₅ to A	intron 4	*	n.d.	NODPOP	HOM	(Perry et al., ^g)	
<i>castor-35</i>	SL1052-1	G ₄₆₈ to A	E ₁₂₂ to K	n.d.	n.d.	NODPOP	HET	(Perry et al., ^g)	
<i>castor-36</i>	SL0818-1	C ₃₃₅₄ to T	intron 7	n.d.	n.d.	NODPOP	HET	(Perry et al., ^g)	

^aThe *CASTOR* genomic sequence is deposited to GenBank under accession number AB162016 and is used as *Lotus japonicus* Gifu reference. Adenine of the ATG initiator codon is designated as position 1. ^bPhenotypes that are scored only in the initial M2 generation are denoted by *; no star stands for additional screening in the M3 generation. In the nodulation phenotype “+/-” designates non-functional symbiosis (e.g. few small white nodules). Annotation in brackets indicate lines harbouring more than one mutation in nodulation genes. ^cGenotype of progenitor or mutant plant in the M2 generation is given as HOM= homozygous or HET=heterozygous. ^dLines SL0820-2,3 carry the mutant alleles *castor-13* and *ccamk-8*. ^eLines contain in addition a *har1-1* mutation. ^fLine S46-1 carries the mutant alleles *castor-25*, *nin-10*, and *har1-1*. ^gLine 282-643M1M1M3 carries the mutant alleles *castor-28*, *ccamk-8*, and *nup85-9*. ^hLine SL4162-2 carries the mutant alleles *castor-32* and *pollux*. ⁱManuscript in preparation.

Table 3.**List of *pollux* mutant alleles**

Allele	Progenitor/ mutant line	Genomic mutation ^a	Effect	Nodulation phenotype ^b	AM phenotype ^b	Detected by TILLING	Geno- type of M2 plant ^c	Re- ference
<i>pollux-1</i>	EMS70	G ₁₁₅₂ to A	G ₃₀₃ to S	-	-	NODPOP	HOM	This study
<i>pollux-2</i>	EMS167	G ₁₁₅₂ to A	G ₃₀₃ to S	-	-	NODPOP	HOM	This study
<i>pollux-3</i>	29-2A	T ₅₆₆₈ to A	L ₈₄₁ to stop	-	n.d.			This study
<i>pollux-4</i>	SL0571-2	C ₄₃₄ to T	S ₁₄₅ to F	-	-	NODPOP	HET	This study
<i>pollux-5</i>	SL3130-2,4	G ₁₂₀₄ to A	W ₃₂₀ to stop	*,-	n.d.,-	both NODPOP	in both HOM	This study
<i>pollux-6</i>	SL5691-3,4	C ₁₂₁₀ to T	S ₃₂₂ to F	+*,-*	n.d., n.d.	both NODPOP	in both HOM	This study
<i>pollux-7</i>	SL1899-2,4	G ₂₃₁₃ to A	G ₅₃₀ to E	+/-,+	n.d., n.d.	both NODPOP	in both HOM	This study
<i>pollux-8</i>	SL0159-2,3,5,6	G ₅₄₈₆ to A	W ₇₈₀ to stop	-*,-*,-	n.d.,n.d.,-,-	all NODPOP	in all HOM	This study
<i>pollux-9</i>	SL0405-2,3,5,6	G ₅₆₃₄ to A	E ₈₃₀ to K	*,-*,-*,*	n.d.,n.d.,n.d.,n. d.	all NODPOP	in all HOM	This study
<i>pollux-10</i>	SL1070-2	G ₆₀₂₁ to A	G ₈₈₂ to S	-	n.d.	NODPOP	HOM	This study
<i>pollux-11</i>	B12-1A ^e	G ₁₂₀₅ to A	W ₃₂₀ to stop	(-)	(-)			(Murray et al., 2006)
<i>pollux-12</i>	B50-C ^c	G ₁₆₄₄ to A	splice site	(+/-)	(-)	NODPOP	HOM	(Murray et al., 2006)
<i>pollux-13</i>	S49-D ^e	G ₅₆₈₂ to A	splice site	(-)	(-)	NODPOP	HOM	(Murray et al., 2006)
<i>pollux-14</i>	Sup3 ^e	C ₄₈₀₄ to T	P ₇₁₉ to L	(-)	(-)	NODPOP	HOM	(Murray et al., 2006)
<i>pollux-15</i>	S24-1B ^g	A ₄₅₈ -C ₄₆₃ del	Q ₁₃₃ -H ₁₅₄ del	n.d.	(+)	NODPOP	HOM	(Murray et al., 2006)
<i>pollux-16</i>	SL5998-2,3,4,5,6	G ₄₉₆ to A	splice site	-*,-*,-*,-*,*	n.d.,-, n.d., n.d., n.d.	all NODPOP	in all HOM	(Perry et al., ^m)
<i>pollux-17</i>	SL1657-2	G ₁₁₄₇ to A	G ₃₀₁ to E	-	-	NODPOP	HOM	(Perry et al., ^m)
<i>pollux-18</i>	SL0317-3 ^h	G ₁₁₇₉ to A	G ₃₁₂ to S	(+*)	n.d.	NODPOP	HET	(Perry et al., ^m)
<i>pollux-19</i>	SL5821-3,5	G ₁₆₄₄ to A	splice site	-*,*	n.d.,-	both NODPOP	in both HOM	(Perry et al., ^m)
<i>pollux-20</i>	SL0729-6,10	G ₃₃₈₈ to A	W ₆₅₁ to stop	*,-*	-,-	both NODPOP	in both HOM	(Perry et al., ^m)
<i>pollux-21</i>	SL1075-2	G ₃₄₁₆ to A	splice site	-	-	NODPOP	HOM	(Perry et al., ^m)
<i>pollux-22</i>	SL0283-4	G ₄₆₉₈ to A	E ₆₈₄ to K	n.d.	n.d.	NODPOP	HET	(Perry et al., ^m)
<i>pollux-23</i>	SL4162-2 ⁱ	C ₃₄₁ to T	T ₁₁₄ to I	(-)	(-)	NODPOP	HOM	(Perry et al., ^m)
<i>pollux-24</i>	SL1913-7,8 ^k	C ₁₉₂₂ to T	intron 4	(+),-*	(+), n.d.	both NODPOP	in both HET	(Perry et al., ^m)
<i>pollux-25</i>	SL5546-2,3	C ₃₅₆₈ to T	intron 8	+*,+*	n.d.	both NODPOP	in both HET	(Perry et al., ^m)
<i>pollux-26</i>	SL0405-4	G ₂₈₃₇ to A	intron 6	-*	n.d.	NODPOP	HET	(Perry et al., ^m)
<i>pollux-27</i>	SL0299-2	G ₂₆₇₂ to A	intron 6	-*	n.d.	NODPOP	HOM	(Perry et al., ^m)
<i>pollux-28</i>	SL0456-2 ^l	T ₅₈₉₇ to G	intron 11	(+)	n.d.	NODPOP	HET	(Perry et al., ^m)
<i>pollux-29</i>	SL0387-3	G ₄₆₄₆ to A	L ₆₆₆ to L	-*	n.d.	NODPOP	HOM	(Perry et al., ^m)

^aThe *POLLUX* genomic sequence is deposited to GenBank under accession number AB162017 and is used as *Lotus japonicus* Gifu reference. Adenine of the ATG initiator codon is designated as position 1.

^bPhenotypes that are scored only in the initial M2 generation are denoted by *; no star stands for additional screening in the M3 generation. In the nodulation phenotype “+/-” designates non-functional symbiosis (e.g. few small white nodules). Annotation in brackets indicate lines harbouring more than one mutation in nodulation genes.

^cGenotype of progenitor or mutant plant in the M2 generation is given as HOM= homozygous or HET=heterozygous.

^d*pollux-1* and *pollux-2* are the same allele

^eLines contain in addition a *har1-1* mutation

^f*pollux-12* and *pollux-19* are the same

^gLine S24-1B carries the mutant alleles *pollux-15* and *symrk-28*

^hLine SL0317-3 carries the mutant alleles *nup133-14* and *pollux-18*

ⁱLine SL4162-2 carries the mutant alleles *castor-32* and *pollux-23*

^kLine SL1913-7 carries the mutant alleles *pollux-24* and *symrk-60*

^lLine SL0456-2 carries the mutant alleles *nfr1-5* and *pollux-28*

^mManuscript in preparation

To ascertain the role of these AS in the symbiosis process, we tested whether *CASTOR* and *POLLUX* cDNA under the regulation of the cauliflower mosaic virus 35S promoter (*P35S*) can mediate nodulation and arbuscule formation in *castor-12* and *pollux-5* mutants, respectively (Table 2, Table 3 and Figure 3). In both *castor-12* and *pollux-5* mutants, a guanosine residue is mutated to an adenosine leading to premature termination codons (PTCs) at the positions W93 and W321, respectively. The PTCs are produced before any alternative splicing sites, depleting the mutant of AS variants (Figure 3). Transgenic roots of the *castor-12* and *pollux-5* plants carrying *CASTOR* and *POLLUX* full-length cDNA, respectively, formed pink nodules after 5 weeks inoculation with *M. loti* (Table 4). *Castor-12* and *pollux-5* are also impaired in AM. *CASTOR* and *POLLUX* full-length cDNA restored the AM defect in transgenic roots of this line (Table 4). All together, the results confirm the identification of *CASTOR* and *POLLUX* and demonstrate that *CASTOR* and *POLLUX* full-length cDNA are sufficient to support both fungal and bacterial endosymbiosis in *L. japonicus* without AS variants.

Table 4.

Restoration of root nodules symbioses in <i>L. japonicus castor-12</i> and <i>pollux-5</i> mutants				
Plant genotype	Transgene	Nod +	Nodule/Nodulated plant	AM +
<i>L. japonicus</i> wild-type	marker only*	30/30	13.0	15/15
<i>pollux-5</i>	<i>POLLUX</i>	45/45	12.2	8/8
<i>pollux-5</i>	marker only*	0/30	0	0/6
<i>castor-12</i>	<i>CASTOR</i>	24/24	11.4	10/10
<i>castor-12</i>	marker only*	0/18	0	0/10

Numbers refer to *A. Rhizogenes* root systems of *L. japonicus* mutants or wild-type. Nod +, number of root systems showing nodules containing bacteria; AM +, number of roots system showing AM 2 weeks after inoculation with *Glomus intraradices* BEG 195 on nodulated plants; *Plants transformed with the binary vector pH7WG2D (Karimi et al., 2002) lacking *CASTOR* and *POLLUX* expression cassettes.

2.2 Sequence analyses

CASTOR and *POLLUX* are two homologous genes which share 62.6% identity. Southern blot experiment indicates that *CASTOR – POLLUX* homologues exist in one or two copies in other dicotyledonous and monocotyledonous plants including *Medicago truncatula*, *Pisum sativum*, *Glycin max*, *Arabidopsis thaliana* and *Oryza sativa*

(Imaizumi-Anraku et al., 2005). BLASTN searches of National Center for Biotechnology Information (NCBI) identified expressed sequence tags (ESTs) in the same species for both *CASTOR* and *POLLUX*, confirming that the sequence homologues represent expressed genes. BLASTP searches of NCBI non-redundant protein sequences databases predicted homologs in the same monocotyledonous and dicotyledonous species as well as more distant homologs in the moss *Physcomitrella patens*. *CASTOR*- and *POLLUX*-related sequences were not identified in the full sequence genomes of animals, fungi, or green algae. However, relative close homologs were identified in bacteria genera, namely *Nocardiodes sp.* JS61, *Mesorhizobium loti* and *Streptomyces ambofaciens*.

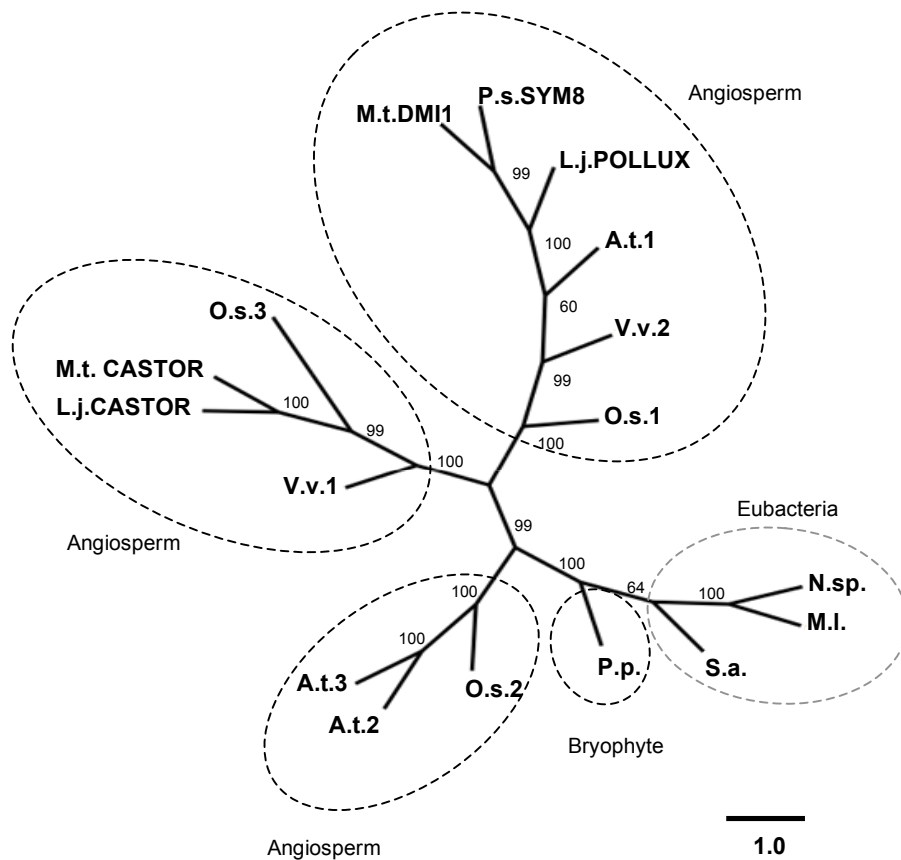


Figure 4. Unrooted radial phylogenetic tree of *CASTOR* and *POLLUX* homologs.

Homologous full-length protein sequences with E value $\leq 10^{-41}$ were aligned using ClustalX and MacClade programs. The protein tree was constructed using the consensus parsimony method (PHYLIP 3.67 program). Percentage bootstrap support based on 1000 replicates is given to the side of each branch. L.j., *Lotus japonicus*; M.t., *Medicago truncatula*; A.t., *Arabidopsis thaliana*; O.s., *Oryza sativa*; V.v., *Vitis vinifera*; P.p., *Physcomitrella patens*; S.a., *Streptomyces ambofaciens*; N.sp., *Nocardiodes sp.*; M.l., *Mesorhizobium loti*; P.s., *Pisum sativum*. L.j. *CASTOR*, gi:62286596; L.j. *POLLUX*, gi:62287141; O.s.1, gi:115441303; O.s.2, gi:115456529; O.s.3, gi:125546404; M.t.DMI1, gi:62286545; P.s.SYM8, gi:161105392; V.v.1, gi:157353778; V.v.2, gi:157354359; A.t.1, gi:186530826; A.t.2, gi:186519621; A.t.3, gi:30679833; P.p., gi:168003777; S.a., gi:117165168; N.sp., gi:119714272; M.l., gi:13471039; MtCASTOR, gi:57494651. Bar: number of amino acid substitution per site between two sequence.

Phylogenetic analyses using a character-based method, the parsimony analysis, were conducted with PHYLIP to ascertain the relationship of CASTOR and POLLUX to other homologous proteins. Analyses of full-length proteins from plants, moss and bacterial species yielded four well-supported clades corresponding to three orthologous groups of plant proteins and a single group of bacterial proteins (Figure 4).

CASTOR and POLLUX have 28% and 31% identity, respectively, with the deduced partial protein *Physcomitrella patens*, which is consistent with an origin in the nonvascular plants. Taken together with the absence of homologs in the fungal, animal and green algal lineages, these results suggest that the CASTOR and POLLUX proteins represent a plant specific innovation that potentially arose near the base of the land plant lineage. The relationship between the prokaryotic sequence and the eucaryote derivative is difficult to deduce from the limited prokaryotic sequence data. On the one hand, the weak sequence identity between the bacterial and moss proteins (< 20%) suggests that the plant and bacterial proteins date back to a primordial precursor. On the other hand, the absence of homologs in archaea and green algae may suggest a horizontal gene transfer between an ancient plant genome(s) and a bacterial species.

CASTOR and *POLLUX* encode predicted integral membrane proteins of 853 and 917 amino acids, respectively, with at least four transmembrane regions (Figure 5A). Overall, the two proteins are very similar to each other with the exception of the N-terminal regions which are more divergent (Figure 5A). Other than these general features, *CASTOR* and *POLLUX* lack similarity to functionally characterized proteins. The middle region of each protein includes a domain of unknown function (DUF) 1012 found in both eukaryotes and bacteria (Figure 5A). The *POLLUX* DUF1012 domain overlaps with a region of low, but global similarity to the TrkA-N domain, a nicotinamide adenine dinucleotide (NAD) binding domain, found in a wide variety of proteins, including potassium channel, phosphoesterases and various other transporters (Schlosser et al., 1993). Similarly, the *CASTOR* DUF1012 domain overlaps with a predicted NAD(P) binding domain. Overlapping with the two transmembrane domains (TM) and the putative NAD binding domain, a PRK10537 domain is predicted in both *CASTOR* and *POLLUX* (Figure 5A).

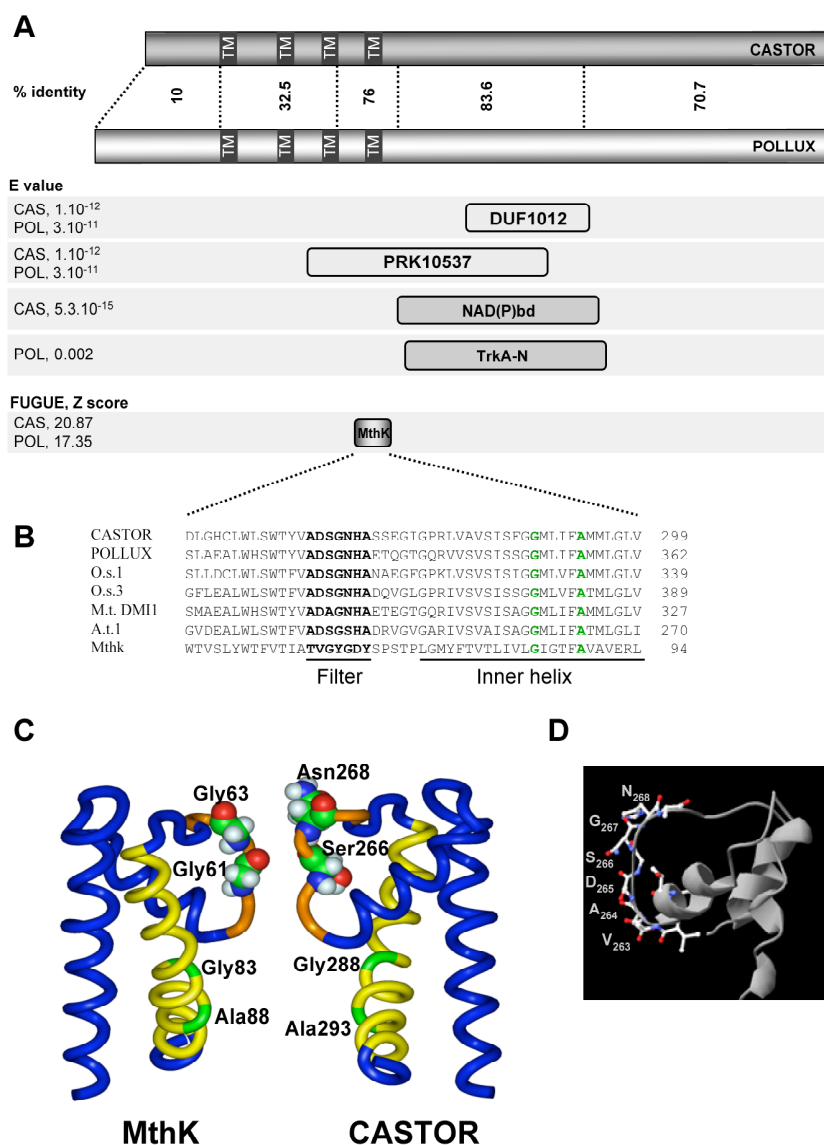


Figure 5. Sequence analyses of CASTOR and POLLUX.

(A) Prediction of conserved domains in CASTOR (853 a.a.) and POLLUX (918 a.a.) were conducted with the programs: Membrane Protein Explorer 3.0 to predict transmembrane domains (TM), NCBI/BlastP to predict domain of unknown function (DUF) 1012, TrkA-N (PF02254) and PRK10537, EMBL/InterProScan to predict NAD(P)bd, and FUGUE to predict the partial sequence-structure homolog *Methanobacterium thermoautotrophicum* calcium-gated potassium channel MthK (027564). (B) Alignment of the filter and inner helical region of the MthK channel with the structural homologous region of CASTOR, POLLUX and plant homologues. This region of MthK forms the core of the pore predicted in (C). (C) X-ray crystal structure of the ion pore region of the MthK channel (Protein Data Bank code 1LNQ), and a model of the homologous region in CASTOR. The filter region is coloured orange: inner helices are coloured yellow. Residues Gly61 and Gly63 in the MthK structure, and the corresponding Ser and Asn residues in CASTOR, are shown in space-filling mode. Conserved residues Gly83 and Ala88 in the inner helix are highlighted in green. (D) Model of the ion pore region of one CASTOR monomer. Amino acid residues constituting the selectivity filter are labeled with the carbonyl oxygen backbone facing the pore. Red: oxygen atoms, blue: amino groups, white: carbon atoms.

The PRK10537 domain is typically conserved in proteobacteria voltage-gated potassium channels. However, CASTOR and POLLUX sequences do not include any voltage sensor domains which are characterized by positively charged residues periodically aligned in transmembrane segments (Bezanilla, 2000). Search based on sequence-structure homology using FUGUE (Shi et al., 2001) resulted in low structural matches to the calcium-gated potassium channel of *Methanobacterium thermoautotrophicum*, MthK, for which a crystal structure has been resolved (Jiang et al., 2002a) (Figure 5A). CASTOR and POLLUX share a structural homology only with a short stretch of MthK sequence covering the pore region, which includes the filter and the inner helix (Figure 5B). Alignment of the pore region of MthK with CASTOR, POLLUX and plant homologues revealed that two important residues of the inner helix, Gly83 and Ala88, are conserved (Figure 5B). Both Gly83 and Ala88 are involved in the mechanics of MthK pore gating. The Gly83 confers the flexibility to the helix to bend and Ala88 constitutes the narrowest point in the intracellular entryway (Jiang et al., 2002b). Despite these similarities between MthK and CASTOR-POLLUX, the potassium signature, TxGYG (Heginbotham et al., 1994), which confers to MthK its potassium selectivity, is not conserved (Figure 5B). Homology modelling of the filter region of CASTOR indicates that the differences could result in a more helical backbone, and this would modify the diameter and the electrostatic properties of the pore (Figure 5C). However, the carbonyl oxygen backbone facing the pore is conserved between MthK and CASTOR, suggesting a cation selectivity (Figure 5D). Nevertheless, the absence of the highly conserved potassium signature sequence and the low structural homology between either protein and MthK left the function totally unclear and prompted us to study the biochemical and electrophysiological properties of CASTOR and POLLUX.

2.3 Nuclear localization of CASTOR and POLLUX

CASTOR and POLLUX are predicted to carry potential chloroplast transit peptides of 69 and 57 amino acids at their N-termini (TargetP scores 0,953 and 0,959), respectively. Although TargetP (<http://www.cbs.dtu.dk/services/TargetP/>) predicted a plastid

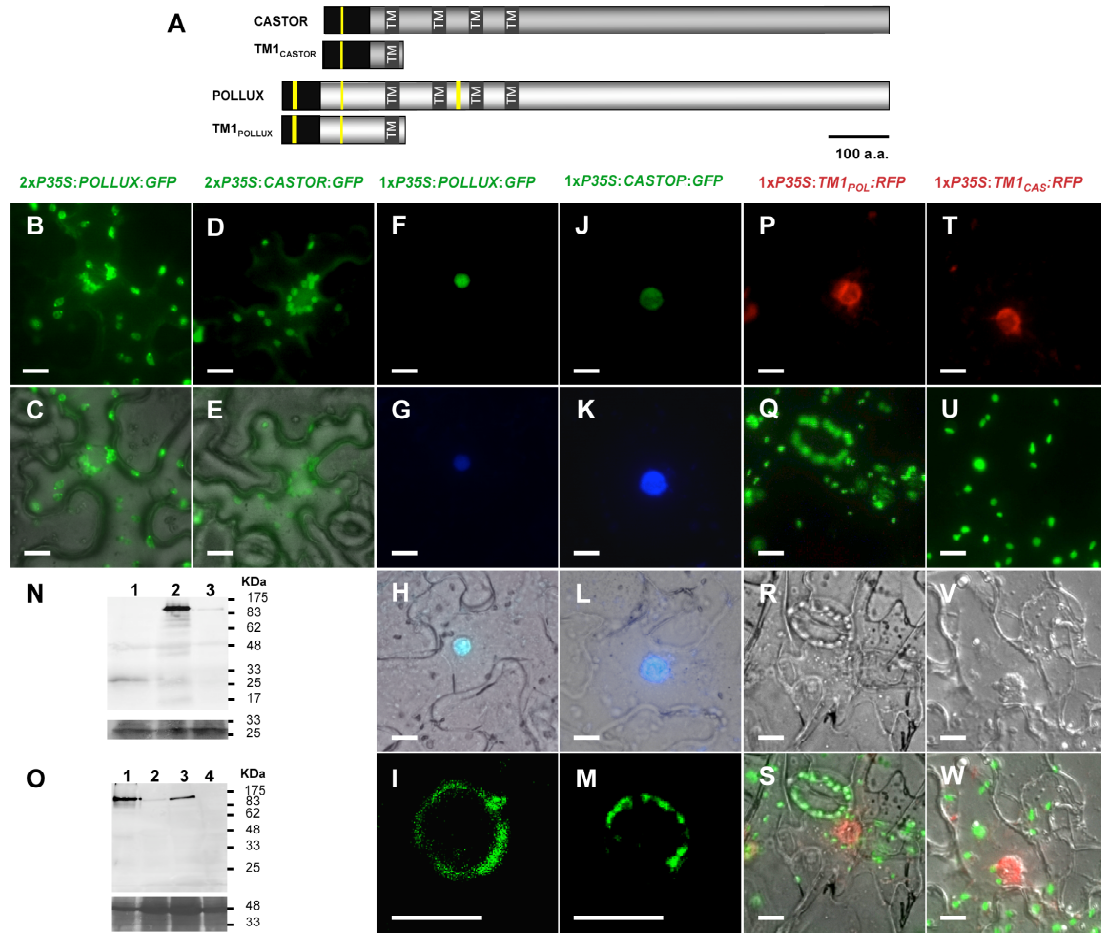


Figure 6. Localization in tobacco leaf epidermal cells of CASTOR and POLLUX.

(A) Representation of CASTOR, POLLUX and truncated versions. TM, Transmembrane domain; yellow line, nuclear localisation signals of CASTOR (HRRR) and POLLUX (left to right PPLKKT, RKRR, PLKKRVA); black boxes, potential chloroplast transit peptide. (B) and (D) Microscopic pictures of leaf epidermal cells expressing a POLLUX:GFP fusion and (D) and (E) a CASTOR:GFP fusion under the control of a double cauliflower mosaic virus 35S promoter (2xP35S). (F) to (I) Confocal laser scanning images of tobacco leaf epidermal cells transiently expressing a POLLUX:GFP fusion and (J) to (M) a CASTOR:GFP fusion under the control of a single cauliflower mosaic virus 35S promoter (1xP35S). (F) and (J) GFP fluorescence, (G) and (K) 4', 6-diamidino-2-phenylindole (DAPI), (H) and (L) GFP, DAPI and Bright field merged, (I) and (M) Confocal microscopic images of individual optical sections of GFP fluorescence. (P) to (S) Microscopic pictures of leaf epidermal cells expressing the TM1_{POL}:RFP fusion, and (T) to (W) a TM1_{CAS}:RFP fusion under the control of a single cauliflower mosaic virus 35S promoter (1xP35S). (P) and (T) RFP fluorescence, (Q) and (U) control leaf epidermal cells expressing N-terminal of the signal peptide of spinach ferredoxin NADP(H) oxidoreductase, a thylakoid bound enzyme (FNR) fused to GFP, (R) and (V) bright field, (S) and (W) RFP, GFP and Bright field merged. Bars = 10 mm. (N) Detection of 2xP35S:CASTOR:GFP and 2xP35S:POLLUX:GFP, and (O) 1xP35S:CASTOR:GFP and 1xP35S:POLLUX:GFP fusion proteins in tobacco by immunoblot. (N) Total protein extracts from leaves expressing GFP alone (1), POLLUX:GFP (2) and CASTOR:GFP (3). (O) Total protein extracts from leaves expressing POLLUX:GFP (1) and CASTOR:GFP (2-3) and empty vector (4). Top panel: immunoblot with anti-GFP. Lower panel: Coomassie stained blot.

localization for CASTOR and POLLUX, Wolf PSORT and Prosite (<http://wolfsort.seq.cbrc.jp/>; <http://www.expasy.org/prosite/>) predicted three and one putative nuclear localization signal (NLS) within CASTOR and POLLUX sequences, respectively (Figure 6A). Moreover, in addition to the predicted NLS, the subprediction methods SVMaac of MultiLoc/TargetLoc (<http://www-bs.informatik.uni-tuebingen.de/Services/MultiLoc/>) reveals that CASTOR and POLLUX may have the properties to be targeted in plastid (SVMaac scores, CASTOR; 0.94 and POLLUX; 0.88) or in the ER (SVMaac scores, CASTOR; 0.68 and POLLUX; 0.63).

In order to determine the localization of CASTOR and POLLUX in *planta*, both *CASTOR* and *POLLUX* fused to the green fluorescent protein (GFP) were transiently expressed under the control of cauliflower mosaic virus 35S promoter (*P35S*) via particle bombardment in onion epidermal and pea root cells (Imaizumi-Anraku et al., 2005). In these expression systems, both CASTOR and POLLUX displayed plastid localization patterns (Imaizumi-Anraku et al., 2005). The plastid localization was further confirmed with *CASTOR* and *POLLUX* expressed under the control of double *P35S* in *Nicotiana benthamiana* leaves via *Agrobacterium tumefaciens* mediated transformation (Figure 6R to 6U). As a marker for the plastid localization, the transit peptide of spinach ferredoxin NADP(H) oxidoreductase, a thylakoid bound enzyme (FNR) (Lohse et al., 2005) was cloned and fused to the GFP (Figure 6C and 6G). Surprisingly, *CASTOR* and *POLLUX* expressed under the control of a single *P35S* in *Nicotiana benthamiana* leaves via *Agrobacterium tumefaciens* mediated transformation displayed a localization in the nuclear envelope (Figure 6J to 6Q). In all experiments, the expression of the full length CASTOR and POLLUX was detected by immunoblot with anti-GFP excluding a possible localization of truncated proteins or free GFP (Figure 6V and 6W). To assess whether CASTOR and POLLUX N-termini sequences containing both the predicted chloroplast transit peptides and first NLS would localize the proteins in the plastid or in the nuclear periphery, we generated additional fusion between the red fluorescent protein (RFP) and N-terminal fragment encompassing the first 139 amino acids and 208 amino acids of CASTOR and POLLUX (TM1_{CASTOR}:RFP and TM1_{POLLUX}:RFP), respectively (Figure 6A). In *Nicotiana benthamiana* leaves, for both TM1_{CASTOR}:RFP and TM1_{POLLUX}:RFP expressed under a single *P35S*, the red fluorescence was observed at the periphery of nuclei (Figure 6B and 6F). No colocalization of either TM1_{CASTOR}:RFP or

TM1_{POLLUX}:RFP with the plastid control (FNR:GFP) could be observed (Figure 6E and 6I), confirming an exclusive localization of TM1_{CASTOR}:RFP and TM1_{POLLUX}:RFP in the nuclear rim. These results indicate that the N-termini sequences of CASTOR and POLLUX contain active nuclear localization signals sufficient to target the protein to the nuclear rim under the expression straight of a single *P35S*. However, when *CASTOR:GFP* and *POLLUX:GFP* are expressed under the control of double *P35S*, the green fluorescence was observed in plastids which all together demonstrate that entirely different localization patterns are detectable in transient assays.

In order to assess the localization in *L. japonicus* root cells and to exclude possible artefacts associated with the transgenic expression of fusion proteins, we targeted the endogenous proteins using specific antibodies. Rabbit polyclonal antibodies were raised against hydrophilic peptides of CASTOR and POLLUX. In immunoblots, the purified CASTOR antibodies allowed a specific detection of CASTOR (Figure 7A), whereas the POLLUX antibody was unspecific (data not shown). The immunogold labelling with anti-CASTOR was performed on wild type *L. japonicus* and on *castor-12*, a mutant carrying a single point mutation leading to a premature stop codon at position W93 (Table 2). By electron microscopical analysis of immunogold labelled sections, a strong and specific accumulation of gold particles was observed at the position of the nuclear envelope of the wild type. This labelling was absent in samples of the *castor-12* mutant (Figure 7B to 7E). The separation of the membranes was not well preserved by the immunolocalization compatible embedding method used. Therefore, we could not determine whether CASTOR resides in the inner or outer membrane of the nuclear envelope, or in both. Only non-specific background labelling was observed in plastids in both wild type and *castor-12* (Figure 7B). Collectively, these data provide evidence for a localization of CASTOR in the nuclear envelope.

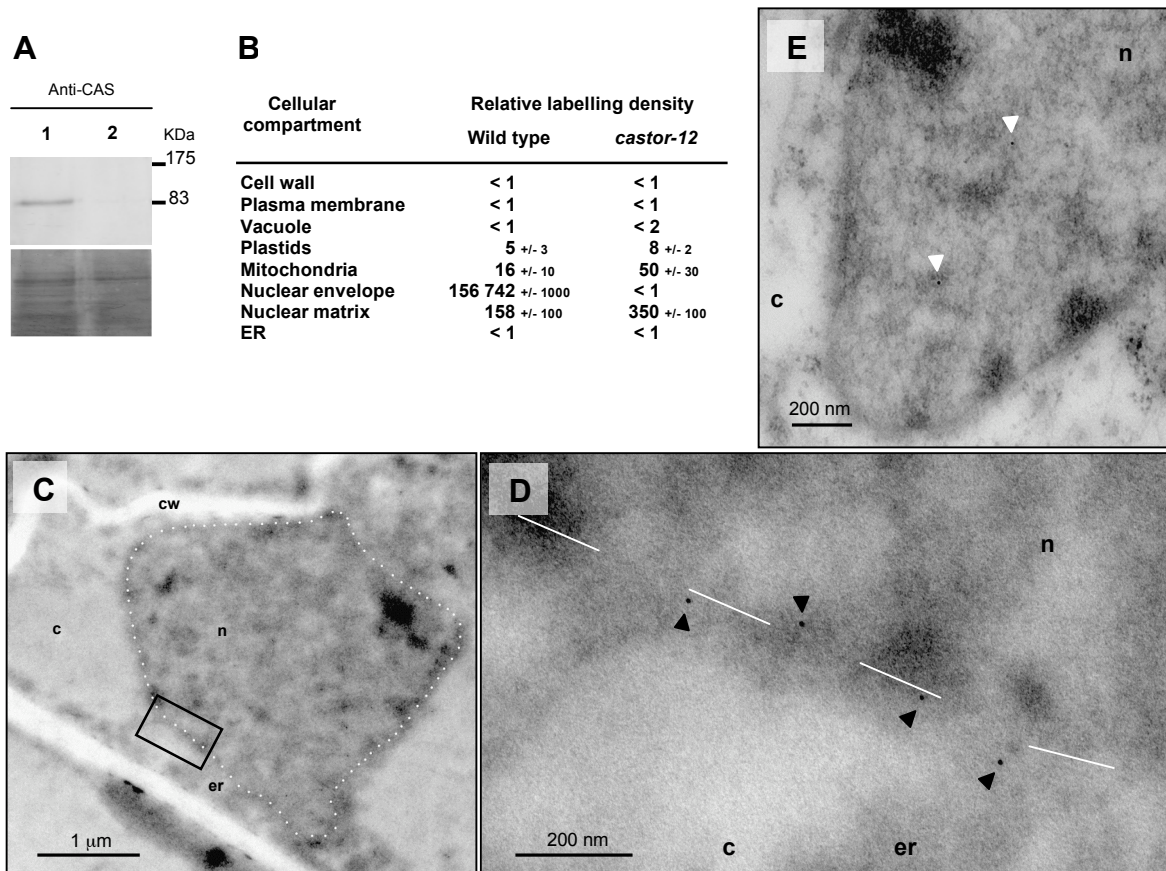


Figure 7. Immunogold localization of CASTOR in *Lotus japonicus* with anti-CASTOR.

(A) Immunoblot detection with anti-CASTOR in total extract of transformed roots of *Lotus japonicus* mutant *castor-12* (W93*). 1; *castor-12* complemented with *P35S:CASTOR* via *A. rhizogenes* hairy root transformation, 2; *castor-12* transformed roots with empty vector as negative control, lower panel; loading shown by Coomassie staining of the blot.

(B) Relative density of gold particles in different cellular compartments of *L. japonicus* Gifu wild type and mutant *castor-12* roots after immunogold labelling with anti-CASTOR.

(C) to (E) Electron microscopic pictures of *L. japonicus* Gifu wild type nucleus (C) and *castor-12* nucleus (E). (D) Zoom of the black box of picture (C). Dashed white line: delimitation of the nuclear envelopes. c cytoplasm; cw, cell wall; n, nucleus; er, endoplasmic reticulum. Black arrowheads mark positive immunodetection of CASTOR. White arrowheads mark background labelling in the nuclear matrix.

2.4 Homodimerization of CASTOR and POLLUX

One common feature of ion channels is their organization in homo- or hetero-tetrameric complexes of identical or similar subunits, respectively (Christie, 1995). We checked the potential of the C-terminal soluble domains of CASTOR (cCASTOR; H322-E853) and POLLUX (cPOLLUX; H386-D917) to form homo- or heteromers. In yeast-two-hybrid assays, cCASTOR and cPOLLUX were each capable of self-interaction (Figure 8A). The interaction between POLLUX and CASTOR was only observed using cCASTOR fused to the GAL4 activator domain (AD) and cPOLLUX to the GAL4 binding domain (BD), but never when cCASTOR and cPOLLUX were fused to BD and AD, respectively (Figure 8A). To assess the specificity of AD:cCASTOR interaction, we mutated *cCASTOR* according to a series of *castor* mutant alleles carrying a point mutation or deletion (Table 2). Five *ccastor* mutant versions, *ccastor-1* (Δ LA 479-480), *ccastor-7* (V598I), *ccastor-13* (D444N), *ccastor-17* (R590H) and *ccastor-28* (D537G), were tested for cCASTOR dimerization in yeast-two-hybrid assays. AD:cCASTOR and BD:*ccastor-1*, expressed in yeast (Figure 8B), did not interact indicating that interactions of AD:cCASTOR with either BD:cCASTOR or BD:cPOLLUX were specific (Figure 8C). Furthermore, the AD:cPOLLUX dimerization was tested with two mutant versions, *cpollux-7* (V531E) and *cpollux-8* (W781*) (Table 3), (Figure 8D). AD:cPOLLUX and BD:*cpollux-8*, expressed in yeast (data not shown), did not interact, demonstrating the specificity of POLLUX dimerization, as well as the requirement of a full C-terminal sequence for interaction. All together, these results demonstrate that cCASTOR and cPOLLUX can homo-dimerize. Furthermore, the homo-dimerization requires their C-termini domains.

To address the question of CASTOR and POLLUX hetero- or homo-dimerization in *planta*, we used a bimolecular fluorescence complementation (BiFC) approach in tobacco epidermal cells (Figure 9A). The full length *CASTOR* and *POLLUX* were fused to either the N- or C-terminal half of the yellow fluorescent protein (*YFP*) gene. The expression of all fusion proteins was confirmed by immunoblots (Figure 9B). All BiFC *CASTOR* and *POLLUX* fusion constructs complemented *L. japonicus castor* or *pollux* mutant alleles, respectively, suggesting that these constructs are functional (Table 5). In line with the yeast-two-hybrid and localization results, the YFP fluorescence due to the full-length *CASTOR* or *POLLUX* self-interactions was clearly observed around the nucleus and the latter was abolished by the *castor-1* mutation (Figure 9A). Although AD:cCASTOR and

BD:cPOLLUX interact in yeast, the heterodimerization of CASTOR and POLLUX, both tested either in fusion with the N- or C-terminal half of the YFP, was never seen in tobacco epidermal cells (Figure 9A, data not shown). All together, these observations suggest that, in *planta*, CASTOR and POLLUX form two distinct complexes for which the assembly involves the C-terminal region of the proteins.

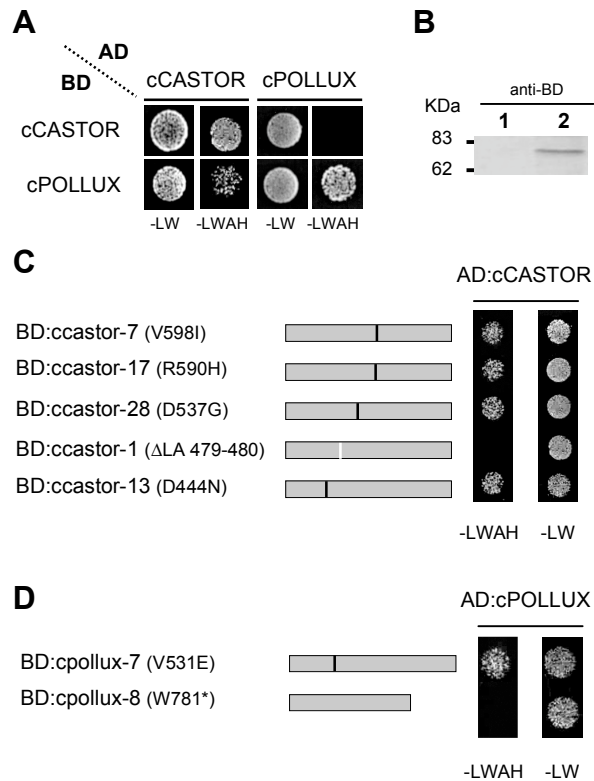


Figure 8. Yeast-two-hybrid assay for interactions of cCASTOR and cPOLLUX.

(A) Interaction assays were performed in the yeast strain AH109 cotransformed with the bait (BD) and prey (AD) vectors containing either cCASTOR (H322-E853) or cPOLLUX (H386-D917). The cotransformants and interacting partners were analysed on synthetic dropout nutrient medium lacking leucine and tryptophan (-LW), and lacking leucine, tryptophan, adenine and histidine (-LWAH), respectively. (B) Expression analyses of BD:cCASTOR Δ LA 479-480 by immunoblot. Total extract from yeast transformed with empty vector (1) and vector expressing BD: cCASTOR Δ LA 479-480 (2). (C) Yeast-two-hybrid interaction analyses of ccastor mutant versions. All tested mutations originate from symbiosis-defective *castor* mutant alleles; castor-1 (Δ LA 479-480), castor-7 (V598I), castor-13 (D444N), castor-17 (R590H) and castor-28 (D537G) (Table 2). (D) Yeast-two-hybrid interaction analyses of cpollux mutant versions. All tested mutations originate from symbiosis-defective *pollux* mutant alleles; pollux-7 (V531E) and pollux-8 (W781*) (Table 3). Dark line; single amino acid change, White line; deletion.

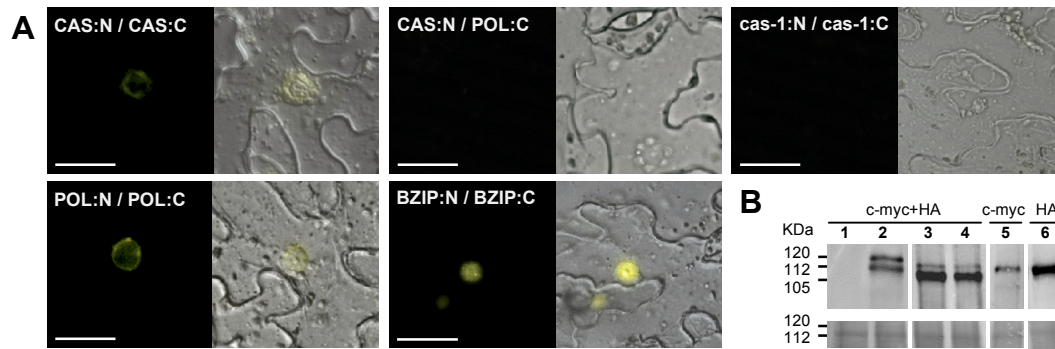


Figure 9. Formation of CASTOR and POLLUX homocomplexes in planta.

(A) BiFC analysis of CASTOR (CAS) and POLLUX (POL) interaction in transiently transformed *N. benthamiana* leaf epidermal cells. CASTOR and POLLUX driven by the cauliflower mosaic virus 35S promoter were fused to the N-terminal half of yellow fluorescent protein (YFP) and a c-myc tag (N), or to the C-terminal half of YFP and a HA tag (C). Self-interactions between CASTOR Δ LA-479-480 (cas-1) and the nuclear localized transcription factor bZIP63 (BZIP) from *A. thaliana* were used as negative and positive controls, respectively. The experiment was visualized with an inverted epifluorescence microscope. Left panel: YFP fluorescence, right panel: bright field and YFP fluorescence merged. Bars = 20 μ m. (B) Protein expression analysis by immunoblot. The protein extracts from leaves transiently transformed with empty vector (1), or vectors expressing POL:C and POL:N (2), CAS:C and CAS:N (3), cas-1:N and cas-1:C (4), CAS:N and POL:C (5), CAS:N and POL:C (6) were analyzed. Expected sizes of POLLUX: 102 kDa, CASTOR: 95 kDa, N-terminal half of the yellow fluorescent protein fused to c-myc tag (N): 18 kDa, C-terminal half of the yellow fluorescent protein fused to HA tag (C): 10 kDa. Top panel: immunoblot. Lower panel: Coomassie stained blot documenting protein loading.

Table 5. Restoration of Root Nodule Symbioses in *A. rhizogenes*-transformed root systems of *L. japonicus* mutants *pollux-2* and *castor-12* with the different *POLLUX* and *CASTOR* split YFP versions, respectively.

Plant genotype	Transgene	Fraction of nodulated plants	Nodule / nodulated plants
wild type	35S:N	32/49	4.6
wild type	35S:C	28/30	4.1
<i>pollux-2</i>	35S:N	0/89	0
<i>pollux-2</i>	35S:POL:N	30/57	4.2
<i>pollux-2</i>	35S:POL:C	43/72	3.8
<i>castor-12</i>	35S:N	0/64	0
<i>castor-12</i>	35S:CAS:N	59/85	3.4
<i>castor-12</i>	35S:CAS:C	54/78	5.1

2.5 Expression of *POLLUX* and *DMII* under the control of *P35S* restores the nodulation phenotype of *castor-12* mutant

Both CASTOR and POLLUX are two complexes formed by homo-units assembling. The expression level of *CASTOR* and *POLLUX* mRNA in root, nodule, leaf, seed pod and flower bud was examined by quantitative RT-PCR (Imaizumi-Anraku et al., 2005). *CASTOR* and *POLLUX* were both constitutively expressed. *M. loti* inoculation or Nod-factor treatment did slightly repress the expression of *CASTOR* and *POLLUX* genes during the first two days (Imaizumi-Anraku et al., 2005). To determine the spatial expression pattern of *CASTOR* and *POLLUX* in *L. japonicus* roots before and after *M. loti* inoculation, we used the β -glucuronidase (*GUS*) reporter gene fused with a 5'-upstream region of 2.3kb and 2.8kb for *CASTOR* and *POLLUX*, respectively. In *A. rhizogenes* transformed roots expressing the *GUS* reporter gene driven by either *CASTOR* or *POLLUX* promoters, the patterns of *GUS* activity were similar in all roots with the strongest staining at the growing tips (Figure 10). No differences in the expression pattern of either construct were observed before and after 24h inoculation with *M. loti*.

The similar sequences, expression patterns and localization of *CASTOR* and *POLLUX* suggest that they have similar roles. However, mutations in either *castor* or *pollux* alone lead to symbiosis-deficiency. Taken together, these data raise the hypothesis that a certain threshold of *CASTOR* and *POLLUX* is required for symbiosis. In order to test this, we expressed *CASTOR* and *POLLUX* under the control of a single *P35S* in *castor-12* and *pollux-5* mutant alleles via *A. rhizogenes* transformation system. *Pollux-5* contains a nonsense mutation W321* leading to a truncated protein with three transmembrane domains while *castor-12* (W93*) does not retain any (Table 2 and 3). The *P35S:CASTOR* construct complemented *castor-12* but not *pollux-5* (Figure 11A and 11B). However, the *P35S:POLLUX* construct complemented *pollux-5* as well as *castor-12* (Figure 11A and 11B). This result clearly demonstrates that the homocomplex *POLLUX* can compensate the loss of *CASTOR* when expressed under the control of *P35S*, which strongly suggests that *POLLUX* has a biochemical function similar to *CASTOR*. In line with the BiFC results, these data imply also that *POLLUX* localizes to the same nuclear membrane as *CASTOR* in *planta*.

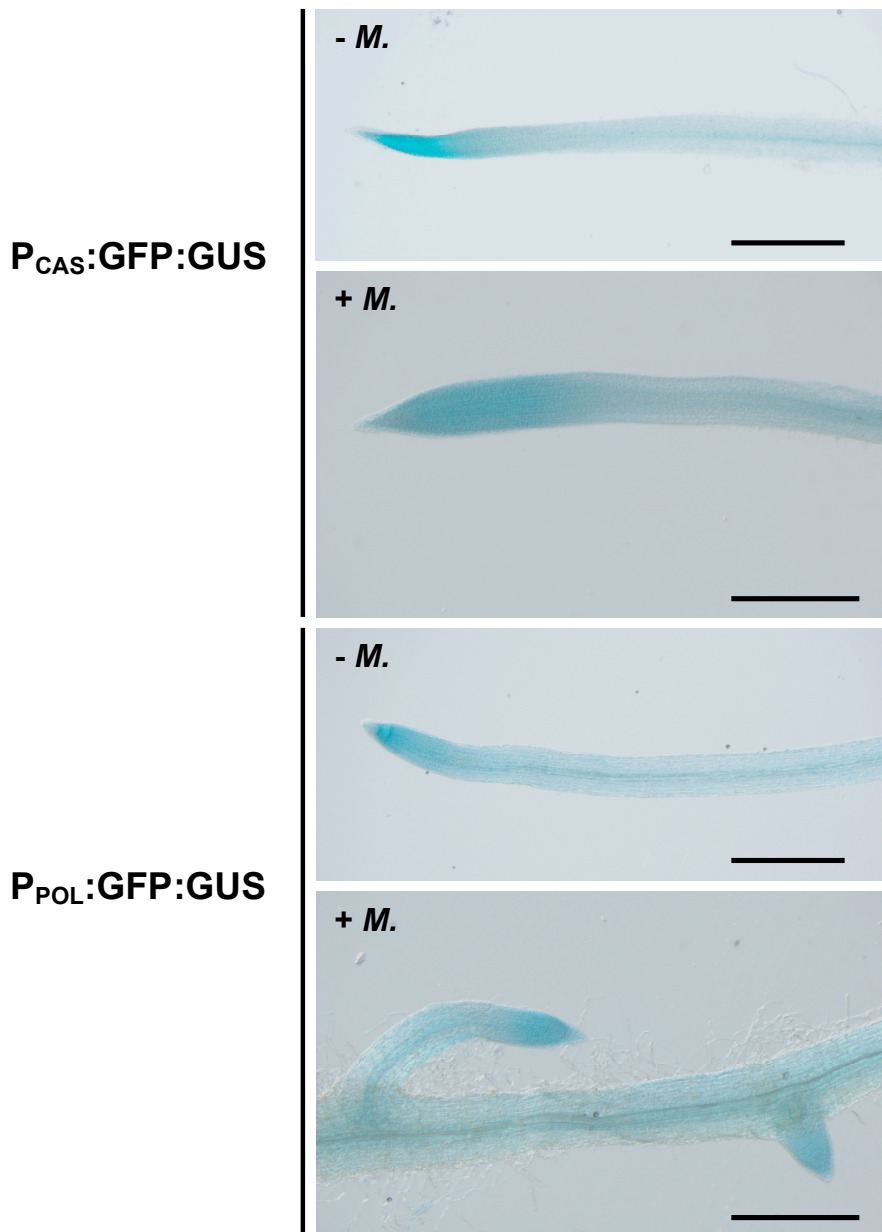
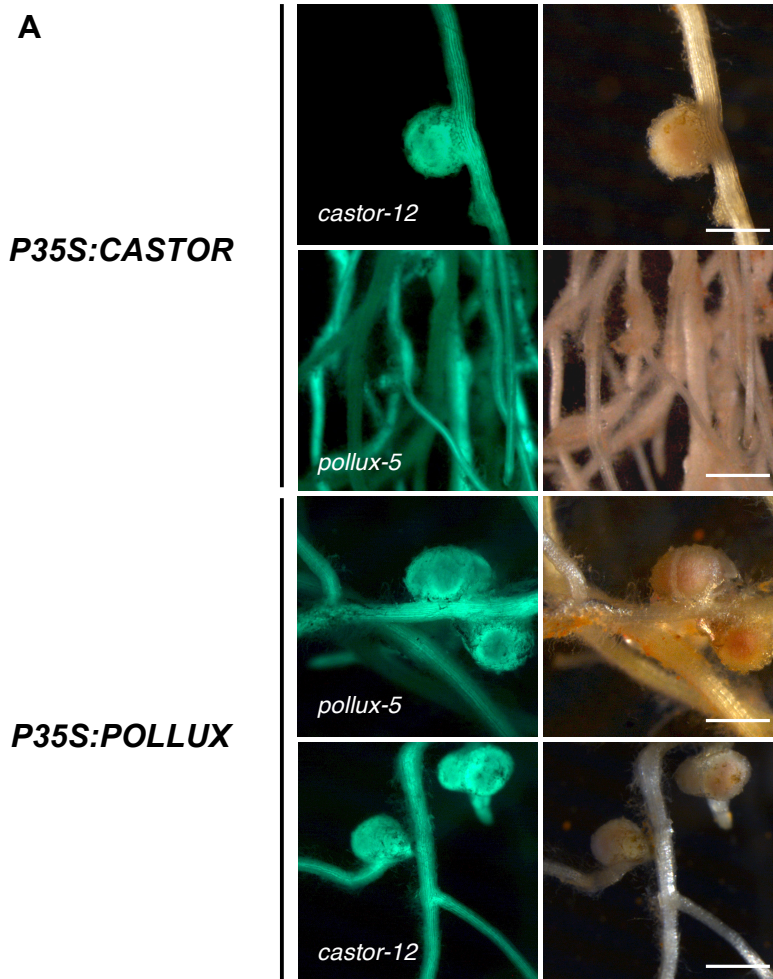


Figure 10. Expression patterns of *CASTOR* and *POLLUX* promoter:GUS fusions in *L. japonicus* roots before and after inoculation with *Mesorhizobium loti*.

A. *Rhizogenes*-transformed root systems of *L. japonicus* expressing the GUS reporter gene fused to the *CASTOR* and *POLLUX* promoters ($P_{CAS}:GFP:GUS$ and $P_{POL}:GFP:GUS$) were examined for GUS activity without and with *M. loti* strain R7A 24h after inoculation. Bars = 200 mm.



B

Plant genotype	Transgene	Fraction of nodulated plants	Nodules/Nodulated plant
Wild type	marker only	23/23	3.43 (+/- 1.0)
<i>castor-12</i>	marker only	0/39	0
<i>castor-12</i>	<i>P35S:CASTOR</i>	19/20	3.1 (+/- 0.8)
<i>castor-12</i>	<i>P35S:POLLUX</i>	14/18	2.5 (+/- 0.5)
<i>pollux-5</i>	marker only	0/12	0
<i>pollux-5</i>	<i>P35S:POLLUX</i>	31/33	3.75 (+/- 1.1)
<i>pollux-5</i>	<i>P35S:CASTOR</i>	0/23	0

Figure 11. Restoration of root nodule symbiosis in *A. Rhizogenes*-transformed root systems of *L. japonicus* mutants.

(A) Pictures of transgenic hairy roots three weeks after inoculation with *Mesorhizobium loti* R7A. The T-DNA carried the green fluorescent protein (GFP) as a marker gene. Left panel; GFP fluorescence, right panel; bright field. Bars = 1 mm.

(B) Nodulation of transgenic roots. The fraction of nodulated plants and the number of nodules per nodulated plants were determined three weeks after inoculation with the *Mesorhizobium loti* R7A strain. The standard deviations are indicated between brackets.

In order to determine whether the *M. truncatula* *DMI1* (Does not Make Infection 1) (Ane et al., 2004), the *POLLUX* putative ortholog, could restore the nodulation phenotype of the *castor* and *pollux* mutant, transgenic roots of these plants carrying the fusion construct *DMI1:GFP* under the control of a single *P35S* were generated and inoculated with the *M. loti* R7A strain. Similarly to *POLLUX*, *DMI1* fully restored the nodulation phenotype of *castor-12* and *pollux-1* mutant (Figure 12A and 12B). Furthermore, in line with the previous report showing *DMI1* localized around the nucleus (Riely et al., 2007), *DMI1* localizes at the nuclear periphery in *castor-12* and *pollux-1* mutants (Figure 12C).

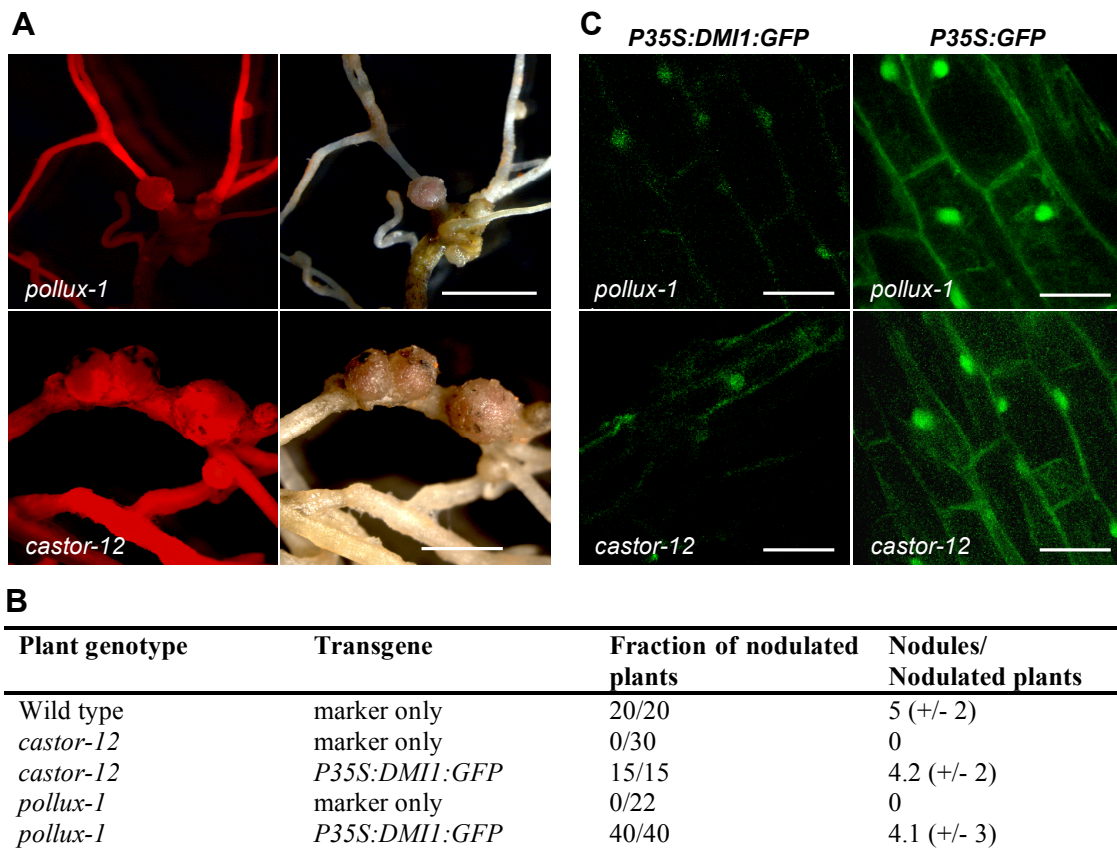


Figure 12. Restoration of root nodule symbiosis in *A. rhizogenes*-transformed root systems of *L. japonicus* mutant with the *M. truncatula* *DMI1* gene under the control of single *P35S*.

(A) Pictures of transgenic hairy roots four weeks after inoculation with the *Mesorhizobium loti* R7A strain. The T-DNA carried the *Discosoma sp.* red fluorescent protein (DsRed) as a marker gene. Left panel; DsRed fluorescence, right panel; bright field. Bars = 2 mm. (B) Nodulation of transgenic roots. The fraction of nodulated plants and the number of nodules per nodulated plants were determined four weeks after inoculation with the *Mesorhizobium loti* R7A strain. The standard deviations are indicated between brackets. (C) Confocal laser scanning images of *A. rhizogenes*-transformed root systems of *L. japonicus* *pollux-1* and *castor-12* mutant with either *DMI1:GFP* fusion under the regulation of *P35S* (Riely et al., 2007) (bars = 30 μ m) or *GFP* under the regulation of *P35S* (bars = 35 μ m).

Collectively, these data confirm that POLLUX and its *M. truncatula* ortholog DMI1 have a function similar to CASTOR. Furthermore, the complementation of *castor* mutant with *POLLUX* highlights an identical localization of CASTOR and POLLUX in *L. japonicus*.

2.6 Functional characterization

The amino acid sequence of CASTOR and POLLUX filters did not match to any known conserved signature, giving no information concerning ion selectivity. However, the model of CASTOR predicted a decoration of the pore with carbonyl oxygen atoms suggesting a cation selectivity (Figure 5D). We therefore tested, *via* yeast complementation and electrophysiological approaches, the hypothesis that CASTOR and POLLUX act as cation channels.

2.6.1 Yeast complementation assays

2.6.1.1. *cch1Δmid1Δ* and *trk1Δ* yeast mutants complementation assays

CCH1 and MID1 are components of a high-affinity Ca^{2+} permeable channel (Fischer et al., 1997; Iida et al., 1994), whereas TRK1 is a high-affinity K^+ transporter conferring to the yeast K^+ uptake system a higher K^+/Na^+ discrimination under Na^+ stress (Gaber et al., 1988). The CCH1/MID1 complex is involved in the generation of calcium influx in response to various biotic or abiotic factors; budding, alpha-mating pheromone, cold or iron stress (Fischer et al., 1997; Peiter et al., 2005). The *cch1Δmid1Δ* mutant also displays reduced tolerance to monovalent cations such as Li^+ (Paidhungat and Garrett, 1997), whereas the absence of TRK1 confers to *trk1Δ* mutant a higher sensitivity to Na^+ (Calero et al., 2000; Gaber et al., 1988).

In order to check if CASTOR and POLLUX could complement the reduced tolerance to lithium for *cch1Δmid1Δ* mutant or to sodium for *trk1Δ* mutant, both proteins tagged to a herpes simplex virus protein, VP16, were expressed under the regulation of the *S. cerevisiae* alcohol dehydrogenase 1 promoter. POLLUX could be detected in the

microsomal fraction by immunoblot with anti-VP16 (Figure 13A and 14B), whereas the full-length CASTOR expressed with different vectors could either not be detected or appears to be cleaved in the yeast mutants (Figure 13A and 14B).

The expression of POLLUX did not suppress the phenotypes of *cch1Δmid1Δ* or *trk1Δ* strains (Figure 13B and 13C). In contrast, expression of POLLUX in *trk1Δ* mutant reduced the mutant growth by 20 % (Figure 13C). These data demonstrate that POLLUX increases the sodium sensitivity of the mutant.

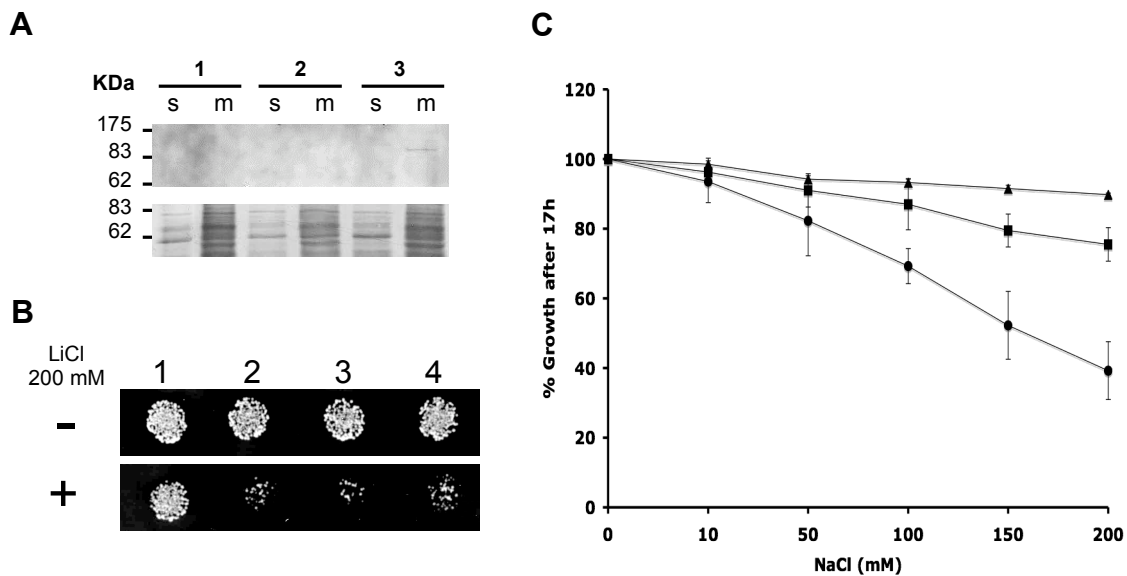


Figure 13. Complementation of the yeast double mutant *cch1Δmid1Δ* and *trk1Δ* strains. (A) Expression analyses of CASTOR and POLLUX in the yeast *cch1Δmid1Δ* mutant JK9-3 da strain. Upper panel: immunoblot detection with anti-VP16, lower panel: Coomassie blue staining of the membrane. Protein extracts from *cch1Δmid1Δ* mutant transformed with the empty vector pTMBV4 (1), pTMBV4 vector carrying *CASTOR* (2) or *POLLUX* (3) under the regulation of the *S. cerevisiae* alcohol dehydrogenase 1 promoter and fused to the tag VP16 (Hepres simplex VP16 transactivator). m; microsomal fraction, s; soluble fraction. (B) Growth assay of *cch1Δmid1Δ* mutant JK9-3 da strain transformed with either *CASTOR* or *POLLUX* on yeast synthetic defined medium lacking leucine (SD-L) containing 200 mM LiCl. Growth of JK9-3 da wild type strain transformed with the empty vector pTMBV4 (1), growth of *cch1Δmid1Δ* mutant JK9-3 da strain transformed with pTMBV4:*CASTOR* (2), pTMBV4:*POLLUX* (3) or empty vector pTMBV4 (4). (C) Growth of NaCl sensitive mutant *trk1Δ* on SD-L medium supplemented with different concentrations of NaCl. ●; *trk1Δ* mutant transformed with pTMBV4:*POLLUX*, ■; *trk1Δ* mutant transformed with empty vector pTMBV4, ▲; wild type transformed with empty vector pTMBV4. Standard errors of the means from 3 experiments.

2.6.1.3 MAB 2d yeast mutant complementation assays

In order to check whether POLLUX could trigger a potassium influx, we assayed POLLUX for complementation of a yeast mutant, MAB 2d, in which the main potassium importers

and exporters are deleted (*trk1Δ trk2Δ ena1-4Δ nha1Δ*) (Kolacna et al., 2005; Maresova and Sychrova, 2005; Rodriguez-Navarro, 2000). The deletion of both the potassium efflux and influx systems enables the MAB 2d strain to grow on acidic minimal medium supplied with otherwise toxic potassium concentrations of 600 mM (Kolacna et al., 2005). A second aspect of the potassium-uptake deficient phenotype is the inability of the mutant to grow at potassium concentrations from 10 to 50 mM (Kolacna et al., 2005). The expression of POLLUX under the regulation of the *Saccharomyces cerevisiae* alcohol dehydrogenase promoter in the strain MAB 2d impaired the growth of the mutant at potassium concentrations between 300 and 600 mM KCl, and promoted the growth on medium containing between 10 to 50 mM KCl (Figure 14). These results demonstrate that in MAB 2d, POLLUX acts as a channel triggering an influx of potassium which can be detrimental or advantageous for the yeast depending on the concentration of potassium available in the medium.

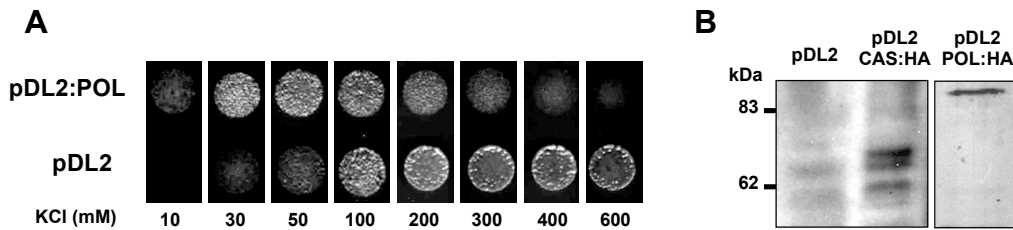


Figure 14. Complementation of MAB 2d mutant.

(A) Growth of MAB 2d cells transformed with pDL2:POLLUX (POL) under the *S. cerevisiae* alcohol dehydrogenase 1 promoter, or the empty vector (pDL2) at indicated KCl concentrations on minimal medium pH 4. (B) CASTOR and POLLUX were expressed in the yeast strain MAB2d. Only degradation products of CASTOR were detected, while a single band corresponding to the predicted size of the POLLUX full length protein (102 kDa) was observed

All together, these data indicate that POLLUX could trigger both an influx of potassium and an influx of sodium inside the yeast, which suggests that POLLUX is a non selective cation channel localized to the yeast plasma membrane. The attempts to confirm the localization of POLLUX in yeast were unsuccessful. However, *in planta*, POLLUX under the control of a different promoter could end up in a different sub-cellular

membrane. Therefore, considering our results, the plasma membrane localization of a fraction of POLLUX in yeast cannot be excluded.

2.6.2 Electrophysiological analysis

2.6.2.1 CASTOR is a cation channel

In order to determine whether CASTOR is an ion channel, we expressed CASTOR using an *in vitro* transcription-translation system (Figure 15A and 15B). The protein was purified by selective solubilization (Figure 15C and 15D), denatured and subsequently reconstituted into liposomes by dialysis. Proteoliposomes were then fused into planar lipid bilayers (Morera et al., 2007). The modeling of CASTOR filter based on the structural homology with MthK predicted a decoration of the pore with carbonyl oxygen atoms from the peptide backbone, suggesting selectivity for cations (Figure 5D). To test this prediction experimentally, we checked the permeability of CASTOR for physiologically relevant cations over anions. In asymmetrical KCl or NaCl solutions of 250 and 20 mM, we recorded the reverse potential of CASTOR which corresponds to the membrane potential at which the net flow of ions from one reservoir to the other is zero (Figure 16A and Table 6A). The calculation of the permeability ratio was based on the Goldman-Hodgkin-Katz current equation (Goldman, 1943; Hodgkin and Katz, 1949). The permeability ratios P_{K^+}/P_{Cl^-} of 6.09, P_{Na^+}/P_{Cl^-} of 1.66 and $P_{Ca^{2+}}/P_{Cl^-}$ of 0.52 indicate a preference of CASTOR for potassium (Table 6A). To test if the preference for potassium was not influenced by a conformational change of the filter due to the presence of only one cation in excess (Valiyaveetil et al., 2006), we performed competition assays between K^+ , Ca^{2+} and Na^+ (Table 6B). Solutions of K^+ and Ca^{2+} or K^+ and Na^+ were applied to the left and right side of the planar lipid bilayer, respectively. The permeability ratios P_{K^+}/P_{Na^+} and $P_{K^+}/P_{Ca^{2+}}$ indicated a 2-fold preference for K^+ in comparison to Na^+ and Ca^{2+} . These results demonstrate a moderate preference of CASTOR for K^+ over Na^+ and Ca^{2+} , which suggests that CASTOR is a poorly selective cation channel.

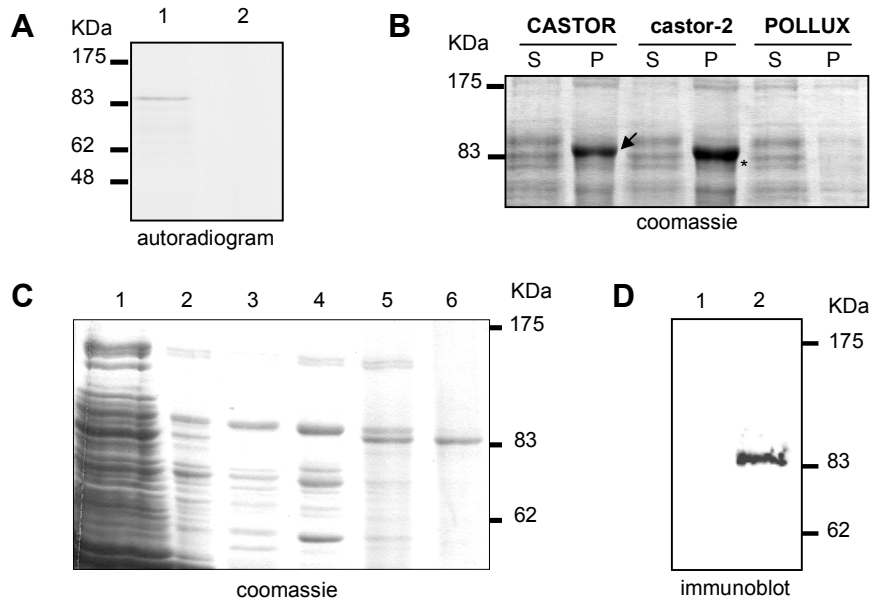


Figure 15. Cell free expression of CASTOR, castor-2 and POLLUX.

(A) Autoradiography of CASTOR (1) and POLLUX (2), expressed in a cell free system and labelled radioactively with L-[³⁵S]methionine. (B) and (C) Coomassie Blue staining of pro-teins samples analyzed by SDS/PAGE in 6% (v/v) tricine gel. (B) Total extract from the cell free expression system. S, soluble fraction; P, pelleted fraction; black arrow, CASTOR; asterisk, castor-2. (C) Purification of CASTOR by selective solubilization. 5 μ L of soluble fraction were analysed after centrifugation of the total cell free CASTOR expressed samples (lane 1), washing in sodium phosphate buffer pH7.2 (lane 2 and 3), washing in sodium phosphate buffer pH7.2 and 2% (v/v) MEGA-9 1h (lane 4 and 5), washing in sodium phosphate buffer pH7.2 and 0,1% (v/v) SDS 1h (lane 6). (D) Immunoblot analyses with anti-CASTOR using 2 μ g of solubilized CASTOR. 1; Total protein of POLLUX expressed in cell free system, 2; CASTOR purified by selective solubilization.

Castor-2 carries a single nucleotide replacement which leads to the substitution of alanine by threonine at the position 264 (Figure 17 and Table 2). The *castor-2* mutant is defective in Ca²⁺ spiking (Naoya Takeda unpublished data) and both root nodule and AM symbioses (Table 2). The mutated alanine is positioned at the hinge of the selectivity filter, which could alter the selectivity of the channel (Figure 17). To test this hypothesis, we determined the reverse potential (Figure 18A) and subsequently the permeability ratio of castor-2 for K⁺ and Na⁺ (Table 6A). We observed that castor-2 was equally permeable to Na⁺ and K⁺ (Table 6). This result indicates that the A264T mutation alters the selectivity of the pore.

Table 6. Reverse potential (E_{rev}) and permeability ratios (P_X/P_{Cl^-}) for CASTOR and castor-2 (A), and reverse potential and permeability ratios P_{K^+}/P_X for CASTOR (B).

A				
Ion (X)	CASTOR		castor-2	
	E_{rev} (mV)	P_X/P_{Cl^-}	E_{rev} (mV)	P_X/P_{Cl^-}
K^+	36 +/- 2 (n=40)	6.0 ^a	28 +/- 2 (n=48)	3.7 ^a
Na^+	11 +/- 1 (n=8)	1.6 ^a	25 +/- 3 (n=13)	3.2 ^a
Ca^{2+}	-29 +/- 2 (n=13)	0.52 ^a	-31 +/- 2 (n=19)	0.6 ^a

B		
Ion (X)	E_{rev} (mV)	P_{K^+}/P_X
Na^+	17.9 +/- 2 (n=5)	2.0 ^a
Ca^{2+}	0.4 +/- 1 (n=17)	2.0 ^b

^a Permeability ratios calculated from reverse potentials using equation: $E_{rev} = RT/zF \times \ln(P_{K^+}[K]_o/P_{Na^+}[Na]_i)$

^b Permeability ratios calculated from reverse potentials using equation: $E_{rev} = RT/F \times \ln(\sqrt{((4P_{Ca^{2+}}[Ca]_o/P_{K^+}[K]_i)^{1/4} - 1/2)})$ with $(RT/F = 25.26 \text{ mV}, Z = 1)$. The junction potential correction; Agar bridge 2M KCl, (A) NaCl (250 mM/20 mM,) $V_m = V_{cmd} + 2.3 \text{ mV}$; KCl (250 mM/20 mM) $V_m = V_{cmd} + 1.2 \text{ mV}$; CaCl2 (125mM/10mM) $V_m = V_{cmd} + 3.1 \text{ mV}$ (B) KCl-NaCl: $V_m = V_{cmd} - 1.1 \text{ mV}$; KCl-CaCl2: $V_m = V_{cmd} - 2.3 \text{ mV}$.

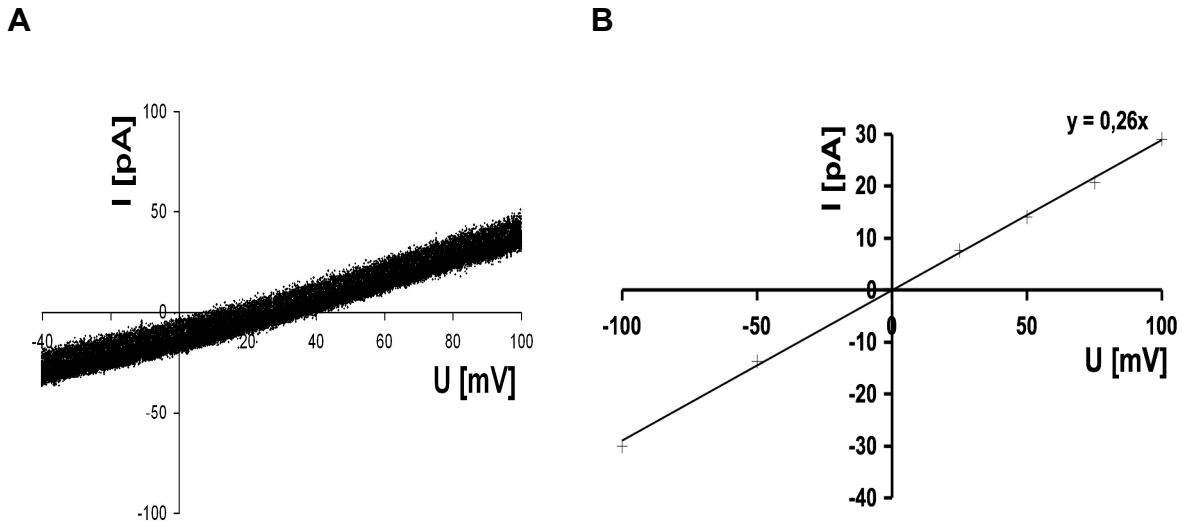


Figure 16. Electrophysiological characterization of CASTOR.

(A) Selectivity of the CASTOR channel. Voltage ramps (10 mV/s) were applied to bilayers containing one copy of CASTOR at asymmetrical electrolyte conditions: 250 mM/20 mM (*cis/trans*). (B) Conductance of CASTOR at different voltages in presence of potassium. The experiment was done with symmetrical 250 mM KCl buffer in each reservoir (*cis/trans*). The conductance was recorded at different voltages; crosses represent individual data points. The slope of the linear regression curve ($y = 0.26x$) indicated a maximal conductance of 260 pS.

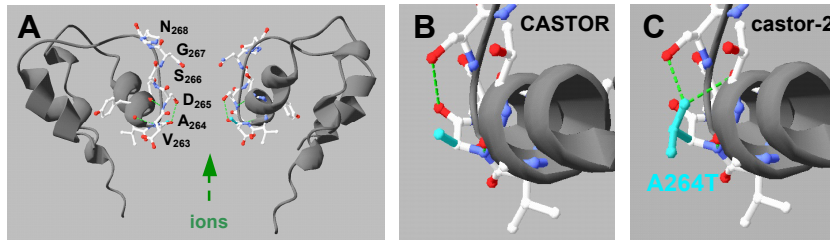


Figure 17. Modelization of the CASTOR pore and the castor-2 mutant pore.

(A) Model of the ion pore region of two CASTOR monomers based on the MthK channel (Protein Data Bank code 1LNQ). Amino acid residues constituting the selectivity filter are labeled with the carbonyl oxygen backbone facing the pore. Red: oxygen atoms, blue: amino groups, white: carbon atoms. The alanine 264 (cyan) in CASTOR (B) is substituted with a threonine in castor-2 (C) which potentially results in the formation of two new hydrogen bonds (dashed green lines).

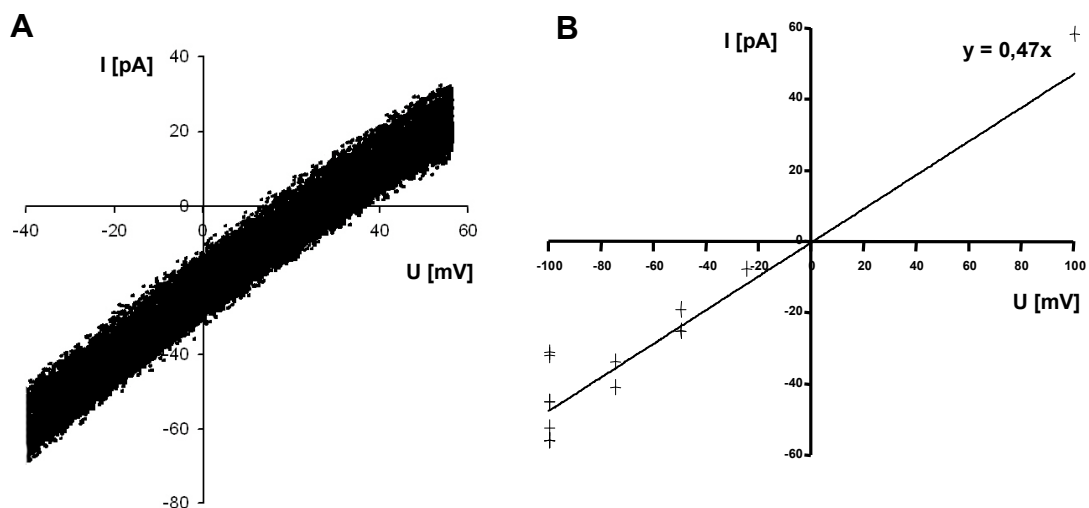


Figure 18. Electrophysiological characterization of castor-2 channel.

(A) Selectivity of the castor-2. Voltage ramps (10 mV/s) were applied to bilayers containing four copies of castor-2 at asymmetrical electrolyte conditions: 250 mM/20 mM (*cis/trans*). (B) Conductance of two copies of castor-2 at different voltages in presence of potassium. The experiment was done with symmetrical 250 mM KCl buffer in each reservoir (*cis/trans*). The conductance was recorded at different voltages; crosses represent individual data points. The slope of the linear regression curve ($y=0.47x$) indicated a maximal conductance of 470 pS.

Quaternary ammonium ions (QAs) such as tetrabutylammonium (TBA) or tetraethylammonium are well established open- K^+ channel blockers (Hille, 2001; Yellen, 1984), as well as blocker of the sarcoplasmic reticulum calcium release channels (Tinker et al., 1992). In contrast, the QAs have no effect on open-cation channels (Demidchik and Tester, 2002). At a holding potential of 25 mV, the subsequent application of 10, 100, 200 and 500 μ M of TBA did not influence the closing of CASTOR or castor-2 inserted in

the lipid bilayer (data not shown). All together, the selectivity ratio and the QAs experiments suggest that CASTOR is a poorly selective cation channel with a better permeability for potassium.

2.6.2.2 Magnesium mediates voltage-dependent blockage of CASTOR

In response to stimuli, ion channels can switch between closed and open state conformations, thereby acting as regulators of ion fluxes in cells. To explore the gating mechanism of CASTOR, we applied different stimuli in order to influence its opening and closing. Voltage gating was evaluated by modulating the membrane potential from 100 mV to -100 mV in a solution of 250 mM KCl, on both sides of the lipid bilayer. Closing and opening of CASTOR was observed without any detectable influence of the voltage (Figure 20A). The current-voltage relation reveals that the channel was active over a large voltage range from -100 mV to 100 mV without any rectification of the current (Figure 16B). The current-voltage relationship of CASTOR was linear over this voltage range with a maximal conductance of 260 pS (Figure 16B). Similarly no rectification of the current was observed in castor-2 (Figure 18B). A maximal conductance of 235 pS was observed for castor-2, which is relatively similar to CASTOR.

We tested the influence of divalent cations such as MgCl_2 on the gating mechanism of CASTOR. At positive voltage, random closing steps of CASTOR and castor-2 were recorded, attesting to the presence of the channels (Figure 19). At these voltages, no differences were observed between CASTOR and castor-2 in the presence or absence of 3 mM of MgCl_2 on the *cis* side. However, at negative voltage, and specifically in the presence of MgCl_2 , closing of CASTOR occurred at a high frequency, while no changes were observed for castor-2 (Figure 19). The differences observed between the mutant and the wild type channels demonstrate the specificity of the closing of wild type CASTOR in the presence of Mg^{2+} . This result suggests that the A264T mutation modifies the pore conformation in such a way that Mg^{2+} dependent blockage is no longer occurring.

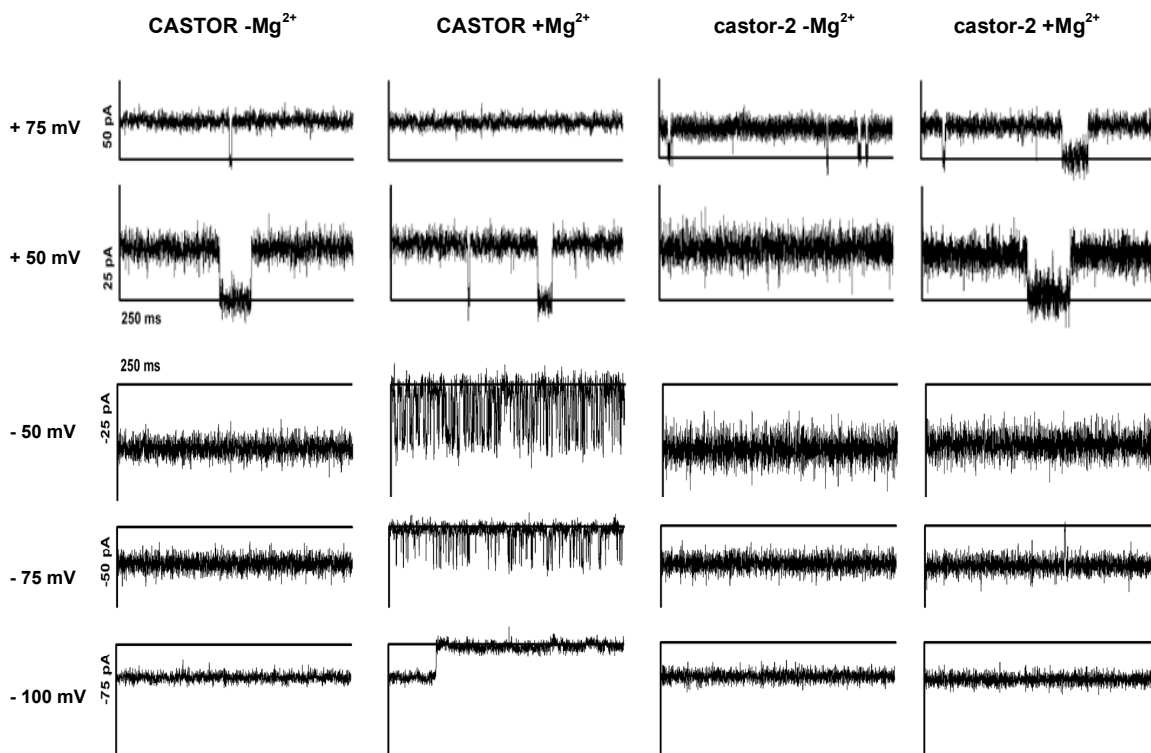


Figure 19. Voltage dependent magnesium-blockage of CASTOR.

CASTOR and castor-2 channel currents were recorded at voltage indicated on the left, in the presence and absence of physiologically relevant concentration of MgCl_2 (3 mM) (Allen and Sanders, 1996). At negative voltage after addition of MgCl_2 , high frequency of closing steps of CASTOR were observed.

2.6.2.3 CASTOR sensitivity to putative binding ligands

Because InsP_3 and Ca^{2+} are discussed as likely modulators of calcium spiking, we analysed the sensitivity of CASTOR gating to calcium and InsP_3 at a holding potential from 100 to -100 mV in a recording solution containing 250 mM KCl. The effect of InsP_3 has been tested at the maximal physiological concentration of 10 μM (Blatt et al., 1990), whereas CaCl_2 has been applied from 0.1 to 10 mM according to the concentration tested on MthK (Zadek and Nimigean, 2006). However, neither InsP_3 nor Ca^{2+} influenced CASTOR gating at the concentrations tested (Figure 20A). A putative NAD(P) binding domain is predicted at the C-terminus part of CASTOR (Figure 5A). Therefore, NADP⁺, NADPH, NAD⁺ and NADH were tested on the channel gating. An absence of closing

was exclusively observed with 1 mM of NADH, suggesting a binding to CASTOR (Figure 20B). However, this experiment has been performed only once and further analyses will be required to get conclusive results.

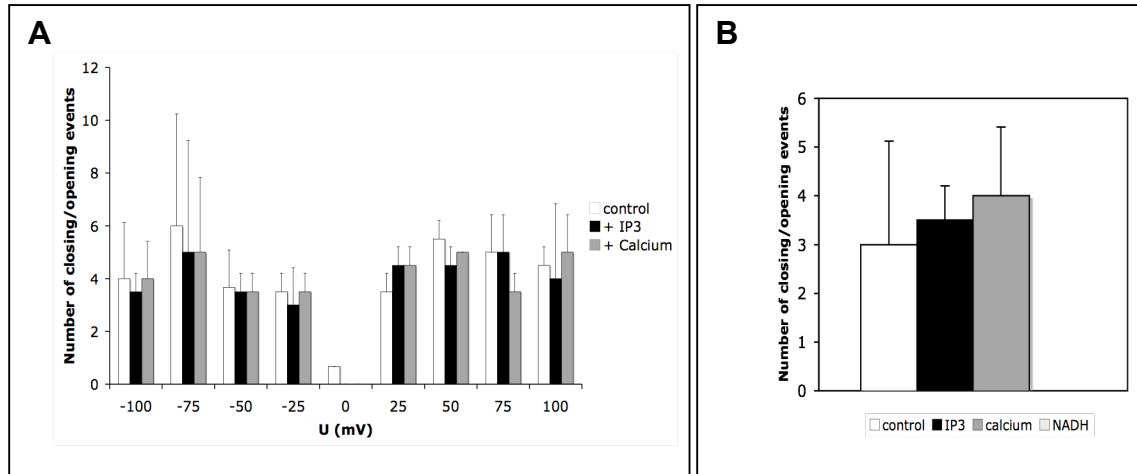


Figure 20. Modulation of CASTOR gating.

(A) Number of closing/opening events at different voltage (control) and after addition of 10 μ M inositol triphosphate (+ IP3) or 1 mM calcium chloride (+ CaCl₂) during 20s. Standard error of the means of three experiments. (B) Number of closing/opening events at a holding potential of -100 mV after addition of 10 μ M IP3, 1 mM CaCl₂ or 7 μ M NADH during 20s. Standard errors of the means of three experiments for control, IP3 and calcium. Only one experiment has been done with NADH.

Collectively these results demonstrate that either CASTOR or POLLUX can trigger a flux of potassium and sodium. The electrophysiology experiment highlighted that in the presence of both cations, CASTOR prefers potassium. Furthermore, the Mg²⁺ seems to play a crucial role in the kinetic of CASTOR by reducing its conductance under negative voltage. In contrast, if the NADH binding is confirmed, this allosteric factor could be involved in keeping the channel open, possibly in association with another ligand essential for CASTOR activation.

2.7 CASTOR interacting component

The modulation of channel activities by regulatory proteins is a well-known mechanism in the mammalian system. By biochemical approaches and screening cDNA libraries using yeast-two-hybrid system, proteins interacting with the C-terminus part of K⁺ or cation channels were identified and shown to be involved in modulating current, promoting the channel assembly or targeting the channel to its active compartment (Martens et al., 1999; McDonald et al., 1997; Michaelievski et al., 2002; Molokanova et al., 2000; Scott et al., 1994). Furthermore, mutation in phosphorylation sites combined with physiological studies provided evidence that K⁺ channels of the shaker family are substrates for cAMP-dependent protein kinase (Drain et al., 1994), protein kinase C (Covarrubias et al., 1994) and Ca²⁺/calmodulin dependent protein kinase (Roeper et al., 1997).

In *planta*, direct interactions between regulatory proteins such as kinase, phosphatase or calmoduline with K⁺ or cation channels have been demonstrated *via* biochemical or yeast two hybrid approaches (Arazi et al., 2000; Cherel et al., 2002; Xu et al., 2006). In the early symbiotic signalling pathway, CASTOR and POLLUX are required for the generation of the calcium spiking as well as the receptor-like kinase, SYMRK, (Stracke et al., 2002). In tobacco cells, SYMRK:YFP has been localized in the plasma membrane, as well as in the nucleus (Merixtell Llovera personal communication). Immunoblot analysis revealed cleavage products of SYMRK which could correspond to the SYMRK-kinase:YFP fusion relocalized in the nucleus (Merixtell Llovera personal communication). As a Ca²⁺ spiking downstream component, a nuclear localized Ca²⁺/calmodulin dependent protein kinase (CCaMK) has been identified and is likely to be a player in deciphering the calcium signature (Levy et al., 2004).

To unravel whether CASTOR activity could be modulated by those symbiotic components, the yeast two hybrid system was used to check interaction between CASTOR, SYMRK and CCaMK, as well as to screen a *M. loti* inoculated-*L. japonicus* roots cDNA library.

2.7.1 Yeast-two-hybrid assay with common symbiotic components

The C-terminal soluble domains of CASTOR (cCASTOR; H322-E853) and POLLUX (cPOLLUX; H386-D917) were assayed for interaction with SYMRK-kinase domain and CCaMK in the yeast two hybrid GAL4 based system. As negative control, the SYMRK extracellular domain (SYMRK-ECD) and a SYMRK interactor, the *Lotus japonicus* seven in absentia 1 (LjSINA1) (Satoko Yoshida personal communication), were used. However, none of the symbiotic components, SYMRK-kinase domain, CCaMK, SYMRK-ECD or LjSINA1 were interacted with CASTOR or POLLUX C-terminal domains (Figure 21).

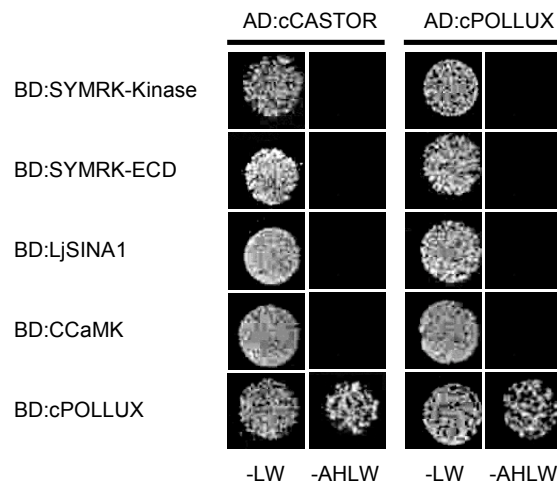


Figure 21. Yeast-two-hybrid assay for interactions of cCASTOR and cPOLLUX with symbiotic components.

Interaction assays were performed in the yeast strain AH109 cotransformed with the bait (BD) and prey (AD) vectors containing either cCASTOR (H322-E853) or cPOLLUX (H386-D917) with SYMRK kinase domain E594-R923 (SYMRK-Kinase), SYMRK extracellular domain T29-Q517 (SYMRK-ECD), CCaMK or LjSINA1. The cotransformants and interacting partners were analysed on synthetic dropout nutrient medium lacking leucine and tryptophan (-LW), and lacking leucine, tryptophan, adenine and histidine (-LWAH), respectively. The constructs BD:SYMRK-Kinase, BD:SYMRK-ECD, BD:LjSINA1 and BD:CCaMK were provided by Satoko Yoshida.

2.7.2 Screening of a *L. japonicus* roots cDNA libraries using yeast-two-hybrid system

The C-terminal soluble domain of CASTOR (cCASTOR; H322-E853) was used as a bait of the yeast two hybrid system to screen a lotus cDNA library constructed in the prey vector pAD-GAL4-2.1 (Poulsen and Podenphant, 2002). The cDNA library was prepared from mRNA extracted from *L. japonicus* seedlings roots 5 and 12 days after *M. loti* inoculation (Poulsen and Podenphant, 2002). Approximately 4 million yeast *S. cerevisia* colonies expressing the cDNA library were assayed for their ability to grow on selective synthetic medium (SD/-AHLW). The prey plasmids were isolated from the positive colonies and cotransformed with the pBD:cCASTOR back to yeast. Colonies that failed to grow in the second round of testing were considered as false positives. Polymerase chain reaction (PCR) and restriction digest with *RsaI* were performed on the positive clones in order to identify similar sequence pattern. One clone per identical pattern was sequenced. The 46 sequences obtained were assembled into 7 contigs (<http://staden.sourceforge.net/>). BlastX search with the 7 putative interactors identified similar protein in other legumes as well as in *A. thaliana* (Table 7). Among them, proteins similar to an *A. thaliana* developmental protein DG118 (named 50), a Zinc finger RING-type protein (named 84) and an *A. thaliana* pentatrικο-peptide (PPR) repeat-containing protein (named 64) were chosen for further analyses. Both the *L. japonicus* sequence-related *A. thaliana* developmental protein DG118 (50) and the *L. japonicus* sequence-related Zinc finger RING-type protein (84) were predicted to localize in the nucleus (Table 7).

The putative cCASTOR interactors full length 50, 84 and 64 were subcloned and tested for *vice versa* interaction, as well as for interaction with cPOLLUX in yeast two hybrid assays. None of the cCASTOR interactors were found to interact with cPOLLUX (Figure 22). Moreover, only the candidate 50 interacted with cCASTOR in both directions reinforcing the hypothesis that 50 is a CASTOR real interactor (Figure 22). The candidate 50 encodes a small soluble protein of 204 amino acids containing a predicted Snf7 (sucrose non-fermenting 7) domain which is involved in protein sorting (Babst et al., 2002; Peck et al., 2004). Therefore, we renamed 50, LjSNF7 for *Lotus japonicus* Snf7 proteins.

Table 7. List of putative cCASTOR interactors.

Interactor numbers	Blast X similarity results	Features
50, 55, 51, 123, 100, 61, 70, 108, 66, 112, 18, 19, 22, 01, 34, 21, 35, 12, 29	gi:18410249, <i>A. thaliana</i> vacuolar protein sorting (VPS) 46.2, E value = 1e-29	Pfam03357 ^b , Snf7 domain, involved in protein sorting Localization ^a : nucl 6
52, 57, 67, 02, 03, 08, 20, 13, 06	gi:145362649, <i>A. thaliana</i> Eucaryotic translation initiation factor 2 subunit beta (eIF-2-beta), E value = 4e-100	Pfam01873 ^b , contain putative zinc finger binding C domain Localization ^a : chlo:4, cyto:4.
65, 120, 64, 04, 05, 17, 32	gi:15233698, <i>A. thaliana</i> pentatricopeptide (PPR) repeat-containing protein, E value = 2e-65	Pfam01535 ^b , PPR repeat Localization ^a : cyto 9.
117, 103, 71, 85, 15	gi:161789859, <i>G. max</i> transcription factor, GT-1, E value = 2e-92	InterProScan ^b : no hit. Localization ^a : nucl 14.
72, 101, 84, 23	gi:124360876, <i>M. truncatula</i> Zinc finger, RING-type, E value = 9e-83	IPR005805 ^b , Rieske iron-sulphur protein domain. Localization ^a : nucl 8
114	gi:163889364, <i>M. truncatula</i> bHLH transcription factor, E value = 7e-41	InterProScan ^b : no hit. Localization ^a : chlo 7
24	gi:15231043, <i>A. thaliana</i> chlorophyll synthase, ATG4/ CHLG/G4, E value = 1e-86	Pfam01040 ^b : UbiA Prenyl-transferase Localization ^a : nucl 6

a, localization predicted with WolfPSort (<http://wolfpsort.org/>). nucl, nuclear; chlo; chloroplastic, cyto; cytoplasmic. b, conserved domains predicted with InterProScan (<http://www.ebi.ac.uk/Tools/InterProScan/>). No information concerning the level of expression of the interactors were available in the *Lotus japonicus* array on the Kazusa website (<http://est.kazusa.or.jp/en/plant/lotus/EST/>)

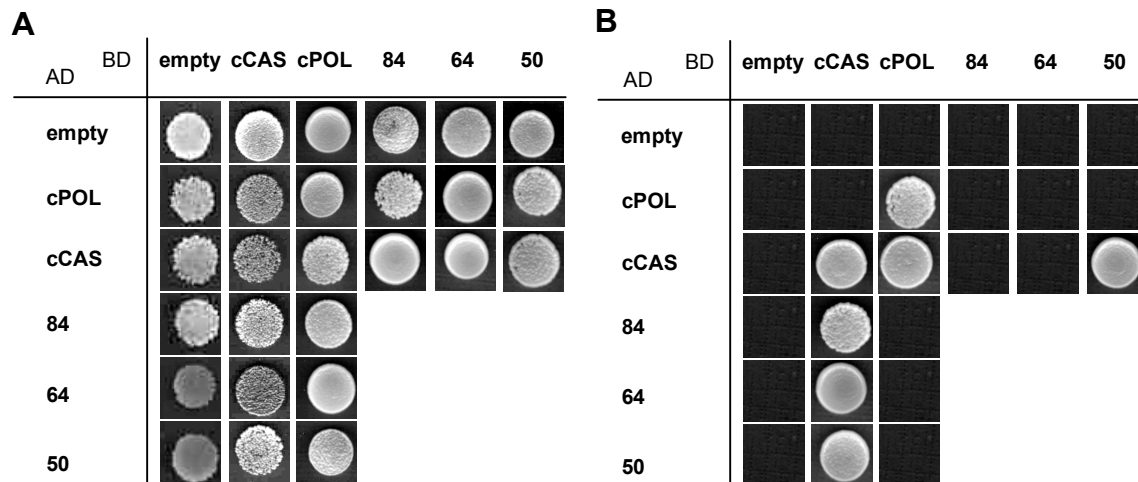


Figure 22. Yeast-two-hybrid assay for interaction between cCASTOR and yeast two hybrid library full-length candidat interactors.

(A) Interaction assays were performed in the yeast strain AH109 cotransformed with the bait (BD) and prey (AD) vectors containing either cCASTOR (H322-E853), cPOLLUX (H386-D917), 84 full length, 50 full length or 64 full length. The cotransformants were analysed on synthetic dropout nutrient medium lacking leucine and tryptophan (-LW). (B) The growth of interacting partners were analysed on synthetic dropout nutrient medium lacking leucine, tryptophan, adenine and histidine (-LWAH).

2.7.2.1 Root nodule phenotype of transformed *L. japonicus* roots expressing RNAiLjSNF7 construct.

In order to attest whether LjSNF7 plays a role in root nodule symbiosis, gene silencing *via* RNA interference (RNAi) of the interacting candidat was performed in transgenic *L. japonicus* roots. A 278 bp sequence corresponding to the 3' end of the gene was subcloned under the regulation of the *L. japonicus* ubiquitin promoter (*Ljubq1*) in the pUB-GWS-GFP binary plasmid carrying the GFP fluorescent marker (Maekawa et al., 2008). As control, the empty vector, as well as the vector carrying a partial sequence of the β -glucuronidase (*GUS*) gene, were used (Maekawa et al., 2008). The binary vectors were transformed in the *Agrobacterium rhizogenes* AR1193 strain. The transformed strain was then used to inoculate *L. japonicus* seedling hypocotyls in order to regenerate transformed roots. The transgenic roots were scored for nodule formation 3 weeks after inoculation with the *M. loti* R7A strain. An average of 2.7 and 2.6 nodules were formed on the *L. japonicus* transgenic roots carrying the silencing *GUS* construct or the empty vectors, respectively. In contrast, an average of 0.5 nodules appears on the pUB-GWSLjSNF7-GFP transgenic roots (Figure 23 A). In the pUB-GWSLjSNF7-GFP

transgenic roots, the LjSNF7 expression levels were reduced by 50 % in comparison to the wild type (Figure 23B), which is in line with the 50 % reduction of nodule formation.

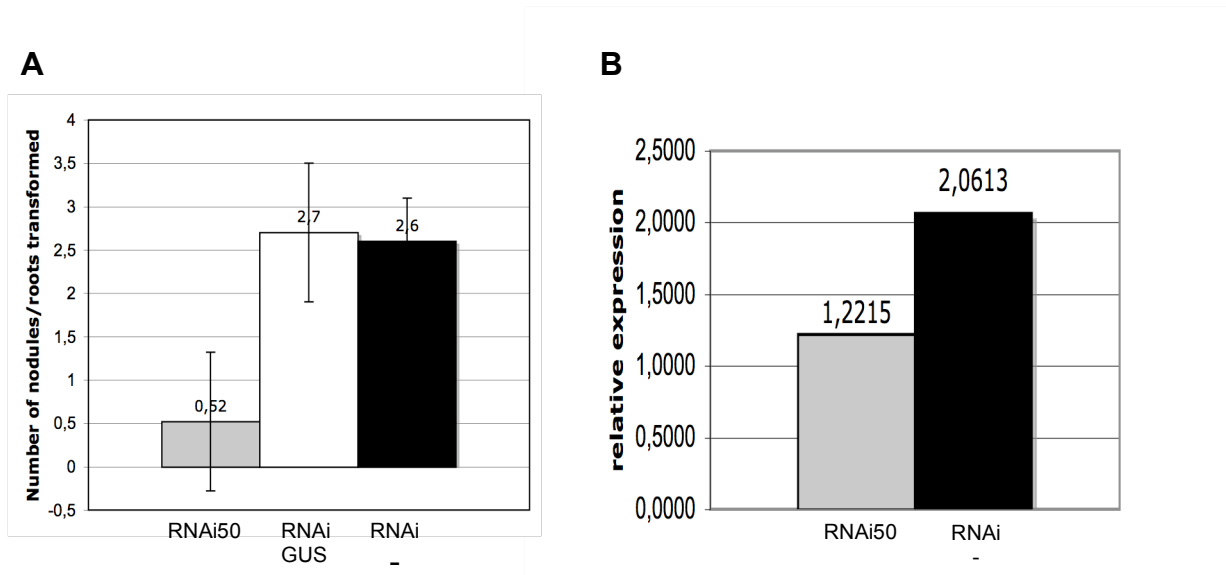


Figure 23. Downregulation of LjSNF7 in *A. rhizogenes* transformed roots expressing pUB-GWSLjSNF7-GFP impaired nodulation.

(A) Number of nodules formed after 3 weeks inoculation with the *M. loti* R7A strain on transgenic roots expressing the silencing cassette LjSNF7 (RNAi50), GUS (RNAiGUS) or the empty cassette (RNAi -) under the regulation of the *L. japonicus* ubiquitin promoter (*Ljubq1*). Standard errors of the mean of 23 roots. (B) Relative expression levels of LjSNF7 measured by quantitative RT-PCR in roots expressing pUB-GWSLjSNF7-GFP (RNAi50) or in roots expressing the empty vector pUB-GWS-GFP (RNAi -).

2.7.2.2 Sub-cellular localization of LjSNF7

To determine the sub-cellular localization of LjSNF7, a *LjSNF7::RFP* fusion construct was transiently expressed under the regulation of a single *P35S* promoter in cell culture derived *L. japonicus* protoplasts. The fluorescence of the LjSNF7:RFP was compared to various organelle markers including the plastid marker (FNR:GFP), the endoplasmic reticulum marker (GFP:HDEL), and as cytoplasmic and nucleoplasmic marker, the free RFP (Figure 24). The analyses of the LjSNF7:RFP-expressing protoplasts showed that the red fluorescence was confined in an uncharacterized compartment surrounding the nucleus which does not correspond to either ER, plastid or a free diffusion of LjSNF7:RFP (Figure 24M to 24O). In order to determine whether the LjSNF7 fluorescence pattern could correspond to the CASTOR localized compartment, we generated a fusion construct between the CASTOR N-terminal fragment encompassing

the first 69 amino acids, including the predicted NLS (Figure 5A), and the RFP. The red fluorescence generated by the expression of TPcas:RFP was observed in nuclear-localized patches (Figure 24J to 24L). Although the fluorescence of both fusion constructs were observed in a nuclear-localized compartment, further experiments including colocalization, BiFC and co-immunoprecipitation will be required to determine whether CASTOR and LjSNF7 are really interacting in *planta*.

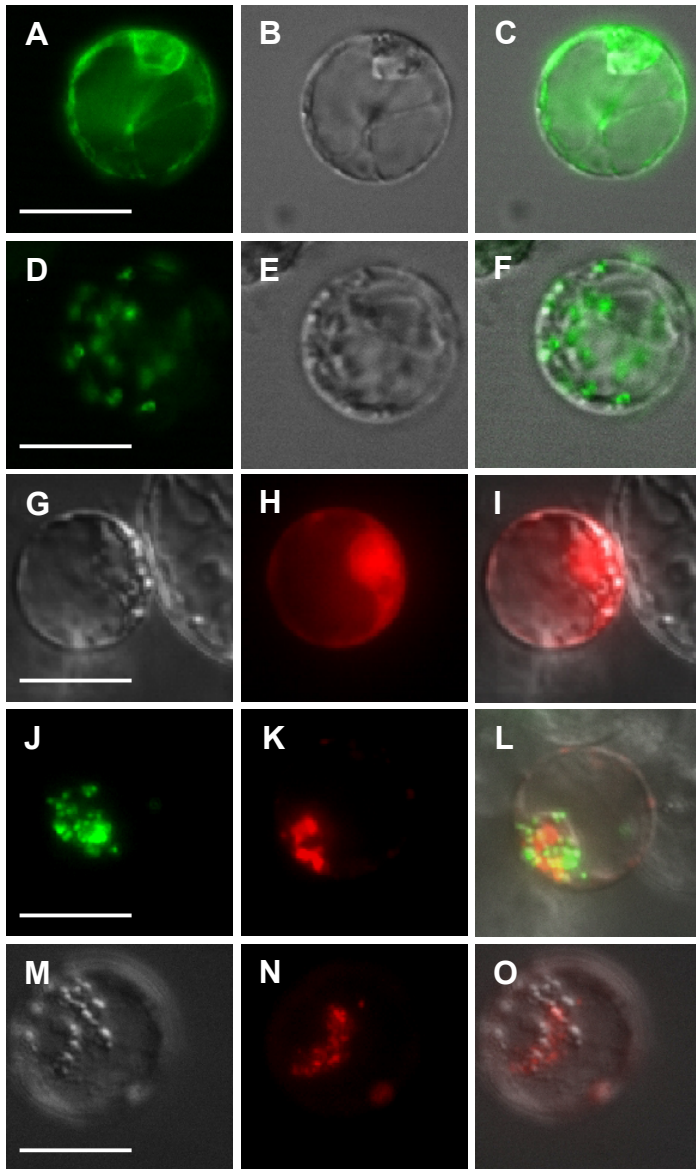


Figure 24. Subcellular localization of LjSNF7:RFP in *L. japonicus* cell culture protoplast.

(A) to (C) Epifluorescence microscope pictures of protoplasts expressing the GFP:HDEL fusion proteins (ER control), (D) to (F) the FNR:GFP fusion proteins (plastid control), (G) to (I) RFP (cytosolic and nucleosomal control), (J) to (L) coexpressing FNR:GFP and TPcas:RFP fusion proteins, (M) to (O) the LjSNF7:RFP fusion proteins. (A), (D) and (J) GFP fluorescence; (H), (K) and (N) RFP fluorescence; (B), (E), (G) and (M) bright field images; (C), (F), (I), (L) and (O) Fluorescence and bright field images merged. Bar = 20 μ m.

3. Discussion

Nod factor perception at the plasma membrane triggers perinuclear Ca^{2+} oscillations (Ehrhardt et al., 1996). *CASTOR* and *POLLUX* are required for Nod factor induced Ca^{2+} spiking (Miwa et al., 2006). To understand how *CASTOR* and *POLLUX* are linked to the Ca^{2+} spiking machinery, we investigated the structural and biochemical features of these two sequence-related proteins.

3.1 Nuclear localization of *CASTOR* and *POLLUX*

The immunogold labeling of endogenous *CASTOR* in *L. japonicus* clearly demonstrates the localization of *CASTOR* in the nuclear envelope. The complementation of a *castor* mutant with *P35S:POLLUX* suggests a similar localization of *POLLUX*. This result is in line with the WoLFPSORT analyses, which predict three and one nuclear localization signals (NLS) in *POLLUX* and *CASTOR*, respectively. However, the difference between *CASTOR* and *POLLUX* in number and sequences of predicted NLS suggests that they may not reside in the same location. The absence of *pollux-5* complementation with *P35S:CASTOR* could be explained by this possible distinct targeting. In order to reach the inner nuclear membrane, membrane proteins must move across the three continuous membrane domains that make up the nuclear envelope: the ONM, the pore membrane and the INM where they reside. Divers mechanisms have been proposed to explain the migration of the membrane protein to the INM. Based on study in HeLa cells, one model suggests that the migration in the pore membrane could be energy dependent (Ohba et al., 2004). On the other hand, the movement of the integral INM proteins might be promoted *via* direct interaction of the membrane protein with specific nucleoporins. An important feature of the second model would be the recognition of specific signal sequence similarly to the NLS of soluble nuclear localized proteins. Evidence for the role of NLS in targeting the inner membrane protein comes from studies in yeast. Mutation or deletion of NLS of the protein helix-extension-helix-2, *Heh2*, caused the dispersal of the protein through the ER (King et al., 2006). Moreover, *Heh2* that lacks the NLS were excluded from the INM (King et al., 2006). The sequence of the NLS identified is enriched in

lysine similarly to POLLUX NLS. Although the studies has been done in yeast, the nucleopore complex machinery seems to be well conserved among plant, fungal and animal lineages (Baptiste et al., 2005). Therefore, in a hypothetical scenario, given that the NLS will be membrane tethered, CASTOR resides in the outer nuclear envelope while POLLUX is required in both the inner and the outer nuclear membrane. Such partially overlapping localization could explain the absence of *pollux-5* complementation with *P35S:CASTOR*. However, further experiments will be required to confirm this hypothesis. Previously, the localization CASTOR and POLLUX, predicted by TargetP to carry a chloroplast transit peptide, has been reported in plastids of onion and pea root cells (Imaizumi-Anraku et al., 2005). In this study, we observed plastid localization of CASTOR and POLLUX GFP fusion constructs in tobacco epidermal cells when driven by *2xP35S*. In the same cellular system, but expressed under the control of *1xP35S*, CASTOR and POLLUX were only observed in the nuclear envelope. Although a previous report demonstrates that a protein initially targeted to the ER could then be delivered to the plastid (Villarejo et al., 2005), it is unclear from our study whether CASTOR and POLLUX are localized to the plastid after being targeted to the secretory pathway, or directly delivered to the plastid when highly expressed in heterologous cells. All together, these experiments suggest that CASTOR and POLLUX have the potential to be dual targeted to the plastid or to the nuclear envelope.

3.2 CASTOR and POLLUX are non-selective cation channels

The functional complementation of a *castor* mutant by *P35S:POLLUX* revealed that the two distinct complexes formed by CASTOR or POLLUX have identical biochemical function.

In order to characterize the function of CASTOR and its kinetics properties, we employed electrophysiological assays on CASTOR reconstituted in planar lipid bilayers. The CASTOR model predicted a decoration of the pore with carbonyl oxygen atoms which suggests a cation selectivity. With a permeability of approximately 6:1 and 2:1 for P_K/P_{Cl} and P_{Na}/P_{Cl} , respectively, CASTOR is confirmed as a cation channel weakly selective for cation over anion. The P_{Ca}/P_{Cl} of 0.5 demonstrates that CASTOR has a

lower permeable for Ca^{2+} than for Cl^- . Considering the oxygen backbone facing the pore and conferring an electronegative environment, in the presence of Ca^{2+} , a size exclusion mechanism could explain the chloride flux observed. Although the selectivity of CASTOR for cation is weak, it appears identical to other endomembrane cation channels such as the slow and fast vacuolar cation channel of sugarbeet for which a $P_{\text{K}}/P_{\text{Cl}}$ of 6:1 has been recorded (Hedrich and Neher, 1987). In the presence of equimolar concentration of NaCl or CaCl_2 , the preference for K^+ was confirmed. However, with a 2-fold preference for K^+ over Na^+ and Ca^{2+} , CASTOR is only weakly selective for potassium. Moreover, in line with numerous cation channels characterized (Davenport and Tester, 2000; Demidchik et al., 2002), CASTOR is also insensitive to QAs K^+ channel inhibitor. Furthermore, the high conductance of CASTOR is of the same range as other cation channels revealed by patch clamp analyses of parsley protoplast (Demidchik et al., 2002; Zimmermann et al., 1997). Interestingly, a high-conductance cation channel has also been recorded in beet root nuclear envelope (Grygorczyk and Grygorczyk, 1998).

CASTOR and POLLUX share the same selectivity filter sequences. The expression of POLLUX in *trk1Δ* mutant and the complementation of the yeast mutant strain MAB 2d indicate that POLLUX behaves as a cation channel permeable to both potassium and sodium.

All together, the electrophysiology and yeast assays indicate unequivocally that CASTOR and POLLUX are non-selective cation channels permeable to both sodium and potassium. In the cytoplasm, a low Na^+ and high K^+ concentration are essential for the maintenance of a number of enzymatic processes and protein synthesis (Bhandal and Malik, 1988; Tester and Davenport, 2003). Considering the preference of CASTOR for potassium, together with the fact that potassium has a concentration as high as 100 to 200 mM within the cytoplasm (Gierth and Mäser, 2007; Walker et al., 1996), we propose that potassium is likely to be the major ion going through CASTOR and POLLUX *in vivo*. In this model, the potassium is supposed to go down a concentration gradient from the cytoplasm to the perinuclear membrane space.

3.3 Channel gating

To explore possible opening and closing mechanisms of CASTOR, we tested effectors either known to regulate cation channel gating or proposed to be involved in the signalling pathway leading to Ca^{2+} spiking. Our results revealed a regulatory mechanism involving a divalent cation. At negative voltage and in presence of Mg^{2+} , a blockage of CASTOR conductance was observed. This behaviour is reminiscent of voltage-dependent divalent cation blockage, a phenomenon which has been studied in detail in potassium and cation channels (Armstrong et al., 1982; Lu and MacKinnon, 1994; Stern et al., 1987; Zhang et al., 2006). Different voltage-dependent cation blocking mechanisms have been observed. A ring of negatively charged amino acids in the conduction pathway formed by the inner helices is involved in this electrostatic mechanism in a subset of potassium channels (Zhang et al., 2006). In contrast, in cation channels, the external site of the selectivity filter can bind divalent cations that serve to block monovalent cation conduction (Armstrong et al., 1982; Stern et al., 1987). To be active, the voltage-dependent magnesium blocking mechanism requires a membrane potential positive at the side of the magnesium source. Cationic lipophilic dyes which accumulate in the organelle depending on the membrane potential, have been utilized extensively to measure membrane potential (Marchetti et al., 2004). In living plant cells the cyanine dye 3,3'-dihexyloxycarbocyanine iodide (DiOC6(3)) (Metivier et al., 1998), was shown to accumulate in the nuclear envelope suggesting the generation of a membrane potential across the inner and outer membrane (Matzke and Matzke, 1986). This experiment suggests that nuclear membrane potential would be negative inside the perinuclear space relative to the outside cytoplasmic space. In a hypothetical model, the voltage-dependent magnesium blocking mechanism is active while the nuclear membrane potential difference reaches a precise negative voltage, attracting the magnesium in the conducting pathway and limiting the potassium conductance.

The absence of blocking in castor-2 revealed that the A264T mutation modifies the structure of the pore and filter in such a way that magnesium blockage could no longer occur. A structural modification of the pore of castor-2 is further supported by the equal selectivity to K^+ and Na^+ . Our data suggest that the phenomenon of voltage-dependent Mg^{2+} blockage also occurs in CASTOR. The absence of this regulatory

mechanism in castor-2 could influence potassium fluxes, which may be inappropriate for calcium spiking.

CASTOR and POLLUX each have large C-terminal domain, which is required for the homocomplex assembly. In addition, the large C-terminal domain of channels have been involved in regulating channel conductance *via* binding of allosteric effectors (Li et al., 2007). As in *M. truncatula*, pharmacological studies implicated PLD and PLC upstream of Ca^{2+} spiking (den Hartog et al., 2003; Engstrom et al., 2002), phospholipid derived signaling compounds may be directly or indirectly involved in triggering the Ca^{2+} oscillation. However, our experiments did not reveal a direct influence of InsP_3 or calcium on CASTOR gating. Nevertheless, an absence of closing of CASTOR in the presence of NADH suggests a binding of NADH possibly to the predicted NAD binding domain keeping the channel in an open configuration. However, the experiment was done at -100 mV in absence of magnesium. Therefore it would be interesting to test whether in presence of both magnesium and NADH, CASTOR stays in an open configuration.

3.4 Hypothetical role of LjSNF7 in the root nodule symbiosis

A combination of *S. cerevisiae* genetics and biochemistry has led to the identification of Snf7 proteins as part of the endosomal sorting complex required for transport of proteins into the intraluminal vesicles of endosomes (Babst et al., 2002). In this process, Snf7 proteins interact with a vacuolar protein-sorting (Vps20) which bind to the endosomal membrane in order to form the endosomal vesicular bodies.

Further studies have linked Snf7 to other signalling pathways which involve or not protein trafficking. Yeast two hybrid analyses and large scale proteomic experiments demonstrate interaction of Snf7 proteins with multiple proteins including a protease, Rim13p, and a calpain-like protease, Rim20p (Gavin et al., 2002; Ito et al., 2001). Rim13p and Rim20p belong to the *RIM101* conserved pathway which confer the ability of fungi to sense and respond to neutral-alkaline environments changes (Davis et al., 2000b; Li et al., 2004). Rim101p is a transcription factor which promotes changes in gene expression, acting as inducer of neutral-alkaline response genes and a repressor of acidic response genes (Bensen et al., 2004; Davis et al., 2000a). Rim20p and Rim13p are

proposed to control activation of the transcription factor Rim101p by cleaving it and releasing the active N-terminal domain which contain the zinc fingers (Xu et al., 2004). Although the exact function of Snf7p in the *RIM101* pathways is unclear, its role as a scaffold protein bringing the proteases Rim20p and Rim13p to the substrate Rim101p is suggested (Xu and Mitchell, 2001).

Homologous LjSNF7 proteins are present in numerous monocotyledones and dicotyledones including *A. thaliana* (Figure 25). Although putative homologs of all the main ESCRT-related proteins have been identified in plants (Winter and Hauser, 2006), only few, excluding the *A. thaliana* putative homologs, have been functionally studied. Nevertheless, the roles of SNF7 proteins described have in common the function to recruit proteins. Therefore, if LjSNF7 protein is a real CASTOR interactor, it potentially could be involved in the recruitment of protein to CASTOR in order to activate CASTOR gating or to anchor CASTOR to the outer nuclear membrane.

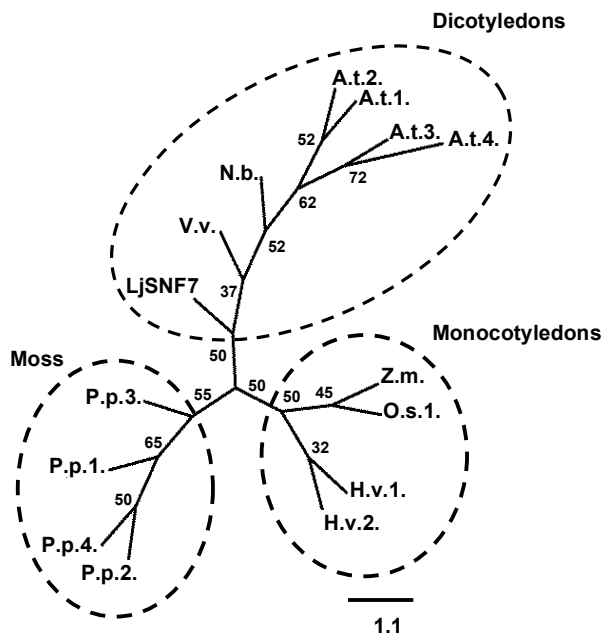


Figure 25. Unrooted radial phylogenetic tree of LjSNF7 homologs.

Homologous full-length protein sequences with E value $\leq 10^{-68}$ were aligned using ClustalX and MacClade programs. The protein tree was constructed using the consensus parsimony method (PHYLIP 3.67 program). Percentage bootstrap support based on 1000 replicates is given to the side of each branch. A.t., *Arabidopsis thaliana*; N.b., *Nicotiana benthamiana*; V.v., *Vitis vinifera*; O.s., *Oryza sativa*; Z.m., *Zea mays*; H.v., *Hordeum vulgare*; P.p., *Physcomitrella patens*. N.b., gi28916459; V.v., gi147855645; A.t.1., gi15220819; A.t.2., gi9802746; A.t.3., gi18410249; A.t.4., gi21537090; Z.m., gi162461720; O.s.1., gi115469156; H.v.1., gi165932189; H.v.2., gi165932187; P.p.1., gi168001188; P.p.2., gi168023705; P.p.3., gi168065046; P.p.4., gi168015068. Bar: number of amino acid substitution per site between two sequence.

3.5 CASTOR and POLLUX are required for calcium spiking

Because Ca^{2+} spiking occurs in both the nucleoplasm and the nuclear associated cytoplasm, the ER and nuclear envelope complex have been proposed to serve as the corresponding Ca^{2+} stores (Oldroyd and Downie, 2006). Collectively, our results demonstrate that CASTOR and POLLUX are cation channels permeable to potassium. Since potassium contributes significantly to endomembrane potentials, an opening of CASTOR and POLLUX is likely to influence the potential of the membrane they reside in. The mutant phenotype and nuclear localization of these channels suggests that they may be part of the Ca^{2+} spiking machinery. Furthermore, the high conductance of CASTOR is similar to that of the potassium channels acting as counter ion channels balancing the positive charge released from the sarcoplasmic reticulum (Wang and Best, 1994). We therefore propose that CASTOR and POLLUX may act as counter ion channels facilitating an influx of potassium, which compensates for the rapid release of positive charge from the calcium store during each spike (Figure 26). A Nod factor-induced ligand may be involved in CASTOR and POLLUX opening, which would be temporally coordinated with the yet-to-be-identified Ca^{2+} channel. To be able to bind the effector, the putative carboxyterminal regulatory domain would have to be exposed to the cyto- or nucleoplasm. The predicted direction of ion flow into the nuclear envelope cavity is consistent with orientation of the pore in such a way that the carboxyterminal portion is exposed to the outside of the nuclear envelope membranes. Magnesium is an ion present in millimolar concentrations within the cyto- and nucleoplasm constitutively available under physiological conditions in the cell (Allen and Sanders, 1996). The Mg^{2+} blockage mechanism is likely to be involved in decreasing CASTOR and POLLUX conductance during spiking, which could lead to a concomitant stop of Ca^{2+} efflux. The calcium store would then be replenished by the activity of calcium ATPases. In previous studies, cyclopiazonic acid, an inhibitor of type IIa calcium-ATPase, inhibited Nod factor induced Ca^{2+} spiking (Engstrom et al., 2002), suggesting their involvement in the generation of Ca^{2+} spiking.

However, due to the potassium permeability of CASTOR and POLLUX, their opening could affect the nuclear membrane potential. In mammals, the membrane potential influences the activation of calcium-induced calcium release channels (Stehno-

Bittel et al., 1995). Therefore, CASTOR and POLLUX may, in addition or alternatively to their role as counter ion channels, be directly involved in regulating electronically coupled Ca^{2+} channels on the same membrane system. In *M. truncatula*, mastoparan was observed to induce Ca^{2+} spiking in wild-type as well as in *dmi1* mutant root hairs (Sun et al., 2007). By interrogation of public sequence databases, we identified a putative *CASTOR* orthologue of *M. truncatula*, *MtCASTOR* (Figure 4). The successful complementation of *castor* with *POLLUX* demonstrates that the twin channels have similar functions. Moreover, quantitative gene expression levels appear to be critical in determining the channel mutant phenotypes. It is therefore possible that the mastoparan-induced Ca^{2+} spiking in the absence of DMI1 works *via* an over-activated *MtCASTOR* sufficient to bypass the requirement for DMI1.

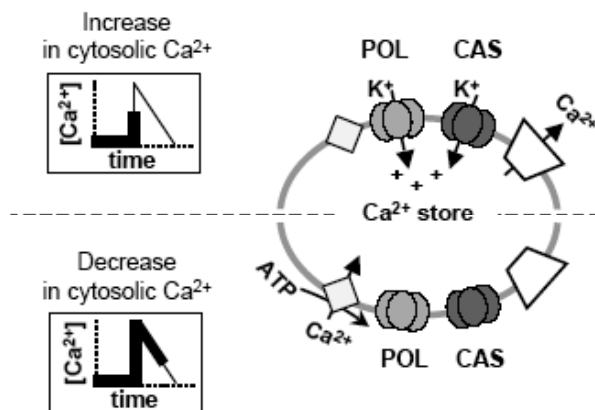


Figure 26. Proposed role of CASTOR and POLLUX as counter ion channels.

During calcium spiking, calcium is released from the nuclear envelope through a yet unidentified calcium channel (white trapezoid). CASTOR and POLLUX facilitate a counter movement of potassium cations to compensate the charge release. A calcium ATPase (white diamond) would then be responsible for actively replenishing the calcium store.

CASTOR and POLLUX are the founder members of a novel cation channel family. Sequence-related genes to *CASTOR* and *POLLUX* are widespread across higher plants. The presence of members in *Arabidopsis thaliana*, an asymbiotic species (Figure 4), suggests additional roles of these classes of potassium permeable channels. Ca^{2+} oscillations are involved in the regulation of different biological process such as pollen tube growth or guard-cell turgor (Franklin-Tong et al., 1996; McAinsh et al., 1995). Interestingly, guard cells can integrate information from multiple stimuli such as abscisic acid, external K^+ or Ca^{2+} , to mount appropriate Ca^{2+} signatures that lead to stomatal

closure (Leckie et al., 1998; McAinsh et al., 1995). It will be interesting to determine whether the *A. thaliana* channels related to CASTOR and POLLUX are involved in the generation of Ca²⁺ oscillations in guard cells.

4. Material and methods

4.1 Material

4.1.1 Plants and chemicals

Lotus japonicus ecotype Gifu accession B-129 (Handberg and Stougaard, 1992), *L. japonicus* ecotype Gifu accession B-129 EMS mutants (Table 2 and Table 3) and *Nicotiana benthamiana* (Wydro et al., 2006) seeds were used in this study.

Chemicals used were purchased from Sigma Aldrich (München, Germany), Roth (Karlsruhe, Germany), Roche (Penzberd, Germany), Merck (Darmstadt, Germany), Amersham Bioscience (Freiburg, Germany) and Invitrogen (Karlsruhe, Germany).

4.1.2 Enzymes and kits

The enzymes used in this study were obtained from New England Biolabs (Frankfurt, Germany), Invitrogen (Karlsruhe, Germany) and MBI Fermentas (St. Leon-Rotl, Germany). For plasmid DNA extraction the NucleoSpin® Plasmid kit from Macherey-Nagel (Düren, Germany) was used. For plant RNA extraction the NucleoSpin RNA Plant kit from Macherey-Nagel (Düren, Germany) was used. For directional cloning strategy the pENTR™ Directional TOPO® cloning Kits from Invitrogen (Karlsruhe, Germany) were used. The *in vitro* transcription-translation was performed with the RTS 100 *E. coli* HY and RTS 500 ProteoMaster *E. coli* HY kits from Roche (Penzberd, Germany).

4.1.3 Strains, oligonucleotides, vectors and clones

The following bacterial and fungal strains have been used in this study: the *E. coli* TOP10, DH5α and DB3.1 (Invitrogen), the *A. tumefaciens* Agl1 (Lazo et al., 1991) and

GV3101pMP90RK (Koncz and Schell, 1986), the *A. rhizogenes* AR1193 (Stougaard et al., 1987b), the yeast AH109 (Clontech), the yeast mutant MAB 2d (Maresova and Sychrova, 2005), the *cch1Δmid1Δ* mutant (Peiter et al., 2005) and *trk1Δ* mutant (ORF Y17000 from Euroscarf collection; http://web.uni-frankfurt.de/fb15/mikro/euroscarf/col_index.html), as well as their respective parental strain JK9-3da (Peiter et al., 2005) and BY4742 (Euroscarf), the *M. loti* R7A (Sullivan et al., 1995) and the *G. intraradices* BEG195 (<http://www.kent.ac.uk/bio/beg/englishhomepage.htm>). The oligonucleotides used were purchased from Metabion (Munich, Germany). The constructs used in this study are listed in the Table 8A and 8B.

Table 8A. Construct used in this study

Localization of CASTOR and POLLUX		
Vectors	Insert	Construct name
pK7FWG2 (Karimi et al., 2002)	<i>CASTOR</i>	1x35S:CASTOR:GFP
pK7FWG2 (Karimi et al., 2002)	<i>POLLUX</i>	1x35S:POLLUX:GFP
pK7RWG2 (Karimi et al., 2002)	<i>TMI_{CAS}</i>	1x35S:TMI _{CAS} :RFP
pK7RWG2 (Karimi et al., 2002)	<i>TMI_{POL}</i>	1x35S:TMI _{POL} :RFP
pamPAT-MCS (GenBank, AY436765)	<i>CASTOR</i>	2x35S:CASTOR:GFP
pamPAT-MCS (GenBank, AY436765)	<i>POLLUX</i>	2x35S:POLLUX:GFP
pK7FWG2 (Karimi et al., 2002)	<i>FNR</i>	1x35S:FNR:GFP
Formation of CASTOR and POLLUX homocomplexes		
Vectors	Insert	Construct name
pAD-GAL4-GW	<i>cCASTOR</i>	AD:cCASTOR
pAD-GAL4-GW	<i>cPOLLUX</i>	AD:cPOLLUX
pBD-GAL4-GW	<i>cCASTOR</i>	BD:cCASTOR
pBD-GAL4-GW	<i>cPOLLUX</i>	BD:cPOLLUX
pBD-GAL4-GW	<i>ccastor-7</i> (V598I)	BD:ccastor-7
pBD-GAL4-GW	<i>ccastor-17</i> (R590H)	BD:ccastor-17
pBD-GAL4-GW	<i>ccastor-28</i> (D537G)	BD:ccastor-28
pBD-GAL4-GW	<i>ccastor-1</i> (ΔLA 479-480)	BD:ccastor-1
pBD-GAL4-GW	<i>ccastor-13</i> (D444N)	BD:ccastor-13
pBD-GAL4-GW	<i>cpollux-7</i> (V531E)	BD:cpollux-7
pBD-GAL4-GW	<i>cpollux-8</i> (W781*)	BD:cpollux-8
pSPYCE 35S-GW (Walter et al., 2004)	<i>CASTOR</i>	CASTOR:C
pSPYCE 35S-GW (Walter et al., 2004)	<i>POLLUX</i>	POLLUX:C
pSPYNE 35S-GW (Walter et al., 2004)	<i>CASTOR</i>	CASTOR:N
pSPYNE 35S-GW (Walter et al., 2004)	<i>POLLUX</i>	POLLUX:N
pSPYCE 35S-GW (Walter et al., 2004)	<i>castor-1</i> (ΔLA 479-480)	castor-1:C
pSPYNE 35S-GW (Walter et al., 2004)	<i>castor-1</i> (ΔLA 479-480)	castor-1:N
pKGWFS7 (Karimi et al., 2002)	Promoter <i>CASTOR</i> (2309 bp)	P _{CAS} :GFP:GUS
pKGWFS7 (Karimi et al., 2002)	Promoter <i>POLLUX</i> (2843 bp)	P _{POL} :GFP:GUS
pRedRoot_P35S:DMI1:GFP (Riely et al., 2007)		
Functional characterization		
Vectors	Insert	Construct name
pTMBV4 (Dualsystems Biotech AG)	<i>CASTOR</i>	pTMBV4:CASTOR
pTMBV4 (Dualsystems Biotech AG)	<i>POLLUX</i>	pTMBV4:POLLUX
pDL2xN (Dualsystems Biotech AG)	<i>CASTOR</i>	pDL2:CASTOR
pDL2xN (Dualsystems Biotech AG)	<i>POLLUX</i>	pDL2:POLLUX
pDEST17 (Invitrogen)	<i>CASTOR:12His</i>	pDEST17:CASTOR
pDEST17 (Invitrogen)	<i>POLLUX:12His</i>	pDEST17:POLLUX
pDEST17 (Invitrogen)	<i>castor-2</i> (A264T):12His	pDEST17:castor-2

Table 8B. Construct used in this study

CASTOR interacting protein		
Vectors	Insert	Construct name
pAD-GAL4-GW	<i>SNF7</i>	AD:50
pAD-GAL4-GW	<i>84</i>	AD:84
pAD-GAL4-GW	<i>64</i>	AD:64
pBD-GAL4-GW	<i>SNF7</i>	BD:50
pBD-GAL4-GW	<i>84</i>	BD:84
pBD-GAL4-GW	<i>64</i>	BD:64
pUB-GWS-GFP (Maekawa et al., 2008)	<i>SNF7</i>	pUB-GWS50-GFP
pK7RWG2 (Karimi et al., 2002)	<i>SNF7</i>	P35S:SNF7:RFP
p K7RWG2 (Karimi et al., 2002)	<i>TP_{CAS}</i>	<i>TP_{CAS}:RFP</i>

4.1.4 Antibodies

The protein expression levels were monitored by immunoblotting using the antibodies gathered in Table 9.

Table 9. Antibodies used in this study.

Antibodies		Dilution
Primary antibodies		
Mouse monoclonal anti-BD	(Clontech)	1:1000
Mouse monoclonal anti-c-MYC	(Roche)	1:5000
Mouse monoclonal anti-HA	(Roche)	1:5000
Rabbit polyclonal anti-CASTOR	(Eurogentec)	1:200
Secondary antibodies		
IRDye800-conjugated anti-mouse IgG	(Biomol)	1:10 000
Alexa Fluor 680 anti-rabbit IgG	(Invitrogen)	1:10 000
HRP conjugated anti- rabbit IgG	(Amersham)	1: 20 000

4.2 Methods

4.2.1 Bioinformatics

Assembly of sequences and mutation detection were performed using the software Staden Package (<http://staden.sourceforge.net/>).

CASTOR and *POLLUX* gene structures from start to stop codons were predicted using the CODDLE (Codons Optimized to Discovered Deleterious Lesions) program (<http://www.proweb.org./coddle>).

To find homologous genes and conserved domains, sequences were analysed by BLAST (<http://www.ncbi.nlm.nih.gov/BLAST/>), Membrane protein explorer (<http://blanco.biomol.uci.edu/mpex/>), EMBL nucleotide sequence database (<http://www.ebi.ac.uk/embl/>) and Pfam (<http://www.sanger.ac.uk/software/Pfam/>). Localization signals were predicted by TargetP version 1.01 (<http://www.cbs.dtu.dk/services/targetP/>) and WolfPsort (<http://wolfpsort.org/>).

Regarding the phylogenetic analyses, ClustalX and MacClade were used to produce the protein sequence alignment. The consensus parsimony tree was conducted using PHYLIP 3.67 and displayed using FigTree v1.0. The reliability of the tree was estimated using the bootstrapping method with 1000 replicates and a random number generator seed 111.

Sequence-structure homology search was performed using FUGUE v2.0 against a library of 9673 proteins (Shi et al., 2001). The modelisation was analysed using the DeepView Swiss-PdbViewer (<http://www.expasy.org/spdbv/>).

4.2.2 Genetics methods

The map-based cloning of *CASTOR* was initiated with two populations: an intraspecific cross between *L. japonicus* Gifu mutant EMS1749 (*castor-2*) and *L. japonicus* “Miyakojima”, and an interspecific cross between *L. japonicus* Gifu mutant EMS1749 (*castor-2*) and *L. filicaulis*. F2 individuals were previously screened with amplified

fragment length polymorphism (AFLP) markers which resulted in located *CASTOR* at the south telomeric region of chromosome one (L. Mulder). From one AFLP marker P21M44 cosegregating with *CASTOR*, a cleaved amplified polymorphic sequence (CAPS) marker P21M44/*Nla*III was developed and positioned by screening the F2 population to 0.07 cM north of *CASTOR* on the TAC LjT02K14 or M3 (Figure 2A). Given that the *Lotus* genome size is 367 cM (Sandal et al., 2002) or 432 Mb (1 cM = 1.2 Mb), this marker was evaluated at 82 Kb from *CASTOR* which justified a BAC/TAC library screening. As no BAC or TAC could be identified or available, a phage library screening was performed. The Lambda FIXTM IICustom *L. japonicus* B-129 genomic library (Stratagene; J. Stougaard) was screened using the P21M44 marker according to the user manual (<http://www.stratagene.com/manuals/936001.pdf>).

4.2.3 Molecular biological methods

4.2.3.1 General molecular biological methods

The general molecular biological methods including bacteria electroporation, bacteria growth culture, DNA extraction, DNA precipitation, restriction digest, ligation, agarose gel electrophoresis were performed as described (Sambrook and Russell, 2001). Thereby, the reaction conditions were adjusted to the recommendations of manufacturers. The Nanodrop-1000 spectrophotometer (www.nanodrop.com) was used to determine DNA and RNA amount.

4.2.3.2 TILLING

TILLING was carried out using the general TILLING population and the pre-selected nodule mutant population described previously (Perry et al., 2003). Primers amplifying a 1-1.5 kb region were designed using the CODDLE program to identify the region that had the maximum likelihood of being affected by EMS mutation to produce a deleterious allele. *CASTOR* and *POLLUX*-specific forward and reverse primers were directly labelled with the fluorescent dyes 6-carboxyfluorescein and 4,7,2',7'-tetrachloro-6-carboxyfluorescein, respectively, for analysis with an ABI377 sequencer as previously described (Perry et al., 2003).

Genomic DNA isolated from the two populations was diluted to 5ng/μL. Normalized DNA was pooled 4-fold and 1 μL pooled DNA was used in 10 μL PCR reaction using the labelled primers as described (Colbert et al., 2001), but without the addition of unlabeled primers. The touchdown PCR program used was; 95°C 2 min, 7 x [94°C 20s, T_m + 3°C to T_m - 4°C for 30s, -1°C per cycle, gradient to 72°C at 0.5°C/s, 72°C 1 min], 44 x [94°C 20s, T_m-5°C 30s, gradient to 72°C at 0.5°C/s, 72°C 1 min], 69 x [72°C 5 min, 99°C 10 min, 70°C for 20s, -0.3°C per cycle], 15 °C for ever, with an annealing temperature (T_m) of 65°C.

4.2.3.3 Cloning strategies

PCR fragments containing a 3'-A overhangs were cloned into the pGEM®-T Easy vector (Promega) according to the user manual (www.promega.com). For expression in eukaryotic system, cDNA were excised from the pGEM®-T Easy vector with compatible restriction enzyme and subcloned as described (Sambrook and Russell, 2001).

PCR fragments containing a 5'-CACC overhang were cloned into the Gateway entry vectors pENTR/SD/D-TOPO® or pENTR/D-TOPO® (Invitrogen), and subsequently subcloned into destination expression vectors for prokaryotic and eukaryotic expression according to the user manual (<http://www.invitrogen.com/>).

4.2.3.4 RNA isolation

RNA isolation from *L. japonicus* roots was performed according to the user manual (http://www.mn-net.com/Portals/8/attachments/Redakteure_Bio/Protocols/RNA%20and%20mRNA/UM_TotalRNAPlant.pdf).

4.2.3.5 Reverse transcription (RT)-PCR, Rapid Amplification of cDNA ends (RACE)-PCR and quantitative Reverse Transcription (qRT)-PCR

The RT- and RACE-PCR were done following the user manual of SMART™ RACE cDNA Amplification from Clontech (<http://www.genex.cl/stock/clon634914.html>), whereas the qRT-PCR was performed with 100 ng of RNA following the instruction of the manufacturer, Invitrogen (http://tools.invitrogen.com/content/sfs/manuals/superscript_2_step_qrtPCR_sybr_man.pdf).

4.2.3.6 Site directed mutagenesis

The mutations were generated by site directed mutagenesis as described (Horton et al., 1989).

4.2.3.7 Yeast transformation methods

Yeast two hybrid library screening and interaction analyses were performed in the yeast strain AH109 according to the user manual (Yeast Protocols Handbook, PT3024-1, Clontech).

AH109, *trk1* Δ , BY4742, *cch1* Δ *mid1* Δ , JK9-3da and MAB 2d yeast strains were transformed using the lithium acetate method (Gietz and Woods, 2001). Transformants were screened on SD medium containing 0.67% yeast nitrogen base, 2% glucose, and lacking appropriate nutrients.

4.2.4 Biochemical methods

4.2.4.1 General biochemical methods

The protein concentration was determined by Bradford assay (Bradford, 1976) using the Bio-rad protein assay dye reagent concentrate according to the manufacturer manual (<http://www.technomedica.com/publikazii/belur/Bio-Rad.pdf>). Precipitation of protein by acetone or trichloroacetic acid, SDS-PAGE and gel staining by Coomassie Brilliant Blue R250, were done according to published procedures (Sambrook and Russell, 2001). For immunodetection proteins were transferred on polyvinylidene fluoride (PVDF) membrane (Amersham) by electroblotting. Immunodecoration and detection either by using the alkaline phosphatase system or infrared fluorescence were performed according to (Sambrook and Russell, 2001).

4.2.4.2 Protein extraction from *L. japonicus* root

In order to get the total protein extract from *L. japonicus* roots, 3-week-old roots were ground with liquid nitrogen, subsequently mixed with extraction buffer (100 mM Tris-HCl pH 7.2, 150 mM NaCl, 5 mM EDTA, 10 mM DTT, 5% SDS, 4 M Urea) and boiled

10 min. Debris were precipitated before adding 2xSDS sample buffer and loading 10% SDS-PAGE.

4.2.4.3 Protein extraction from *N. benthamiana* leaves

Total crude protein from 2 cm² of transformed leaves was extracted as described (Walter et al., 2004).

4.2.4.4 Protein extraction from *S. cerevisiae*

The crude yeast protein extraction was performed as described in the user manual (DUALmembrane kit 3, P01001, Dualsystems Biotech) with the following modifications; 50 mL of selective media were inoculated with 500 µL of preculture at 30°C until OD₆₀₀ reaches 0.6.

4.2.4.5 *In vitro* expression and purification

CASTOR, *castor-2* and *POLLUX* coding sequence were subcloned into the pDEST17 vector (Invitrogen). To test the expression of *CASTOR* and *POLLUX* in a cell free system, a rapid expression screen was performed with the RTS 100 *E. coli* HY kit (Roche) according to the manufacturer instructions. To scale up the protein amount, *CASTOR* and *castor-2* were expressed using the RTS 500 ProteoMaster *E. coli* HY Kit (Roche) according to the manufacturer instructions. The solubilization and purification of proteins were performed by selective solubilization. The pellets of the cell-free reaction containing *CASTOR* or *castor-2* were washed twice in 1 mL of washing buffer (100 mM NaH₂PO₄, 10 mM Tris, pH 7.2) and centrifuged for 5 min at 5000 g. To remove *E. coli* proteins, the pellet was suspended in *E. coli* protein solubilization buffer (100 mM NaH₂PO₄, 2% MEGA-9, 10 mM Tris, pH 7.2), 45 min at 40°C under shaking and centrifuged for 30 min at 50,000 g. This step was repeated twice. Protein was solubilized in 100 mM NaH₂PO₄, 0,05 % SDS, 10 mM Tris, pH 7.2) for 2 h at room temperature with shaking. Insoluble proteins were precipitated by centrifugation for 30 min at 50,000 g.

4.2.5 Electrophysiological methods

Purified CASTOR proteins were dialysed against 100 mM NaH₂PO₄, 10 mM Tris, 8 M urea pH 7.2 for 2h at room temperature. To remove any remaining SDS, the dialysed proteins were incubated with Serdolit® PAD I beads (SERVA) for 3 hours. The protein concentrations were determined by Bradford assays (Biorad).

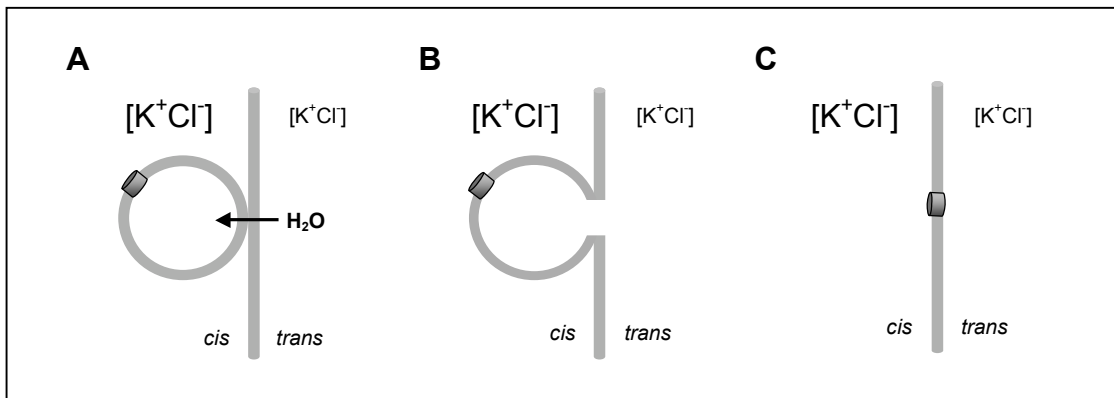


Figure 27. Representation of the fusion of proteoliposome with the planar lipids bilayer.

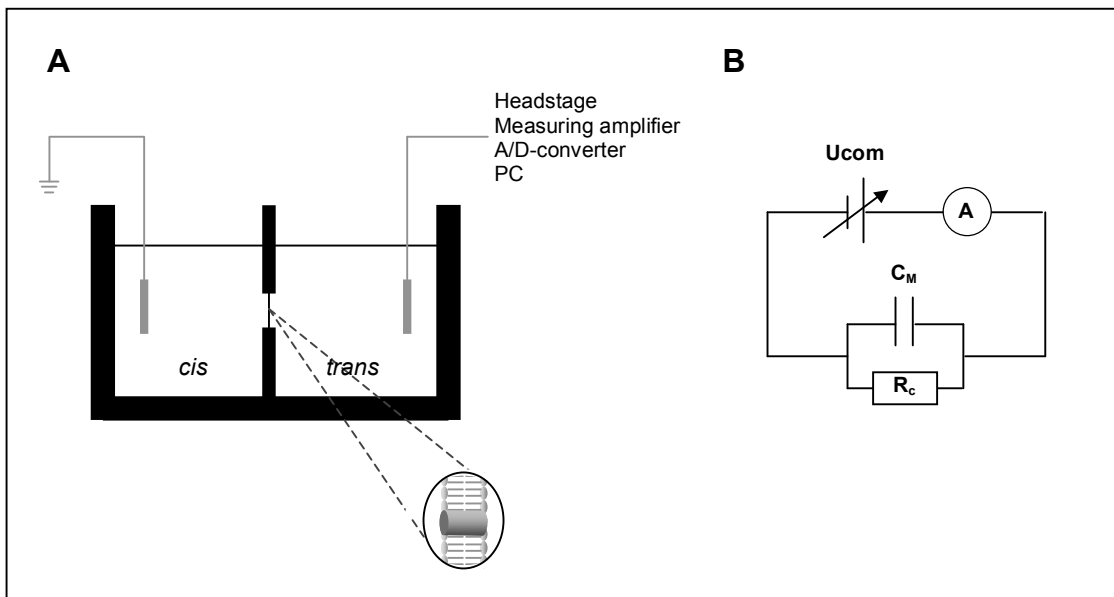


Figure 28. Lipid-bilayer-measurement system.

(A) Representation schematic of the system. An ion channel is inserted in a lipid bilayer which split the *cis* and *trans* chambers. In each chamber, ion solution is exchanged by perfusion (B) Electrical view of the system. A; Amperemeter, Ucom; voltage generator, C_M; lipid bilayer as a capacitor, R_c; canal protein as a resistor.

The reconstitution of proteoliposomes and electrophysiological measurements were performed according to (Ertel et al., 2005) with the following modification: after

formation of a stable lipid bilayer, the solution of the *cis* chamber was exchanged with 250 mM KCl, 10 mM MOPS/Tris, pH 7.0. After fusion of the proteoliposome to the planar lipid bilayer (Figure 27), the recording of the reverse potential was done in a 10 mM MOPS/Tris, pH 7.0 solutions containing in the *cis/trans* chambers (Figure 28) either 250 mM/20 mM KCl, 250 mM/20 mM NaCl or 125 mM/10 mM CaCl₂. The conductance and current properties were determined in equal solutions of 250 mM KCl, 10 mM MOPS/Tris, pH 7.0. The background noise of the bilayer was around 8 pS.

4.2.6 Plant transformation methods

4.2.6.1 *A. tumefaciens* mediated transient transformation

BiFC and localization of the GFP fusion proteins were performed in 5-week-old *Nicotiana benthamiana* plants following *Agrobacterium tumefaciens* GV3101pMP90RK (Koncz and Schell, 1986) and *Ag1* strain-mediated transient transformation, respectively, according to (Lazo et al., 1991; Walter et al., 2004).

4.2.6.2 *A. rhizogenes*-mediated transient transformation

The *A. rhizogenes* strain AR1193 (Stougaard et al., 1987a) was used to transform *Lotus japonicus* (ecotype Gifu) wild type and mutant. Seeds were sterilised as previously described (Hansen et al., 1989) and incubated at 4°C overnight, followed by germination on B5 medium (Gamborg et al., 1968) in a growth chamber (3 days dark, 3 days short light, 70% humidity, 24°C). The emerging roots were cut and hypocotyls dipped in AR1193 carrying the relevant plasmids (OD₆₀₀=1). Transformed plants were grown on B5 medium (containing 40 mg/mL kanamycin for plants transformed with the BiFC construct) in a growth chamber (2 days dark/3 days short light), and then transferred to B5 medium containing cefotaxim (300 mg/mL). Shoots with developed hairy roots were dipped into a dilution of a *Mesorhizobium loti* strain R7A culture (OD₆₀₀=0.01) and transplanted into sterile pots containing 300 mL of seramis (Seramis®) and 100 mL Fahraeus medium (Fahraeus, 1957). Regarding the silencing experiments, the untransformed roots were cut before inoculation with *M. loti* R7A strain to avoid autoregulatory inhibition of nodule formation (Caetano-Anolles and Gresshoff, 1991).

4.2.7 Cell biological methods

4.2.7.1 *L. japonicus* cell culture protoplast transfection

L. japonicus protoplasts were isolated from 5-day-old cell culture. 50 mL of cell culture was harvested at 860 g, 3 min, washed in 25 mL 240 mM CaCl₂ solution and subsequently incubated in enzyme solution containing 3.5% Cellulase (Onozuka R10), 0.6% Macerozyme (Serva R-10) in 240 mM CaCl₂, 14h, 24°C, under 60 rpm shaking. The protoplasts were filtered through 40 µm nylon mesh, precipitated 3 min at 860 g, and washed with 240 mM CaCl₂. The pellet was resuspended in 25 mL P5 medium (1x Gamborg B5 medium, 283 mM sucrose, 4.5 µM 2,4 Dichlorophenoxyacetic acid, pH 5.7 with NaOH). The protoplast solution was centrifuged at 300 g 5 min. The floating protoplasts were harvested and diluted in 15 mL P5 medium to be centrifuged 5 min at 300 g.

The density of viable protoplasts was evaluated by counting the protoplast stained with 0.24 µM Fluorescein diacetate in a Mallassez counting chamber. The following calculation was applied: if (a) represents the dilution of the sample and (n) the total number of cells in a unit sample with a volume of (b), then, the load, expressed in millions of cells per mL, can be calculated by using the equation: millions of cells/mL = $a \times n / b \times 4$.

A minimum amount of 10⁶ protoplasts in a 200 µL volume were transfected as follows: in a 2 mL eppendorf tubes 10 to 30 µg DNA, 10 µg salmon sperm single stranded DNA, 200 µL protoplasts, 200 µL polyethylene glycol (PEG) solution (25% PEG6000, 100 mM Ca(NO₃)₂, 450 mM mannitol, pH 9.0 with KOH) were added in this order before shaking. The reaction was incubated 30 min. The protoplasts were precipitated with 1.5 mL 275 mM Ca(NO₃)₂ 30s at 860 g, to be finally resuspended in 0.5 mL P5 medium. The results were checked after 24h incubation at 24°C.

4.2.8 Histochemical methods

4.2.8.2 Immunogold electron microscopy

CASTOR and POLLUX peptides antibodies were raised in rabbits against the peptides: H₂N-SSPSQYGRRFHTNSNT-CONH₂ and H₂N-CRRGSLPKDFVYPKSP-CONH₂ for CASTOR, and H₂N-TTRKRRPSSVKPPST-CONH₂ and H₂N-GFFPRIPDAPKYPEK-CONH₂ for POLLUX. One-week-old seedlings were used for immunogold electron microscopy. Pieces of roots were fixed immediately after collection with 2.5% formaldehyde in 75 mM sodium cacodylate, 2 mM MgCl₂, pH 7.0 for 2 h at room temperature. The tissue was washed 4 times at room temperature with 1% glycine, 2.5% formaldehyde in 75 mM sodium cacodylate, 2 mM MgCl₂, pH 7.0. After two washing steps in distilled water, the tissue pieces were dehydrated with a graded series of acetone (20-100%). Tissue samples were then infiltrated and embedded in Spurr's low-viscosity resin. After polymerisation, sections with a thickness of 70-90 nm were cut with a diamond knife and mounted on collodion-coated nickel grids. Ultra-thin sections were incubated first in 50 mM glycine in PBS buffer (136 mM NaCl, 2 mM KCl, 4 mM Na₂HPO₄, 1 mM KH₂PO₄, pH 7.4) for 20 min, then in blocking buffer (0.5% BSA, 0.01% Tween 20, 0.05% gelatine, in PBS buffer) for 1 h. Sections were incubated with purified anti-CASTOR serum (Eurogentec) in blocking buffer (diluted 1:20 to 1:100) overnight at 4°C. After six washing steps with blocking buffer, anti-rabbit-IgG conjugated with 5 nm gold (Sigma) was added at a dilution of 1:20 (with blocking buffer) and incubated for 90 min at room temperature. After three washings with blocking buffer, 1% glycine in PBS buffer and distilled water, sections were post stained with aqueous lead citrate. The sections were used either unstained or post stained with aqueous lead citrate (100 mM, pH 13.0). Micrographs were taken with a Zeiss EM 912 electron microscope equipped with an integrated OMEGA energy filter operated in the zero loss mode. Gold particles were counted on 15 micrographs (magnification 40000x) as described (Lucocq, 1994). For the nuclear envelope, the "covered area" was a 5 mm wide strip around the nucleus. The surface of each organelle was calculated and normalized as percentage of the cell. The density of gold particles was calculated by dividing the number of gold particles in each compartment by their normalized surface (in percentage).

4.2.8.2 GUS assay

To performed the GUS staining, transformed seedlings were incubated 40 min at 37 °C with 2 mM 5-bromo-4-chloro-3-indolyl-b-glucuronic acid, 50 mM NaPO₄ pH 7, 1 mM EDTA, 0,1 % Triton X-100 and subsequently washed in 70 % ethanol.

4.2.8.3 Mycorrhiza staining

Root fragments 2 cm long were incubated in 0.8 mL, 96-well plate (ABgene House). The staining was performed with black ink according to (Kosuta et al., 2005).

4.2.9 Fungal and bacterial inoculation methods

4.2.9.1 Inoculation with *G. intraradices*

The *Glomus intraradices* infection has been performed in the chive nurse pot system. Two young chive plants preliminarily infected by *G. intraradices* according to (Kosuta et al., 2005), are grown in pots of 8.5 cm³ containing substrate composed of a 1:1 v/v mixture of vermiculite and Quartz sand. After two to six weeks, *L. japonicus* 2-week-old seedlings are transferred or scarified non-germinated seeds are sown directly in the nurse chive pots. Once a week the chive nurses are watered with nutrient solution (24.65 mg/L MgSO₄-7H₂O, 5.05 mg/L KNO₃, 0.115 mg/L KH₂PO₄, 0.725 mg/L K₂HPO₄, 18.55 mg/L CaCl₂.2H₂O, 0.0715 mg/L H₃BO₃, 0.051 mg/L MnSO₄.4H₂O, 0.011 mg/L ZnSO₄.7H₂O, 0.004 mg/L CuSO₄.5H₂O, 0.0025 mg/L Na₂MoO₄.5H₂O, 0.005 mg/L CoCl₂.4H₂O, 0.835 mg/L Fe-EDTA-di-hydroxy-phenylacetate). The development of arbuscules is checked after 3 weeks.

4.2.9.2 Inoculation with *M. loti*

M. loti strain R7A colony is grown two days at 30°C in TY medium (5 g/L Bacto triptone, 5 g/L Yeast extract, 6 mM CaCl₂). The bacteria are pelleted by centrifugation at 8000 rpm 2 min, washed in saline (0.8% NaCl) 2 times, and resuspended at OD₆₀₀ = 0.01 before inoculation.

5. References

- Akiyama, K., Matsuzaki, K. and Hayashi, H. (2005) Plant sesquiterpenes induce hyphal branching in arbuscular mycorrhizal fungi. *Nature*, **435**, 824-827.
- Albrecht, C., Geurts, R. and Bisseling, T. (1999) Legume nodulation and mycorrhizae formation; two extremes in host specificity meet. *Embo J*, **18**, 281-288.
- Alexander, T., Meier, R., Toth, R. and Weber, H.C. (1988) Dynamics of arbuscule development and degeneration in mycorrhizas of *Triticum aestivum* L. and *Avena sativa* L. with reference to *Zea mays* L. *New Phytologist*, **110**, 363-370.
- Allen, G.J. and Sanders, D. (1996) Control of ionic currents in guard cell vacuoles by cytosolic and luminal calcium. *Plant J*, **10**, 1055-1069.
- Ane, J.M., Kiss, G.B., Riely, B.K., Penmetsa, R.V., Oldroyd, G.E., Ayax, C., Levy, J., Debelle, F., Baek, J.M., Kalo, P., Rosenberg, C., Roe, B.A., Long, S.R., Denarie, J. and Cook, D.R. (2004) Medicago truncatula DMI1 required for bacterial and fungal symbioses in legumes. *Science*, **303**, 1364-1367.
- Arazi, T., Kaplan, B. and Fromm, H. (2000) A high-affinity calmodulin-binding site in a tobacco plasma-membrane channel protein coincides with a characteristic element of cyclic nucleotide-binding domains. *Plant Mol Biol*, **42**, 591-601.
- Ardourel, M., Demont, N., Debelle, F., Mailliet, F., de Billy, F., Prome, J.C., Denarie, J. and Truchet, G. (1994) Rhizobium meliloti lipooligosaccharide nodulation factors: different structural requirements for bacterial entry into target root hair cells and induction of plant symbiotic developmental responses. *Plant Cell*, **6**, 1357-1374.
- Armstrong, C.M., Swenson, R.P., Jr. and Taylor, S.R. (1982) Block of squid axon K channels by internally and externally applied barium ions. *J Gen Physiol*, **80**, 663-682.
- Babst, M., Katzmann, D.J., Estepa-Sabal, E.J., Meerloo, T. and Emr, S.D. (2002) Escrt-III: an endosome-associated heterooligomeric protein complex required for mvb sorting. *Dev Cell*, **3**, 271-282.
- Baptiste, E., Charlebois, R.L., MacLeod, D. and Brochier, C. (2005) The two tempos of nuclear pore complex evolution: highly adapting proteins in an ancient frozen structure. *Genome Biol*, **6**, R85.
- Bensen, E.S., Martin, S.J., Li, M., Berman, J. and Davis, D.A. (2004) Transcriptional profiling in *Candida albicans* reveals new adaptive responses to extracellular pH and functions for Rim101p. *Mol Microbiol*, **54**, 1335-1351.
- Besserer, A., Puech-Pages, V., Kiefer, P., Gomez-Roldan, V., Jauneau, A., Roy, S., Portais, J.C., Roux, C., Becard, G. and Sejalón-Delmas, N. (2006) Strigolactones stimulate arbuscular mycorrhizal fungi by activating mitochondria. *PLoS Biol*, **4**, e226.
- Bezanilla, F. (2000) The voltage sensor in voltage-dependent ion channels. *Physiol Rev*, **80**, 555-592.
- Bhandal, I.S. and Malik, C.P. (1988) Potassium estimation, uptake, and its role in the physiology and metabolism of flowering plants. *International Review of Cytology*, **110**, 205-254.
- Blatt, M.R., Thiel, G. and Trentham, D.R. (1990) Reversible inactivation of K⁺ channels of *Vicia* stomatal guard cells following the photolysis of caged inositol 1,4,5-trisphosphate. *Nature*, **346**, 766-769.

- Bonfante, P., Genre, A., Faccio, A., Martini, I., Schauser, L., Stougaard, J., Webb, J. and Parniske, M. (2000) The Lotus japonicus LjSym4 gene is required for the successful symbiotic infection of root epidermal cells. *Mol Plant Microbe Interact*, **13**, 1109-1120.
- Bradford, M.M. (1976) A rapid and sensitive method for the quantitation of microgram quantities of protein utilizing the principle of protein-dye binding. *Anal Biochem*, **72**, 248-254.
- Buee, M., Rossignol, M., Jauneau, A., Ranjeva, R. and Becard, G. (2000) The pre-symbiotic growth of arbuscular mycorrhizal fungi is induced by a branching factor partially purified from plant root exudates. *Mol Plant Microbe Interact*, **13**, 693-698.
- Caetano-Anolles, G. and Gresshoff, P.M. (1991) Plant genetic control of nodulation. *Annu Rev Microbiol*, **45**, 345-382.
- Calero, F., Gomez, N., Arino, J. and Ramos, J. (2000) Trk1 and Trk2 define the major K(+) transport system in fission yeast. *J Bacteriol*, **182**, 394-399.
- Cardenas, L., Dominguez, J., Quinto, C., Lopez-Lara, I.M., Lugtenberg, B.J., Spaink, H.P., Rademaker, G.J., Haverkamp, J. and Thomas-Oates, J.E. (1995) Isolation, chemical structures and biological activity of the lipo-chitin oligosaccharide nodulation signals from Rhizobium etli. *Plant Mol Biol*, **29**, 453-464.
- Cardenas, L., Feijo, J.A., Kunkel, J.G., Sanchez, F., Holdaway-Clarke, T., Hepler, P.K. and Quinto, C. (1999) Rhizobium nod factors induce increases in intracellular free calcium and extracellular calcium influxes in bean root hairs. *Plant J*, **19**, 347-352.
- Cardenas, L., Vidali, L., Dominguez, J., Perez, H., Sanchez, F., Helper, P.K. and Quinto, C. (1998) Rearrangement of actin microfilaments in plant root hairs responding to Rhizobium etli nodulation signals. *Plant Physiology*, **116**, 871-877.
- Carlson, R.W., Forsberg, L.S., Price, N.P., Bhat, U.R., Kelly, T.M. and Raetz, C.R. (1995) The structure and biosynthesis of Rhizobium leguminosarum lipid A. *Prog Clin Biol Res*, **392**, 25-31.
- Catoira, R., Galera, C., de Billy, F., Penmetsa, R.V., Journet, E.P., Maillet, F., Rosenberg, C., Cook, D., Gough, C. and Denarie, J. (2000) Four genes of Medicago truncatula controlling components of a nod factor transduction pathway. *Plant Cell*, **12**, 1647-1666.
- Catoira, R., Timmers, A.C., Maillet, F., Galera, C., Penmetsa, R.V., Cook, D., Denarie, J. and Gough, C. (2001) The HCL gene of Medicago truncatula controls Rhizobium-induced root hair curling. *Development*, **128**, 1507-1518.
- Chabaud, M., Vénard, C., Defaux-Petras, A., Bécard, G. and Barker, D.G. (2002) Targeted inoculation of Medicago truncatula in vitro root cultures reveals MtENOD11 expression during early stages of infection by arbuscular mycorrhizal fungi. *New Phytologist*, **156**, 265-273.
- Charron, D., Pingret, J.L., Chabaud, M., Journet, E.P. and Barker, D.G. (2004) Pharmacological evidence that multiple phospholipid signaling pathways link Rhizobium nodulation factor perception in Medicago truncatula root hairs to intracellular responses, including Ca²⁺ spiking and specific ENOD gene expression. *Plant Physiol*, **136**, 3582-3593.
- Cherel, I., Michard, E., Platet, N., Mouline, K., Alcon, C., Sentenac, H. and Thibaud, J.B. (2002) Physical and functional interaction of the Arabidopsis K(+) channel AKT2 and phosphatase AtPP2CA. *Plant Cell*, **14**, 1133-1146.

- Christie, M.J. (1995) Molecular and functional diversity of K⁺ channels. *Clin Exp Pharmacol Physiol*, **22**, 944-951.
- Colbert, T., Till, B.J., Tompa, R., Reynolds, S., Steine, M.N., Yeung, A.T., McCallum, C.M., Comai, L. and Henikoff, S. (2001) High-throughput screening for induced point mutations. *Plant Physiol*, **126**, 480-484.
- Covarrubias, M., Wei, A., Salkoff, L. and Vyas, T.B. (1994) Elimination of rapid potassium channel inactivation by phosphorylation of the inactivation gate. *Neuron*, **13**, 1403-1412.
- Davenport, R.J. and Tester, M. (2000) A weakly voltage-dependent, nonselective cation channel mediates toxic sodium influx in wheat. *Plant Physiol*, **122**, 823-834.
- Davis, D., Edwards, J.E., Jr., Mitchell, A.P. and Ibrahim, A.S. (2000a) *Candida albicans* RIM101 pH response pathway is required for host-pathogen interactions. *Infect Immun*, **68**, 5953-5959.
- Davis, D., Wilson, R.B. and Mitchell, A.P. (2000b) RIM101-dependent and-independent pathways govern pH responses in *Candida albicans*. *Mol Cell Biol*, **20**, 971-978.
- de Ruijter, N.C.A., Rook, M.B., Bisseling, T. and Emons, A.M.C. (1998) Lipochito-oligosaccharides re-initiate root hair tip growth in *Vicia sativa* with high calcium and spectrin-like antigen at the tip. *Plant Journal*, **13**, 341-350.
- Demidchik, V., Davenport, R.J. and Tester, M. (2002) Nonselective cation channels in plants. *Annu Rev Plant Biol*, **53**, 67-107.
- Demidchik, V. and Tester, M. (2002) Sodium fluxes through nonselective cation channels in the plasma membrane of protoplasts from *Arabidopsis* roots. *Plant Physiol*, **128**, 379-387.
- den Hartog, M., Musgrave, A. and Munnik, T. (2001) Nod factor-induced phosphatidic acid and diacylglycerol pyrophosphate formation: a role for phospholipase C and D in root hair deformation. *Plant J*, **25**, 55-65.
- den Hartog, M., Verhoef, N. and Munnik, T. (2003) Nod factor and elicitors activate different phospholipid signaling pathways in suspension-cultured alfalfa cells. *Plant Physiol*, **132**, 311-317.
- Doyle, J.J. (1998) Phylogenetic perspectives on nodulation: evolving views of plants and symbiotic bacteria. *Trends Plant Science*, **3**, 473-478.
- Drain, P., Dubin, A.E. and Aldrich, R.W. (1994) Regulation of Shaker K⁺ channel inactivation gating by the cAMP-dependent protein kinase. *Neuron*, **12**, 1097-1109.
- Drissner, D., Kunze, G., Callewaert, N., Gehrig, P., Tamasloukht, M., Boller, T., Felix, G., Amrhein, N. and Bucher, M. (2007) Lyso-phosphatidylcholine is a signal in the arbuscular mycorrhizal symbiosis. *Science*, **318**, 265-268.
- Ehrhardt, D.W., Atkinson, E.M. and Long, S.R. (1992) Depolarization of alfalfa root hair membrane potential by *Rhizobium meliloti* Nod factors. *Science*, **256**, 998-1000.
- Ehrhardt, D.W., Wais, R. and Long, S.R. (1996) Calcium spiking in plant root hairs responding to *Rhizobium* nodulation signals. *Cell*, **85**, 673-681.
- Endre, G., Kereszt, A., Kevei, Z., Mihacea, S., Kalo, P. and Kiss, G.B. (2002) A receptor kinase gene regulating symbiotic nodule development. *Nature*, **417**, 962-966.
- Engstrom, E.M., Ehrhardt, D.W., Mitra, R.M. and Long, S.R. (2002) Pharmacological analysis of nod factor-induced calcium spiking in *Medicago truncatula*. Evidence for the requirement of type IIA calcium pumps and phosphoinositide signaling. *Plant Physiol*, **128**, 1390-1401.

- Ertel, F., Mirus, O., Bredemeier, R., Moslavac, S., Becker, T. and Schleiff, E. (2005) The evolutionarily related beta-barrel polypeptide transporters from *Pisum sativum* and *Nostoc PCC7120* contain two distinct functional domains. *J Biol Chem*, **280**, 28281-28289.
- Esseling, J.J., Lhuissier, F.G. and Emons, A.M. (2003) Nod factor-induced root hair curling: continuous polar growth towards the point of nod factor application. *Plant Physiol*, **132**, 1982-1988.
- Fahraeus, G. (1957) The infection of clover root hairs by nodule bacteria studied by a simple glass slide technique. *J Gen Microbiol*, **16**, 374-381.
- Felle, H.H., Kondorosi, E., Kondorosi, A. and Schultze, M. (1995) Nod signal-induced plasma membrane potential changes in alfalfa root hairs are differentially sensitive to structural modifications of the lipochitooligosaccharide. *Plant Journal*, **7**, 939-947.
- Felle, H.H., Kondorosi, E., Kondorosi, A. and Schultze, M. (1996) Rapid alkalization in alfalfa root hairs in response to rhizobial lipochitooligosaccharide signals. *Plant Journal*, **10**, 295-301.
- Felle, H.H., Kondorosi, E., Kondorosi, A. and Schultze, M. (1998) The role of ion fluxes in Nod factor signalling in *Medicago sativa*. *Plant Journal*, **13**, 455-463.
- Fischer, M., Schnell, N., Chattaway, J., Davies, P., Dixon, G. and Sanders, D. (1997) The *Saccharomyces cerevisiae* CCH1 gene is involved in calcium influx and mating. *FEBS Lett*, **419**, 259-262.
- Fisher, R.F. and Long, S.R. (1992) Rhizobium--plant signal exchange. *Nature*, **357**, 655-660.
- Franklin-Tong, V.E., Drobak, B.K., Allan, A.C., Watkins, P. and Trewavas, A.J. (1996) Growth of Pollen Tubes of *Papaver rhoeas* Is Regulated by a Slow-Moving Calcium Wave Propagated by Inositol 1,4,5-Trisphosphate. *Plant Cell*, **8**, 1305-1321.
- Fukami, K. (2002) Structure, regulation, and function of phospholipase C isozymes. *J Biochem*, **131**, 293-299.
- Furuichi, T., Yoshikawa, S., Miyawaki, A., Wada, K., Maeda, N. and Mikoshiba, K. (1989) Primary structure and functional expression of the inositol 1,4,5-trisphosphate-binding protein P400. *Nature*, **342**, 32-38.
- Gaber, R.F., Styles, C.A. and Fink, G.R. (1988) TRK1 encodes a plasma membrane protein required for high-affinity potassium transport in *Saccharomyces cerevisiae*. *Mol Cell Biol*, **8**, 2848-2859.
- Gamborg, O.L., Miller, R.A. and Ojima, K. (1968) Nutrient requirements of suspension cultures of soybean root cells. *Exp Cell Res*, **50**, 151-158.
- Gavin, A.C., Bosche, M., Krause, R., Grandi, P., Marzioch, M., Bauer, A., Schultz, J., Rick, J.M., Michon, A.M., Cruciat, C.M., Remor, M., Hofert, C., Schelder, M., Brajenovic, M., Ruffner, H., Merino, A., Klein, K., Hudak, M., Dickson, D., Rudi, T., Gnau, V., Bauch, A., Bastuck, S., Huhse, B., Leutwein, C., Heurtier, M.A., Copley, R.R., Edelmann, A., Querfurth, E., Rybin, V., Drewes, G., Raida, M., Bouwmeester, T., Bork, P., Seraphin, B., Kuster, B., Neubauer, G. and Superti-Furga, G. (2002) Functional organization of the yeast proteome by systematic analysis of protein complexes. *Nature*, **415**, 141-147.
- Genre, A. and Bonfante, P. (2007) Dissection of plant cell responses to arbuscular mycorrhizal fungi reveals an unpredicted role for DMI3, a calcium/calmodulin-

- dependent kinase. *XIII International Congress on Molecular Plant-Microbe Interactions*, Sorrento, Italy, p. 188.
- Genre, A., Chabaud, M., Faccio, A., Barker, D.G. and Bonfante, P. (2008) Prepenetration Apparatus Assembly Precedes and Predicts the Colonization Patterns of Arbuscular Mycorrhizal Fungi within the Root Cortex of Both *Medicago truncatula* and *Daucus carota*. *Plant Cell*.
- Genre, A., Chabaud, M., Timmers, T., Bonfante, P. and Barker, D.G. (2005) Arbuscular mycorrhizal fungi elicit a novel intracellular apparatus in *Medicago truncatula* root epidermal cells before infection. *Plant Cell*, **17**, 3489-3499.
- Gerasimenko, O. and Gerasimenko, J. (2004) New aspects of nuclear calcium signalling. *J Cell Sci*, **117**, 3087-3094.
- Gianinazzi-Pearson, V. (1996) Plant Cell Responses to Arbuscular Mycorrhizal Fungi: Getting to the Roots of the Symbiosis. *Plant Cell*, **8**, 1871-1883.
- Gianinazzi-Pearson, V., Arnould, C., Oufattole, M., Arango, M. and Gianinazzi, S. (2000) Differential activation of H⁺-ATPase genes by an arbuscular mycorrhizal fungus in root cells of transgenic tobacco. *Planta*, **211**, 609-613.
- Gierth, M. and Mäser, P. (2007) Potassium transporters in plants - Involvement in K⁺ acquisition, redistribution and homeostasis. *FEBS Letters*, **581**, 2348-2356.
- Gietz, R.D. and Woods, R.A. (2001) Genetic transformation of yeast. *Biotechniques*, **30**, 816-820, 822-816, 828 passim.
- Gleason, C., Chaudhuri, S., Yang, T., Munoz, A., Poovaiah, B.W. and Oldroyd, G.E. (2006) Nodulation independent of rhizobia induced by a calcium-activated kinase lacking autoinhibition. *Nature*, **441**, 1149-1152.
- Godfroy, O., Debelle, F., Timmers, T. and Rosenberg, C. (2006) A rice calcium- and calmodulin-dependent protein kinase restores nodulation to a legume mutant. *Mol Plant Microbe Interact*, **19**, 495-501.
- Goldman, D.E. (1943) Potential, impedance, and rectification in membranes. *J. Gen. Physiol.*, **27**, 37-60.
- Govindarajulu, M., Pfeffer, P.E., Jin, H., Abubaker, J., Douds, D.D., Allen, J.W., Bucking, H., Lammers, P.J. and Shachar-Hill, Y. (2005) Nitrogen transfer in the arbuscular mycorrhizal symbiosis. *Nature*, **435**, 819-823.
- Grygorczyk, C. and Grygorczyk, R. (1998) A Ca²⁺- and voltage-dependent cation channel in the nuclear envelope of red beet. *Biochim Biophys Acta*, **1375**, 117-130.
- Handberg, K. and Stougaard, J. (1992) *Lotus japonicus*, an autogamous, diploid legume species from classical and molecular genetics. *Plant Journal*, **2**, 487-496.
- Hansen, J., Jorgensen, J.-E., Stougaard, J. and Marker, K. (1989) Hairy roots - a shortcut to transgenic root nodules. *Plant Cell Reports*, **8**, 12-15.
- Harris, J.M., Wais, R. and Long, S.R. (2003) Rhizobium-induced calcium spiking in *Lotus japonicus*. *Mol Plant Microbe Interact*, **16**, 335-341.
- Harrison, M.J. (1996) A sugar transporter from *Medicago truncatula*: altered expression pattern in roots during vesicular-arbuscular (VA) mycorrhizal associations. *Plant J*, **9**, 491-503.
- Harrison, M.J., Dewbre, G.R. and Liu, J. (2002) A phosphate transporter from *Medicago truncatula* involved in the acquisition of phosphate released by arbuscular mycorrhizal fungi. *Plant Cell*, **14**, 2413-2429.
- Hayashi, M., Miyahara, A., Sato, S., Kato, T., Yoshikawa, M., Taketa, M., Hayashi, M., Pedrosa, A., Onda, R., Imaizumi-Anraku, H., Bachmair, A., Sandal, N.,

- Stougaard, J., Murooka, Y., Tabata, S., Kawasaki, S., Kawaguchi, M. and Harada, K. (2001) Construction of a genetic linkage map of the model legume *Lotus japonicus* using an intraspecific F2 population. *DNA Res*, **8**, 301-310.
- Hedrich, R. and Neher, E. (1987) Cytoplasmic calcium regulates voltage-dependent ion channels in plant vacuoles. *Nature*, **329**, 833-836.
- Heginbotham, L., Lu, Z., Abramson, T. and MacKinnon, R. (1994) Mutations in the K⁺ channel signature sequence. *Biophys J*, **66**, 1061-1067.
- Heidstra, R., Geurts, R., Franssen, H., Spaink, H.P., Van Kammen, A. and Bisseling, T. (1994) Root Hair Deformation Activity of Nodulation Factors and Their Fate on *Vicia sativa*. *Plant Physiol*, **105**, 787-797.
- Herendeen, P.S., Magallón-Puebla, S., Lupia, R., Crane, P.R. and Kobylinska, J. (1999) *A preliminary conspectus of the Allon flora from the Late cretaceous (late Santonian) of central Georgia, USA*. Annals of the Missouri Botanical Garden.
- Hille, B. (2001) *Ion channels of excitable membranes, 3rd edition*. Sinauer Associates, Inc.
- Hirsch, A.M. (1992) Developmental biology of legume nodulation. *New Phytologist*, **122**, 211-237.
- Hodge, A., Campbell, C.D. and Fitter, A.H. (2001) An arbuscular mycorrhizal fungus accelerates decomposition and acquires nitrogen directly from organic material. *Nature*, **413**, 297-299.
- Hodgkin, A.L. and Katz, B. (1949) The effect of sodium ions on the electrical activity of the giant axon of the squid. *J. Physiol.*, **108**, 37-77.
- Hohnjec, N., Vieweg, M.F., Puhler, A., Becker, A. and Kuster, H. (2005) Overlaps in the transcriptional profiles of *Medicago truncatula* roots inoculated with two different *Glomus* fungi provide insights into the genetic program activated during arbuscular mycorrhiza. *Plant Physiol*, **137**, 1283-1301.
- Horton, R.M., Hunt, H.D., Ho, S.N., Pullen, J.K. and Pease, L.R. (1989) Engineering hybrid genes without the use of restriction enzymes: gene splicing by overlap extension. *Gene*, **77**, 61-68.
- Iida, H., Nakamura, H., Ono, T., Okumura, M.S. and Anraku, Y. (1994) MID1, a novel *Saccharomyces cerevisiae* gene encoding a plasma membrane protein, is required for Ca²⁺ influx and mating. *Mol Cell Biol*, **14**, 8259-8271.
- Imaizumi-Anraku, H., Takeda, N., Charpentier, M., Perry, J., Miwa, H., Umehara, Y., Kouchi, H., Murakami, Y., Mulder, L., Vickers, K., Pike, J., Downie, J.A., Wang, T., Sato, S., Asamizu, E., Tabata, S., Yoshikawa, M., Murooka, Y., Wu, G.J., Kawaguchi, M., Kawasaki, S., Parniske, M. and Hayashi, M. (2005) Plastid proteins crucial for symbiotic fungal and bacterial entry into plant roots. *Nature*, **433**, 527-531.
- Ito, T., Chiba, T., Ozawa, R., Yoshida, M., Hattori, M. and Sakaki, Y. (2001) A comprehensive two-hybrid analysis to explore the yeast protein interactome. *Proc Natl Acad Sci U S A*, **98**, 4569-4574.
- Javot, H., Penmetsa, R.V., Terzaghi, N., Cook, D.R. and Harrison, M.J. (2007) A *Medicago truncatula* phosphate transporter indispensable for the arbuscular mycorrhizal symbiosis. *Proc Natl Acad Sci U S A*, **104**, 1720-1725.
- Jiang, Y., Lee, A., Chen, J., Cadene, M., Chait, B.T. and MacKinnon, R. (2002a) Crystal structure and mechanism of a calcium-gated potassium channel. *Nature*, **417**, 515-522.

- Jiang, Y., Lee, A., Chen, J., Cadene, M., Chait, B.T. and MacKinnon, R. (2002b) The open pore conformation of potassium channels. *Nature*, **417**, 523-526.
- Journet, E.P., El-Gachtouli, N., Vernoud, V., de Billy, F., Pichon, M., Dedieu, A., Arnould, C., Morandi, D., Barker, D.G. and Gianinazzi-Pearson, V. (2001) *Medicago truncatula* ENOD11: a novel RPRP-encoding early nodulin gene expressed during mycorrhization in arbuscule-containing cells. *Mol Plant Microbe Interact*, **14**, 737-748.
- Juge, C., Samson, J., Bastien, C., Vierheilig, H., Coughlan, A. and Piche, Y. (2002) Breaking dormancy in spores of the arbuscular mycorrhizal fungus *Glomus intraradices*: a critical cold-storage period. *Mycorrhiza*, **12**, 37-42.
- Kaiser, B.N., Finnegan, P.M., Tyerman, S.D., Whitehead, L.F., Bergersen, F.J., Day, D.A. and Udvardi, M.K. (1998) Characterization of an ammonium transport protein from the peribacteroid membrane of soybean nodules. *Science*, **281**, 1202-1206.
- Kanamori, N., Madsen, L.H., Radutoiu, S., Frantescu, M., Quistgaard, E.M., Miwa, H., Downie, J.A., James, E.K., Felle, H.H., Haaning, L.L., Jensen, T.H., Sato, S., Nakamura, Y., Tabata, S., Sandal, N. and Stougaard, J. (2006) A nucleoporin is required for induction of Ca²⁺ spiking in legume nodule development and essential for rhizobial and fungal symbiosis. *Proc Natl Acad Sci U S A*, **103**, 359-364.
- Karimi, M., Inze, D. and Depicker, A. (2002) GATEWAY vectors for *Agrobacterium*-mediated plant transformation. *Trends Plant Sci*, **7**, 193-195.
- Kawaguchi, M., Motomura, T., Imaizumi-Anraku, H., Akao, S. and Kawasaki, S. (2001) Providing the basis for genomics in *Lotus japonicus*: the accessions Miyakojima and Gifu are appropriate crossing partners for genetic analyses. *Mol Genet Genomics*, **266**, 157-166.
- Kawasaki, S. and Murakami, Y. (2000) Genome Analysis of *Lotus japonicus*. *J Plant Res*, **113**, 497-506.
- King, M.C., Lusk, C.P. and Blobel, G. (2006) Karyopherin-mediated import of integral inner nuclear membrane proteins. *Nature*, **442**, 1003-1007.
- Kistner, C. and Parniske, M. (2002) Evolution of signal transduction in intracellular symbiosis. *Trends Plant Sci*, **7**, 511-518.
- Kistner, C., Winzer, T., Pitzschke, A., Mulder, L., Sato, S., Kaneko, T., Tabata, S., Sandal, N., Stougaard, J., Webb, K.J., Szczyglowski, K. and Parniske, M. (2005) Seven *Lotus japonicus* genes required for transcriptional reprogramming of the root during fungal and bacterial symbiosis. *Plant Cell*, **17**, 2217-2229.
- Kolacna, L., Zimmermannova, O., Hasenbrink, G., Schwarzer, S., Ludwig, J., Lichtenberg-Frate, H. and Sychrova, H. (2005) New phenotypes of functional expression of the mKir2.1 channel in potassium efflux-deficient *Saccharomyces cerevisiae* strains. *Yeast*, **22**, 1315-1323.
- Koncz, C. and Schell, J. (1986) The promoter of TL-DNA gene 5 controls the tissue-specific expression of chimaeric genes carried by a novel type of *Agrobacterium* binary vector. *Mol. Gen. Genet.*, **204**, 383-396.
- Kosuta, S., Chabaud, M., Lounnon, G., Gough, C., Denarie, J., Barker, D.G. and Becard, G. (2003) A diffusible factor from arbuscular mycorrhizal fungi induces symbiosis-specific MtENOD11 expression in roots of *Medicago truncatula*. *Plant Physiol*, **131**, 952-962.

- Kosuta, S., Hazledine, S., Sun, J., Miwa, H., Morris, R.J., Downie, J.A. and Oldroyd, G.E. (2008) Differential and chaotic calcium signatures in the symbiosis signaling pathway of legumes. *Proc Natl Acad Sci U S A*, **105**, 9823-9828.
- Kosuta, S., Winzer, T. and Parniske, M. (2005) Arbuscular mycorrhiza. In Márquez, A.J. (ed.), *Lotus japonicus handbook*. Springer, pp. 87-95.
- Kurdjian, A.C. (1995) Role of the differentiation of root epidermal cells in Nod factor (from *Rhizobium meliloti*)-induced root-hair depolarization of *Medicago sativa*. *Plant Physiol*, **107**, 783-790.
- LaRue, T. and Weeden, N. (1994) *The symbiosis genes of host*. Officina Press.
- Lazo, G.R., Stein, P.A. and Ludwig, R.A. (1991) A DNA transformation-competent Arabidopsis genomic library in Agrobacterium. *Biotechnology (N Y)*, **9**, 963-967.
- Leckie, C.P., McAinsh, M.R., Allen, G.J., Sanders, D. and Hetherington, A.M. (1998) Abscisic acid-induced stomatal closure mediated by cyclic ADP-ribose. *Proc Natl Acad Sci U S A*, **95**, 15837-15842.
- Lerouge, P., Roche, P., Faucher, C., Maillet, F., Truchet, G., Prome, J.C. and Denarie, J. (1990) Symbiotic host-specificity of *Rhizobium meliloti* is determined by a sulphated and acylated glucosamine oligosaccharide signal. *Nature*, **344**, 781-784.
- Levy, J., Bres, C., Geurts, R., Chalhoub, B., Kulikova, O., Duc, G., Journet, E.P., Ane, J.M., Lauber, E., Bisseling, T., Denarie, J., Rosenberg, C. and Debelle, F. (2004) A putative Ca²⁺ and calmodulin-dependent protein kinase required for bacterial and fungal symbioses. *Science*, **303**, 1361-1364.
- Li, M., Martin, S.J., Bruno, V.M., Mitchell, A.P. and Davis, D.A. (2004) Candida albicans Rim13p, a protease required for Rim101p processing at acidic and alkaline pHs. *Eukaryot Cell*, **3**, 741-751.
- Li, Y., Berke, I., Chen, L. and Jiang, Y. (2007) Gating and inward rectifying properties of the MthK K⁺ channel with and without the gating ring. *J Gen Physiol*, **129**, 109-120.
- Lohse, S., Schliemann, W., Ammer, C., Kopka, J., Strack, D. and Fester, T. (2005) Organization and metabolism of plastids and mitochondria in arbuscular mycorrhizal roots of *Medicago truncatula*. *Plant Physiol*, **139**, 329-340.
- Lombardo, F., Heckmann, A.B., Miwa, H., Perry, J.A., Yano, K., Hayashi, M., Parniske, M., Wang, T.L. and Downie, J.A. (2006) Identification of symbiotically defective mutants of *Lotus japonicus* affected in infection thread growth. *Mol Plant Microbe Interact*, **19**, 1444-1450.
- Long, S.R. (1996) Rhizobium symbiosis: nod factors in perspective. *Plant Cell*, **8**, 1885-1898.
- Lu, Z. and MacKinnon, R. (1994) Electrostatic tuning of Mg²⁺ affinity in an inward-rectifier K⁺ channel. *Nature*, **371**, 243-246.
- Lucocq, J. (1994) Quantitation of gold labelling and antigens in immunolabelled ultrathin sections. *J Anat*, **184 (Pt 1)**, 1-13.
- Madsen, E.B., Madsen, L.H., Radutoiu, S., Olbryt, M., Rakwalska, M., Szczyglowski, K., Sato, S., Kaneko, T., Tabata, S., Sandal, N. and Stougaard, J. (2003) A receptor kinase gene of the LysM type is involved in legume perception of rhizobial signals. *Nature*, **425**, 637-640.
- Maekawa, T., Kusakabe, M., Shimoda, Y., Sato, S., Tabata, S., Murooka, Y. and Hayashi, M. (2008) Polyubiquitin promoter-based binary vectors for overexpression and gene silencing in *Lotus japonicus*. *Mol Plant Microbe Interact*, **21**, 375-382.

- Marchetti, C., Jouy, N., Leroy-Martin, B., Defosse, A., Formstecher, P. and Marchetti, P. (2004) Comparison of four fluorochromes for the detection of the inner mitochondrial membrane potential in human spermatozoa and their correlation with sperm motility. *Hum Reprod*, **19**, 2267-2276.
- Maresova, L. and Sychrova, H. (2005) Physiological characterization of *Saccharomyces cerevisiae* kha1 deletion mutants. *Mol Microbiol*, **55**, 588-600.
- Martens, J.R., Kwak, Y.G. and Tamkun, M.M. (1999) Modulation of Kv channel alpha/beta subunit interactions. *Trends Cardiovasc Med*, **9**, 253-258.
- Marvel, D.J., Torrey, J.G. and Ausubel, F.M. (1987) Rhizobium symbiotic genes required for nodulation of legume and nonlegume hosts. *Proc Natl Acad Sci U S A*, **84**, 1319-1323.
- Matzke, M.A. and Matzke, A.J.M. (1986) Visualization of mitochondria and nuclei in living plant cells by the use of a potential-sensitive fluorescent dye. *Plant, Cell and Environment*, **9**, 73-77.
- McAinsh, M.R., Webb, A., Taylor, J.E. and Hetherington, A.M. (1995) Stimulus-Induced Oscillations in Guard Cell Cytosolic Free Calcium. *Plant Cell*, **7**, 1207-1219.
- McDonald, T.V., Yu, Z., Ming, Z., Palma, E., Meyers, M.B., Wang, K.W., Goldstein, S.A. and Fishman, G.I. (1997) A minK-HERG complex regulates the cardiac potassium current I(Kr). *Nature*, **388**, 289-292.
- Messinese, E., Mun, J.H., Yeun, L.H., Jayaraman, D., Rouge, P., Barre, A., Lougnon, G., Schornack, S., Bono, J.J., Cook, D.R. and Ane, J.M. (2007) A novel nuclear protein interacts with the symbiotic DMI3 calcium- and calmodulin-dependent protein kinase of *Medicago truncatula*. *Mol Plant Microbe Interact*, **20**, 912-921.
- Metivier, D., Dallaporta, B., Zamzami, N., Larochette, N., Susin, S.A., Marzo, I. and Kroemer, G. (1998) Cytofluorometric detection of mitochondrial alterations in early CD95/Fas/APO-1-triggered apoptosis of Jurkat T lymphoma cells. Comparison of seven mitochondrion-specific fluorochromes. *Immunol Lett*, **61**, 157-163.
- Michaevlevski, I., Chikvashvili, D., Tsuk, S., Fili, O., Lohse, M.J., Singer-Lahat, D. and Lotan, I. (2002) Modulation of a brain voltage-gated K⁺ channel by syntaxin 1A requires the physical interaction of Gbetagamma with the channel. *J Biol Chem*, **277**, 34909-34917.
- Miles, G.P., Samuel, M.A., Jones, A.M. and Ellis, B.E. (2004) Mastoparan rapidly activates plant MAP kinase signaling independent of heterotrimeric G proteins. *Plant Physiol*, **134**, 1332-1336.
- Mitra, R.M., Gleason, C.A., Edwards, A., Hadfield, J., Downie, J.A., Oldroyd, G.E. and Long, S.R. (2004) A Ca²⁺/calmodulin-dependent protein kinase required for symbiotic nodule development: Gene identification by transcript-based cloning. *Proc Natl Acad Sci U S A*, **101**, 4701-4705.
- Miwa, H., Sun, J., Oldroyd, G.E. and Downie, J.A. (2006) Analysis of Nod-factor-induced calcium signaling in root hairs of symbiotically defective mutants of *Lotus japonicus*. *Mol Plant Microbe Interact*, **19**, 914-923.
- Molokanova, E., Savchenko, A. and Kramer, R.H. (2000) Interactions of cyclic nucleotide-gated channel subunits and protein tyrosine kinase probed with genistein. *J Gen Physiol*, **115**, 685-696.
- Morera, F.J., Vargas, G., Gonzalez, C., Rosenmann, E. and Latorre, R. (2007) Ion-channel reconstitution. *Methods Mol Biol*, **400**, 571-585.

- Murphy, P.J., Langridge, P. and Smith, S.E. (1997) Cloning plant genes differentially expressed during colonization of roots of *Hordeum vulgare* by the vesicular arbuscular mycorrhizal fungus *Glomus intraradices*. *New Phytologist*, **135**, 291-301.
- Murray, J., Karas, B., Ross, L., Brachmann, A., Wagg, C., Geil, R., Perry, J., Nowakowski, K., MacGillivray, M., Held, M., Stougaard, J., Peterson, L., Parniske, M. and Szczyglowski, K. (2006) Genetic suppressors of the *Lotus japonicus* har1-1 hypernodulation phenotype. *Mol Plant Microbe Interact*, **19**, 1082-1091.
- Nagata, T., Iizumi, S., Satoh, K., Ooka, H., Kawai, J., Carninci, P., Hayashizaki, Y., Otomo, Y., Murakami, K., Matsubara, K. and Kikuchi, S. (2004) Comparative analysis of plant and animal calcium signal transduction element using plant full-length cDNA data. *Mol Biol Evol*, **21**, 1855-1870.
- Nair, M.G., Safir, G.R. and Siqueira, J.O. (1991) Isolation and Identification of Vesicular-Arbuscular Mycorrhiza-Stimulatory Compounds from Clover (*Trifolium repens*) Roots. *Appl Environ Microbiol*, **57**, 434-439.
- Nakamura, Y., Kaneko, T., Asamizu, E., Kato, T., Sato, S. and Tabata, S. (2002) Structural analysis of a *Lotus japonicus* genome. II. Sequence features and mapping of sixty-five TAC clones which cover the 6.5-mb regions of the genome. *DNA Res*, **9**, 63-70.
- Napoli, C.A. and Hubbell, D.H. (1975) Ultrastructure of Rhizobium-induced infection threads in clover root hairs. *Appl Microbiol*, **30**, 1003-1009.
- Navazio, L., Bewell, M.A., Siddiqua, A., Dickinson, G.D., Galione, A. and Sanders, D. (2000) Calcium release from the endoplasmic reticulum of higher plants elicited by the NADP metabolite nicotinic acid adenine dinucleotide phosphate. *Proc Natl Acad Sci U S A*, **97**, 8693-8698.
- Navazio, L., Mariani, P. and Sanders, D. (2001) Mobilization of Ca²⁺ by cyclic ADP-ribose from the endoplasmic reticulum of cauliflower florets. *Plant Physiol*, **125**, 2129-2138.
- Navazio, L., Moscatiello, R., Genre, A., Novero, M., Baldan, B., Bonfante, P. and Mariani, P. (2007) A diffusible signal from arbuscular mycorrhizal fungi elicits a transient cytosolic calcium elevation in host plant cells. *Plant Physiol*, **144**, 673-681.
- Niemietz, C.M. and Tyerman, S.D. (2000) Channel-mediated permeation of ammonia gas through the peribacteroid membrane of soybean nodules. *FEBS Lett*, **465**, 110-114.
- Novero, M., Faccio, A., Genre, A., Stougaard, J., Webb, J., Mulder, L., Parniske, M. and Bonfante, P. (2002) Dual requirement of the *LjSym4* gene for mycorrhizal development in epidermal and cortical cells of *Lotus japonicus* roots. *New Phytologist*, **154**, 741-749.
- Ohba, T., Schirmer, E.C., Nishimoto, T. and Gerace, L. (2004) Energy- and temperature-dependent transport of integral proteins to the inner nuclear membrane via the nuclear pore. *J Cell Biol*, **167**, 1051-1062.
- Oke, V. and Long, S.R. (1999) Bacteroid formation in the Rhizobium-legume symbiosis. *Curr Opin Microbiol*, **2**, 641-646.
- Olah, B., Briere, C., Becard, G., Denarie, J. and Gough, C. (2005) Nod factors and a diffusible factor from arbuscular mycorrhizal fungi stimulate lateral root

- formation in *Medicago truncatula* via the DMI1/DMI2 signalling pathway. *Plant J*, **44**, 195-207.
- Oldroyd, G.E. and Downie, J.A. (2006) Nuclear calcium changes at the core of symbiosis signalling. *Curr Opin Plant Biol*, **9**, 351-357.
- Oldroyd, G.E., Mitra, R.M., Wais, R.J. and Long, S.R. (2001) Evidence for structurally specific negative feedback in the Nod factor signal transduction pathway. *Plant J*, **28**, 191-199.
- Ovtsyna, A.O., Dolgikh, E.A., Kilanova, A.S., Tsyganov, V.E., Borisov, A.Y., Tikhonovich, I.A. and Staehelin, C. (2005) Nod factors induce nod factor cleaving enzymes in pea roots. Genetic and pharmacological approaches indicate different activation mechanisms. *Plant Physiol*, **139**, 1051-1064.
- Paidhungat, M. and Garrett, S. (1997) A homolog of mammalian, voltage-gated calcium channels mediates yeast pheromone-stimulated Ca²⁺ uptake and exacerbates the *cdc1(Ts)* growth defect. *Mol Cell Biol*, **17**, 6339-6347.
- Parniske, M. (2004) Molecular genetics of the arbuscular mycorrhizal symbiosis. *Curr Opin Plant Biol*, **7**, 414-421.
- Pearson, J.N. and Jakobsen, I. (1993) The relative contribution of hyphae and roots to phosphorus uptake by arbuscular mycorrhizal plants, measured by dual labelling with ³²P and ³³P. *New Phytologist*, **124**, 489-494.
- Peck, J.W., Bowden, E.T. and Burbelo, P.D. (2004) Structure and function of human Vps20 and Snf7 proteins. *Biochem J*, **377**, 693-700.
- Peiter, E., Fischer, M., Sidaway, K., Roberts, S.K. and Sanders, D. (2005) The *Saccharomyces cerevisiae* Ca²⁺ channel Cch1pMid1p is essential for tolerance to cold stress and iron toxicity. *FEBS Lett*, **579**, 5697-5703.
- Perry, J.A., Wang, T.L., Welham, T.J., Gardner, S., Pike, J.M., Yoshida, S. and Parniske, M. (2003) A TILLING reverse genetics tool and a web-accessible collection of mutants of the legume *Lotus japonicus*. *Plant Physiol*, **131**, 866-871.
- Pingret, J.L., Journet, E.P. and Barker, D.G. (1998) Rhizobium nod factor signaling. Evidence for a G protein-mediated transduction mechanism. *Plant Cell*, **10**, 659-672.
- Poulsen, C. and Podenphant, L. (2002) Expressed sequence tags from roots and nodule primordia of *Lotus japonicus* infected with *Mesorhizobium loti*. *Mol Plant Microbe Interact*, **15**, 376-379.
- Radutoiu, S., Madsen, L.H., Madsen, E.B., Felle, H.H., Umehara, Y., Gronlund, M., Sato, S., Nakamura, Y., Tabata, S., Sandal, N. and Stougaard, J. (2003) Plant recognition of symbiotic bacteria requires two LysM receptor-like kinases. *Nature*, **425**, 585-592.
- Radutoiu, S., Madsen, L.H., Madsen, E.B., Jurkiewicz, A., Fukai, E., Quistgaard, E.M., Albrechtsen, A.S., James, E.K., Thirup, S. and Stougaard, J. (2007) LysM domains mediate lipochitin-oligosaccharide recognition and Nfr genes extend the symbiotic host range. *Embo J*, **26**, 3923-3935.
- Remy, W., Taylor, T.N., Hass, H. and Kerp, H. (1994) Four hundred-million-year-old vesicular arbuscular mycorrhizae. *Proc Natl Acad Sci U S A*, **91**, 11841-11843.
- Ridge, R.W. and Rolfe, B.G. (1985) Rhizobium sp. Degradation of Legume Root Hair Cell Wall at the Site of Infection Thread Origin. *Appl Environ Microbiol*, **50**, 717-720.

- Riely, B.K., Lougnon, G., Ane, J.M. and Cook, D.R. (2007) The symbiotic ion channel homolog DMI1 is localized in the nuclear membrane of *Medicago truncatula* roots. *Plant J*, **49**, 208-216.
- Robertson, J.G., Wells, B., Brewin, N.J., Wood, E., Knight, C.D. and Downie, J.A. (1985) The legume-Rhizobium symbiosis: a cell surface interaction. *J Cell Sci Suppl*, **2**, 317-331.
- Rodriguez-Navarro, A. (2000) Potassium transport in fungi and plants. *Biochim Biophys Acta*, **1469**, 1-30.
- Roeper, J., Lorra, C. and Pongs, O. (1997) Frequency-dependent inactivation of mammalian A-type K⁺ channel KV1.4 regulated by Ca²⁺/calmodulin-dependent protein kinase. *J Neurosci*, **17**, 3379-3391.
- Ross, E.M. and Higashijima, T. (1994) Regulation of G-protein activation by mastoparans and other cationic peptides. *Methods Enzymol*, **237**, 26-37.
- Saito, K., Yoshikawa, M., Yano, K., Miwa, H., Uchida, H., Asamizu, E., Sato, S., Tabata, S., Imaizumi-Anraku, H., Umehara, Y., Kouchi, H., Murooka, Y., Szczyglowski, K., Downie, J.A., Parniske, M., Hayashi, M. and Kawaguchi, M. (2007) NUCLEOPORIN85 is required for calcium spiking, fungal and bacterial symbioses, and seed production in *Lotus japonicus*. *Plant Cell*, **19**, 610-624.
- Sambrook, J. and Russell, D.W. (2001) *Molecular cloning a laboratory manual, 3rd edition*. Cold spring harbor laboratory press.
- Sandal, N., Krusell, L., Radutoiu, S., Olbryt, M., Pedrosa, A., Stracke, S., Sato, S., Kato, T., Tabata, S., Parniske, M., Bachmair, A., Ketelsen, T. and Stougaard, J. (2002) A genetic linkage map of the model legume *Lotus japonicus* and strategies for fast mapping of new loci. *Genetics*, **161**, 1673-1683.
- Sandal, N., Petersen, T.R., Murray, J., Umehara, Y., Karas, B., Yano, K., Kumagai, H., Yoshikawa, M., Saito, K., Hayashi, M., Murakami, Y., Wang, X., Hakoyama, T., Imaizumi-Anraku, H., Sato, S., Kato, T., Chen, W., Hossain, M.S., Shibata, S., Wang, T.L., Yokota, K., Larsen, K., Kanamori, N., Madsen, E., Radutoiu, S., Madsen, L.H., Radu, T.G., Krusell, L., Ooki, Y., Banba, M., Betti, M., Rispaill, N., Skot, L., Tuck, E., Perry, J., Yoshida, S., Vickers, K., Pike, J., Mulder, L., Charpentier, M., Muller, J., Ohtomo, R., Kojima, T., Ando, S., Marquez, A.J., Gresshoff, P.M., Harada, K., Webb, J., Hata, S., Suganuma, N., Kouchi, H., Kawasaki, S., Tabata, S., Hayashi, M., Parniske, M., Szczyglowski, K., Kawaguchi, M. and Stougaard, J. (2006) Genetics of symbiosis in *Lotus japonicus*: recombinant inbred lines, comparative genetic maps, and map position of 35 symbiotic loci. *Mol Plant Microbe Interact*, **19**, 80-91.
- Schauser, L., Handberg, K., Sandal, N., Stiller, J., Thykjaer, T., Pajuelo, E., Nielsen, A. and Stougaard, J. (1998) Symbiotic mutants deficient in nodule establishment identified after T-DNA transformation of *Lotus japonicus*. *Mol Gen Genet*, **259**, 414-423.
- Schlosser, A., Hamann, A., Bossemeyer, D., Schneider, E. and Bakker, E.P. (1993) NAD⁺ binding to the *Escherichia coli* K(+)-uptake protein TrkA and sequence similarity between TrkA and domains of a family of dehydrogenases suggest a role for NAD⁺ in bacterial transport. *Mol Microbiol*, **9**, 533-543.
- Schüssler, A., Schwarzott, D., Walker, C. (2001) A new fungal phylum, the Glomeromycota phylogeny and evolution. *Mycol. Res.*, 1413-1421.

- Scott, V.E., Rettig, J., Parcej, D.N., Keen, J.N., Findlay, J.B., Pongs, O. and Dolly, J.O. (1994) Primary structure of a beta subunit of alpha-dendrotoxin-sensitive K⁺ channels from bovine brain. *Proc Natl Acad Sci U S A*, **91**, 1637-1641.
- Shaw, S.L. and Long, S.R. (2003) Nod factor elicits two separable calcium responses in *Medicago truncatula* root hair cells. *Plant Physiol*, **131**, 976-984.
- Shi, J., Blundell, T.L. and Mizuguchi, K. (2001) FUGUE: sequence-structure homology recognition using environment-specific substitution tables and structure-dependent gap penalties. *J Mol Biol*, **310**, 243-257.
- Smith, S.E., Smith, F.A. and Jakobsen, I. (2003) Mycorrhizal fungi can dominate phosphate supply to plants irrespective of growth responses. *Plant Physiol*, **133**, 16-20.
- Soltis, D.E., Soltis, P.S., Chase, M.W., Mort, M.E., Albach, D.C., Zanis, M., Savolainen, V., Hahn, W.H., Hoot, S.B., Fay, M.F., Axtell, M., Swensen, S.M., Prince, L.M., Kress, W.J.O.H.N., Nixon, K.C. and Farris, J.S. (2000) *Angiosperm phylogeny inferred from 18S rDNA, rbcL, and atpB sequences*. Botanical Journal of the Linnean Society.
- Spaink, H.P., Sheeley, D.M., van Brussel, A.A., Glushka, J., York, W.S., Tak, T., Geiger, O., Kennedy, E.P., Reinhold, V.N. and Lugtenberg, B.J. (1991) A novel highly unsaturated fatty acid moiety of lipo-oligosaccharide signals determines host specificity of *Rhizobium*. *Nature*, **354**, 125-130.
- Stehno-Bittel, L., Lückhoff, A. and Clapham, D.E. (1995) Calcium release from the nucleus by InsP₃ receptor channels. *Neuron*, **14**, 163-167.
- Stern, J.H., Knutsson, H. and MacLeish, P.R. (1987) Divalent cations directly affect the conductance of excised patches of rod photoreceptor membrane. *Science*, **236**, 1674-1678.
- Stougaard, J. (2000) Regulators and regulation of legume root nodule development. *Plant Physiol*, **124**, 531-540.
- Stougaard, J., Abildsten, D. and KA, M. (1987a) The *Agrobacterium rhizogenes* pRi TL-DNA segment as a gene vector system for transformation of plants. *Molecular General Genetics*, **207**, 251-255.
- Stougaard, J., Abildsten, D. and Marker, K. (1987b) The *Agrobacterium rhizogenes* pRi TL-DNA segment as a gene vector system for transformation of plants. *Molecular General Genetics*, **207**, 251-255.
- Stracke, S., Kistner, C., Yoshida, S., Mulder, L., Sato, S., Kaneko, T., Tabata, S., Sandal, N., Stougaard, J., Szczyglowski, K. and Parniske, M. (2002) A plant receptor-like kinase required for both bacterial and fungal symbiosis. *Nature*, **417**, 959-962.
- Sullivan, J.T., Patrick, H.N., Lowther, W.L. and Scott, D.B. (1995) Nodulating strains of *Rhizobium loti* arise through chromosomal symbiotic gene transfer in the environment. *PNAS*, **92**, 8985-8989.
- Sun, J., Miwa, H., Downie, J.A. and Oldroyd, G.E. (2007) Mastoparan activates calcium spiking analogous to Nod factor-induced responses in *Medicago truncatula* root hair cells. *Plant Physiol*, **144**, 695-702.
- Sutton, J.M., Lea, E.J. and Downie, J.A. (1994) The nodulation-signaling protein NodO from *Rhizobium leguminosarum* biovar *viciae* forms ion channels in membranes. *Proc Natl Acad Sci U S A*, **91**, 9990-9994.
- Swensen, S.M. and Benson, D.R. (2008) Evolution of actinorhizal host plants and *Frankia* endosymbionts. In Pawlowski, K. and Newton, W.E. (eds.), *Nitrogen-fixing actinorhizal symbioses*. Dordrecht:Springer Netherlands, pp. 73-104.

- Takeshima, H., Nishimura, S., Matsumoto, T., Ishida, H., Kangawa, K., Minamino, N., Matsuo, H., Ueda, M., Hanaoka, M., Hirose, T. and et al. (1989) Primary structure and expression from complementary DNA of skeletal muscle ryanodine receptor. *Nature*, **339**, 439-445.
- Tansengco, M.L., Hayashi, M., Kawaguchi, M., Imaizumi-Anraku, H. and Murooka, Y. (2003) crinkle, a novel symbiotic mutant that affects the infection thread growth and alters the root hair, trichome, and seed development in *Lotus japonicus*. *Plant Physiol*, **131**, 1054-1063.
- Tester, M. and Davenport, R. (2003) Na⁺ tolerance and Na⁺ transport in higher plants. *Ann Bot (Lond)*, **91**, 503-527.
- Timmers, A.C., Auriac, M.C. and Truchet, G. (1999) Refined analysis of early symbiotic steps of the *Rhizobium-Medicago* interaction in relationship with microtubular cytoskeleton rearrangements. *Development*, **126**, 3617-3628.
- Tinker, A., Lindsay, A.R. and Williams, A.J. (1992) Block of the sheep cardiac sarcoplasmic reticulum Ca(2⁺)-release channel by tetra-alkyl ammonium cations. *J Membr Biol*, **127**, 149-159.
- Tirichine, L., Imaizumi-Anraku, H., Yoshida, S., Murakami, Y., Madsen, L.H., Miwa, H., Nakagawa, T., Sandal, N., Albrektsen, A.S., Kawaguchi, M., Downie, A., Sato, S., Tabata, S., Kouchi, H., Parniske, M., Kawasaki, S. and Stougaard, J. (2006) Deregulation of a Ca²⁺/calmodulin-dependent kinase leads to spontaneous nodule development. *Nature*, **441**, 1153-1156.
- Trappe, J.M. (1987) *Phylogenetic and ecologic aspects of mycotrophy in the angiosperms from an evolutionary standpoint*.
- Truchet, G., Roche, P., Lerouge, P., Vasse, J., Camut, S., de Billy, F., Promé, J.C. and Dénarié, J. (1991) Sulphated lipo-oligosaccharide signals of *Rhizobium meliloti* elicit root nodule organogenesis in alfalfa. *Nature*, **351**, 670-673.
- Tsyganov, V.E., Voroshilova, V.A., Priefer, U.B., Borisov, A.Y. and Tikhonovich, I.A. (2002) Genetic dissection of the initiation of the infection process and nodule tissue development in the *Rhizobium-pea* (*Pisum sativum* L.) symbiosis. *Ann Bot (Lond)*, **89**, 357-366.
- Turgeon, B.G. and Bauer, W.D. (1985) Ultrastructure of infection-thread development during infection of soybean by *Rhizobium japonicum*. *Planta*, **163**, 328-349.
- Umehara, M., Hanada, A., Yoshida, S., Akiyama, K., Arite, T., Takeda-Kamiya, N., Magome, H., Kamiya, Y., Shirasu, K., Yoneyama, K., Kyojuka, J. and Yamaguchi, S. (2008) Inhibition of shoot branching by new terpenoid plant hormones. *Nature*, **455**, 195-200.
- Valiyaveetil, F.I., Leonetti, M., Muir, T.W. and Mackinnon, R. (2006) Ion selectivity in a semisynthetic K⁺ channel locked in the conductive conformation. *Science*, **314**, 1004-1007.
- van Brussel, A.A., Bakhuizen, R., van Spronsen, P.C., Spaink, H.P., Tak, T., Lugtenberg, B.J. and Kijne, J.W. (1992) Induction of Pre-Infection Thread Structures in the Leguminous Host Plant by Mitogenic Lipo-Oligosaccharides of *Rhizobium*. *Science*, **257**, 70-72.
- Vierheilig, H., Bago, B., Albrecht, C., Poulin, M.J. and Piche, Y. (1998) Flavonoids and arbuscular-mycorrhizal fungi. *Adv Exp Med Biol*, **439**, 9-33.
- Villarejo, A., Buren, S., Larsson, S., Dejardin, A., Monne, M., Rudhe, C., Karlsson, J., Jansson, S., Lerouge, P., Rolland, N., von Heijne, G., Grebe, M., Bako, L. and

- Samuelsson, G. (2005) Evidence for a protein transported through the secretory pathway en route to the higher plant chloroplast. *Nat Cell Biol*, **7**, 1224-1231.
- Wais, R.J., Galera, C., Oldroyd, G., Catoira, R., Penmetsa, R.V., Cook, D., Gough, C., Denarie, J. and Long, S.R. (2000) Genetic analysis of calcium spiking responses in nodulation mutants of *Medicago truncatula*. *Proc Natl Acad Sci U S A*, **97**, 13407-13412.
- Walker, D.J., Leigh, R.A. and Miller, A.J. (1996) Potassium homeostasis in vacuolate plant cells. *Proc Natl Acad Sci U S A*, **93**, 10510-10514.
- Walker, S.A. and Downie, J.A. (2000) Entry of *Rhizobium leguminosarum* bv. *viciae* into root hairs requires minimal Nod factor specificity, but subsequent infection thread growth requires nodO or nodE. *Mol Plant Microbe Interact*, **13**, 754-762.
- Walker, S.A., Viprey, V. and Downie, J.A. (2000) Dissection of nodulation signaling using pea mutants defective for calcium spiking induced by nod factors and chitin oligomers. *Proc Natl Acad Sci U S A*, **97**, 13413-13418.
- Walter, M., Chaban, C., Schutze, K., Batistic, O., Weckermann, K., Nake, C., Blazevic, D., Grefen, C., Schumacher, K., Oecking, C., Harter, K. and Kudla, J. (2004) Visualization of protein interactions in living plant cells using bimolecular fluorescence complementation. *Plant J*, **40**, 428-438.
- Wang, J. and Best, P.M. (1994) Characterization of the potassium channel from frog skeletal muscle sarcoplasmic reticulum membrane. *J Physiol*, **477 (Pt 2)**, 279-290.
- Weidmann, S., Sanchez, L., Descombin, J., Chatagnier, O., Gianinazzi, S. and Gianinazzi-Pearson, V. (2004) Fungal elicitation of signal transduction-related plant genes precedes mycorrhiza establishment and requires the *dmi3* gene in *Medicago truncatula*. *Mol Plant Microbe Interact*, **17**, 1385-1393.
- Wilkinson, D.M. (2001) At cross purposes. *Nature*, **412**, 485.
- Winter, V. and Hauser, M.T. (2006) Exploring the ESCRTing machinery in eukaryotes. *Trends Plant Sci*, **11**, 115-123.
- Wydro, M., Kozubek, E. and Lehmann, P. (2006) Optimization of transient *Agrobacterium*-mediated gene expression system in leaves of *Nicotiana benthamiana*. *Acta Biochim Pol*, **53**, 289-298.
- Xu, J., Li, H.D., Chen, L.Q., Wang, Y., Liu, L.L., He, L. and Wu, W.H. (2006) A protein kinase, interacting with two calcineurin B-like proteins, regulates K⁺ transporter AKT1 in *Arabidopsis*. *Cell*, **125**, 1347-1360.
- Xu, W. and Mitchell, A.P. (2001) Yeast PalA/AIP1/Alix homolog Rim20p associates with a PEST-like region and is required for its proteolytic cleavage. *J Bacteriol*, **183**, 6917-6923.
- Xu, W., Smith, F.J., Jr., Subaran, R. and Mitchell, A.P. (2004) Multivesicular body-ESCRT components function in pH response regulation in *Saccharomyces cerevisiae* and *Candida albicans*. *Mol Biol Cell*, **15**, 5528-5537.
- Yang, W.C., de Blank, C., Meskiene, I., Hirt, H., Bakker, J., van Kammen, A., Franssen, H. and Bisseling, T. (1994) *Rhizobium* nod factors reactivate the cell cycle during infection and nodule primordium formation, but the cycle is only completed in primordium formation. *Plant Cell*, **6**, 1415-1426.
- Yano, K., Tansengco, M.L., Hio, T., Higashi, K., Murooka, Y., Imaizumi-Anraku, H., Kawaguchi, M. and Hayashi, M. (2006) New nodulation mutants responsible for infection thread development in *Lotus japonicus*. *Mol Plant Microbe Interact*, **19**, 801-810.

- Yao, P.Y. and Vincent, J.M. (1969) Host specificity in the root hair "curling factor" of *Rhizobium spp.* *Aust J Biol Sci*, **22**, 413-423.
- Yellen, G. (1984) Ionic permeation and blockade in Ca²⁺-activated K⁺ channels of bovine chromaffin cells. *J Gen Physiol*, **84**, 157-186.
- Yoshida, S. and Parniske, M. (2005) Regulation of plant symbiosis receptor kinase through serine and threonine phosphorylation. *J Biol Chem*, **280**, 9203-9209.
- Zadek, B. and Nimigean, C.M. (2006) Calcium-dependent gating of MthK, a prokaryotic potassium channel. *J Gen Physiol*, **127**, 673-685.
- Zhang, Y., Niu, X., Brelidze, T.I. and Magleby, K.L. (2006) Ring of negative charge in BK channels facilitates block by intracellular Mg²⁺ and polyamines through electrostatics. *J Gen Physiol*, **128**, 185-202.
- Zhu, H., Riely, B.K., Burns, N.J. and Ane, J.M. (2006) Tracing nonlegume orthologs of legume genes required for nodulation and arbuscular mycorrhizal symbioses. *Genetics*, **172**, 2491-2499.
- Zimmermann, S., Nurnberger, T., Frachisse, J.M., Wirtz, W., Guern, J., Hedrich, R. and Scheel, D. (1997) Receptor-mediated activation of a plant Ca²⁺-permeable ion channel involved in pathogen defense. *Proc Natl Acad Sci U S A*, **94**, 2751-2755.

6. Acknowledgement

I would like to express my gratitude to all those who gave me the possibility to complete this thesis. First, I want to thank my supervisor Prof. Dr. M. Parniske for giving me the chance to perform my PhD-thesis in his laboratory, for supporting my work and giving me the opportunity to have a worldwide scientific training.

My colleagues past and present all gave me the feeling to be at home at work. Therefore, I like to thank all members of the laboratory for building a great atmosphere.

I like also to give a special thanks to Lionel Navarro, Cristina Azevedo, Gabor Giczey, Satoko Yoshida, Catherine White and Meritxell Llovera for stimulating discussions, suggestions and encouragement, which helped me in research for this thesis. For all their help, interest and valuable hints, I like to specially thank Rolf Bredemeier and Prof. Dr. Enrico Schleiff. Furthermore, I like to express my sincere thanks to my PhD colleagues, Kristina Haage, Martin Groth and Katharina Markmann for all their help in running the laboratory and their support in a foreign country.

My sincere thanks are also due to all my friends in Munich and family in France for their patience, support, interest, and encouragement in difficult time. I warmly thank my friends Marie and Benoit, as well as my brother for their understanding and encouragement all time of my research. I would like to give my special thanks to René for patient and loving support enabled me to complete this work.

7. Appendix

7.1 List of publications

7.1.1 Papers

Perry, J., Welham, T., Brachmann, A., **Charpentier, M.**, Markmann, K., Wang, T. and Parniske, M. Mining the symbiotic component of the *Lotus japonicus* genome using classical genetics and thematic TILLING. Manuscript in preparation.

Charpentier, M., Bredemeier, R., Wanner, G., Takeda, N., Schleiff, E. and Parniske, M. *Lotus japonicus* CASTOR and POLLUX Are Ion Channels Essential for Perinuclear Calcium Spiking in Legume Root Endosymbiosis. *Plant Cell*, **20**, 1-13

Sandal, N., Petersen, T.R., Murray, J., Umehara, Y., Karas, B., Yano, K., Kumagai, H., Yoshikawa, M., Saito, K., Hayashi, M., Murakami, Y., Wang, X., Hakoyama, T., Imaizumi-Anraku, H., Sato, S., Kato, T., Chen, W., Hossain, M.S., Shibata, S., Wang, T.L., Yokota, K., Larsen, K., Kanamori, N., Madsen, E., Radutoiu, S., Madsen, L.H., Radu, T.G., Krusell, L., Ooki, Y., Banba, M., Betti, M., Rispaill, N., Skot, L., Tuck, E., Perry, J., Yoshida, S., Vickers, K., Pike, J., Mulder, L., **Charpentier, M.**, Muller, J., Ohtomo, R., Kojima, T., Ando, S., Marquez, A.J., Gresshoff, P.M., Harada, K., Webb, J., Hata, S., Sukanuma, N., Kouchi, H., Kawasaki, S., Tabata, S., Hayashi, M., Parniske, M., Szczyglowski, K., Kawaguchi, M. and Stougaard, J. (2006) Genetics of symbiosis in *Lotus japonicus*: recombinant inbred lines, comparative genetic maps, and map position of 35 symbiotic loci. *Mol Plant Microbe Interact*, **19**, 80-91

Imaizumi-Anraku, H., Takeda, N., **Charpentier, M.**, Perry, J., Miwa, H., Umehara, Y., Kouchi, H., Murakami, Y., Mulder, L., Vickers, K., Pike, J., Downie, J.A., Wang, T., Sato, S., Asamizu, E., Tabata, S., Yoshikawa, M., Murooka, Y., Wu, G.J., Kawaguchi, M., Kawasaki, S., Parniske, M. and Hayashi, M. (2005) Plastid proteins crucial for symbiotic fungal and bacterial entry into plant roots. *Nature*, **433**, 527-531.

7.1.2 Posters and conferences

CASTOR and POLLUX in symbiotic signal transduction. Charpentier, M., Bredemeier, R., Schleiff, E. and Parniske, P. International Symposium: 100 years of Endosymbiotic Theory: From Prokaryotes to Eucaryotic Organelles. Hamburg, Germany (2005).

CASTOR and POLLUX in symbiotic signal transduction. Charpentier, M., Bredemeier, R., Schleiff, E. and Parniske, P. Gordon conference: Ion channels. Tilton, NH, USA (2006).

CASTOR and POLLUX ion transporters in symbiotic signal transduction: myth or reality? Charpentier, M., Bredemeier, R., Schleiff, E. and Parniske, P. XV FESPB Congress. Lyon, France (2006)

CASTOR and POLLUX in symbiotic signal transduction. Charpentier, M., Bredemeier, R., Schleiff, E. and Parniske, P. 13th International congress on Molecular Plant-Microbe Interaction. Sorrento, Italy (2007)

7.1.3 Talks

CASTOR and POLLUX in symbiotic signal transduction. Intensifying Training in Europe on Genomic Research Activity in Legumes network (INTEGRAL) Conference. Munich, Germany (2005)

CASTOR and POLLUX in symbiotic signal transduction. INTEGRAL Conference. Ravello, Italia (2006)

Unravelling the function of CASTOR and POLLUX in symbiotic signalling. INTEGRAL Conference. Sevilla, Spain (2007)

New class of cation channels essential for perinuclear calcium spiking. 8th European Nitrogen Fixation Conference. Gent, Belgium (2008)

7.2 List of figures

Figure 1. Positional cloning of <i>CASTOR</i> and <i>POLLUX</i> genes.....	25
Figure 2. A model for the early symbiosis signalling pathway in the epidermis.....	26
Figure 3. Alternative-spliced variants of <i>CASTOR</i> (A) and <i>POLLUX</i> (B).....	28
Figure 4. Unrooted radial phylogenetic tree of <i>CASTOR</i> and <i>POLLUX</i> homologs.....	32
Figure 5. Sequence analyses of <i>CASTOR</i> and <i>POLLUX</i>	34
Figure 6. Localization in tobacco leaf epidermal cells of <i>CASTOR</i> and <i>POLLUX</i>	36
Figure 7. Immunogold localization of <i>CASTOR</i> in <i>Lotus japonicus</i> with anti- <i>CASTOR</i> ...	39
Figure 8. Yeast-two-hybrid assay for interactions of c <i>CASTOR</i> and c <i>POLLUX</i>	41
Figure 9. Formation of <i>CASTOR</i> and <i>POLLUX</i> homocomplexes in <i>planta</i>	42
Figure 10. Expression patterns of <i>CASTOR</i> and <i>POLLUX</i> promoter:GUS fusions in <i>L. japonicus</i> roots before and after inoculation with <i>Mesorhizobium loti</i>	44
Figure 11. Restoration of root nodule symbiosis in <i>A. rhizogenes</i> -transformed root systems of <i>L. japonicus</i> mutants.....	45
Figure 12. Restoration of root nodule symbiosis in <i>A. rhizogenes</i> -transformed root systems of <i>L. japonicus</i> mutant with the <i>M. truncatula DMII</i> gene under the control of single <i>P35S</i>	46
Figure 13. Complementation of the yeast double mutant <i>cchl1Δmid1Δ</i> and <i>trk1Δ</i> strains....	48
Figure 14. Complementation of MAB 2d mutant.....	49
Figure 15. Cell free expression of <i>CASTOR</i> , <i>castor-2</i> and <i>POLLUX</i>	51
Figure 16. Electrophysiological characterization of <i>CASTOR</i>	52
Figure 17. Modelization of the <i>CASTOR</i> pore and the <i>castor-2</i> mutant pore.....	53
Figure 18. Electrophysiological characterization of <i>castor-2</i> channel.....	53
Figure 19. Voltage dependent magnesium-blockage of <i>CASTOR</i>	55
Figure 20. Modulation of <i>CASTOR</i> gating.....	56

Figure 21. Yeast-two-hybrid assay for interaction between cCASTOR and yeast two hybrid library full-length candidat interactors.....	58
Figure 22. Yeast-two-hybrid assay for interactions of cCASTOR and yeast two hybrid library full length candidate interactors.....	61
Figure 23. Downregulation of LjSNF7 in <i>A. rhizogenes</i> transformed roots expressing pUB-GWS50-GFP impaired nodulation.....	62
Figure 24. Subcellular localization of LjSNF7:RFP in <i>L. japonicus</i> cell culture protoplast.....	63
Figure 25. Unrooted radial phylogenetic tree of LjSNF7 homologs.....	69
Figure 26. Proposed role of CASTOR and POLLUX as counter ion channels.....	71
Figure 27. Representation of the fusion of proteoliposome with the planar lipids bilayer...	81
Figure 28. Lipid-bilayer-measurement system.....	81

7.3 List of tables

Table 1. Common <i>L. japonicus</i> <i>SYM</i> genes required for AM and RNS.....	21
Table 2. List of <i>castor</i> mutant alleles.....	29
Table 3. List of <i>pollux</i> mutant alleles.....	30
Table 4. Restoration of root nodules symbioses in <i>L. japonicus castor-12</i> and <i>pollux-5</i> mutants.....	31
Table 5. Restoration of Root Nodule Symbioses in <i>A. rhizogenes</i> -transformed root systems of <i>L. japonicus</i> mutants <i>pollux-2</i> and <i>castor-12</i> with the different <i>POLLUX</i> and <i>CASTOR</i> split YFP versions, respectively.....	42
Table 6. Reverse potential (E_{rev}) and permeability ratios (P_X/P_{Cl^-}) for CASTOR and <i>castor-2</i> (A), and reverse potential and permeability ratios P_{K^+}/P_X for CASTOR (B).....	52
Table 7. List of putative cCASTOR interactors.....	60
Table 8. Construct used in this study.....	74
Table 9. Antibodies used in this study.....	75

7.4 Erklärung

Ich erkläre hiermit an Eides Statt, dass ich die vorgelegte Dissertation über die

Functional Characterisation of Two Channels Proteins
Involved in Leguminous Symbiosis

selbständig angefertigt und mich anderer Hilfsmittel als die in ihr angegebenen nicht bedient habe, insbesondere, dass aus Schriften Entlehnungen, soweit sie in der Dissertation nicht ausdrücklich als solche mit Angabe der betreffenden Schrift bezeichnet sind, nicht stattgefunden haben.

Ich habe weder anderweitig versucht, eine Dissertation einzureichen oder eine Doktorprüfung durchzuführen, noch habe ich diese Dissertation oder Teile derselben einer anderen Prüfungskommission vorgelegt.

München, den.....

.....

Charpentier Myriam

7.5 Curriculum vitae

PERSONAL DATA

Date of Birth Feb. 24, 1978. La Roche Sur Yon (Vendée, France)
Address 106 Les Cerisiers, 85480 Fougeré. France

HIGHER EDUCATION

Sept. 1996-June 2000 Institut Catholique d'Études Supérieures (ICES), La Roche sur yon,
France. Study of Cellular Biology and Physiology

Sept. 2000-June 2001 Paul Sabatier University – Toulouse, France. Master's degree 1:
Physiology and Molecular Plant Biology; (First Class honours).
Supervisor: Dr. Georges Boudart (UMR CNRS_UPS 5546)
Topic: Elicitor activity of a fungal endopolygalacturonase in
tobacco requires a functional catalytic site and cell wall localization

Sept. 2001-Dec. 2002 University Paris VII. France. Master's degree 2: Plant Productivity;
(First Class honours).
Supervisor: Dr. Abdel Ihafid Bendahmane (Plant Genomics
Research Unit, URGV, Evry)
Topic: Map-based cloning of *Pmm* conferring resistance to
Sphaerotheca fulginea in melon

Oct. 2004- Sept. 2008 PhD (Ludwig-Maximilians-Universität München, Genetics: Prof.
Dr. Martin Parniske)
Topic: Functional characterization of CASTOR and POLLUX, new
class of potassium permeable channel involved in arbuscular
mycorrhiza and root nodule symbioses

MISCELLANEOUS

First Aid Training course (France)

Computational skills Microsoft Word/ Excel/Power Point/Adobe Photoshop
Endnote/Vector NII/Staden Package/DeepView.
Experience with both Windows and Macintosh operating systems.

Languages English (IELTS, 6.5), German (basic knowledge)

Hobbies Running; Dancing (salsa); Music (Accordeon)